Chapter 1

Common Theoretical Issues

U. Nierste, Z. Ligeti, A. S. Kronfeld

1.1 Introduction

This chapter provides some of the theoretical background needed to interpret measurements studied by Working Groups 1–3 (and reported in Chapters 6–8, respectively). These three working groups deal with the decay of b-flavored hadrons, and they are independent of the production mechanism. The theory of b decays requires some elementary concepts on symmetries and mixing, some knowledge of the standard electroweak theory, and some information on how the b quark is bound into hadrons. On the other hand, the theory of production, fragmentation, and spectroscopy—the subjects of Working Group 4 (and Chapter 9)—is separate, dealing entirely with aspects of the strong interactions. Hence, the theoretical background needed for Working Group 4 is entirely in Chapter 9, and theoretical issues common to the working groups studying decays are collected together in this chapter.[1] Although the experimental study of CP violation in the B system is just beginning [1–3], there are several theoretical reviews [4–8] that the reader may want to consult for details not covered here.

We start in Sec. 1.2 by reviewing how flavor mixing and CP violation arise in the Standard Model. Experiments of the past decade have verified the $SU(3) \times SU(2) \times U(1)$ gauge structure of elementary particle interactions, in a comprehensive and very precise way. By comparison, tests of the flavor interactions are not yet nearly as broad or detailed. The Standard Model, in which quark masses and mixing arise from Yukawa interactions with the Higgs field, still serves as the current foundation for discussing flavor physics. Sec. 1.2 discusses the standard flavor sector, leading to the Cabibbo-Kobayashi-Maskawa (CKM) matrix, which contains a CP violating parameter for three generations. By construction, the CKM matrix is unitary, which implies several relations among its entries and, hence, between CP conserving and CP violating observables. Furthermore, the same construction shows how, in the Standard Model, neutral currents conserve flavor at the tree level, which is known as the Glashow-Iliopoulos-Maiani (GIM) effect.

We emphasize that in extensions of the Standard Model the CKM mechanisms can exist side-by-side with other sources of CP and flavor violation. Many measurements are

[1] There is, unavoidably, some overlap with theoretical material in Chapters 6–8. We have attempted to use consistent conventions and notation throughout.

therefore needed to test whether the standard patterns prevail. Quark interactions are obscured by confinement, however. Therefore, Sec. 1.2 concludes with a brief summary of the ways of avoiding or reducing uncertainties from nonperturbative QCD, and the much of the rest of the chapter revisits various aspects in greater detail.

Sec. 1.3 covers aspects of B mesons that can be discussed without reference to their underlying dynamics. The strong interactions conserve the quantum numbers P, T, and C of parity, time reversal, and charge conjugation. We therefore start by discussing the transformation properties of currents and hadrons under these discrete symmetry transformations. Once these concepts—and associated phase conventions—are fixed, one can discuss the mixing between neutral mesons. (In the Standard Model, neutral meson mixing is induced through one-loop effects.) Although a flavored neutral meson and its anti-particle form a two-state quantum mechanical system, the particles are not stable, so the two mass eigenstates can have different decay widths in general. Consequently, the physical description of decay during mixing contains formulae that are not always simple and phase conventions that are not always transparent. Sec. 1.3 provides such a general set of formulae, derived with a self-consistent set of conventions.

The general discussion of Sec. 1.3, leads to a useful classification of CP violation. There can be CP violation in mixing, in decay, and in the interference of decays with and without mixing. Sec. 1.4 gives the concrete mathematical definition of these three types of CP violation, illustrated with examples. CP violation in many B decays is principally of one type or another, although in general two or more of these types may be present, as is the case with some kaon decays. We also work through two important examples of CP in the interference of amplitudes: $B \to J/\psi K_S$ and $B_s \to D_s^{\pm} K^{\mp}$, where it is possible to use the CP invariance of QCD to show that the CP asymmetry of these decays is independent of the hadronic transition amplitude.

To gain a comprehensive view of flavor physics, and decide whether the standard model correctly describes flavor-changing interactions, one has to consider QCD. Sec. 1.5 discusses several theoretical tools to separate scales, so that the nonperturbative hadronic physics can be treated separately from physics at higher scales, where perturbation theory is accurate. Indeed, in B decays several length scales are involved: the scale of QCD, $\Lambda_{\rm QCD}$, the mass of the b quark, m_b, the higher masses of the W and Z bosons and the top quark, and, possibly, higher scales of new physics. The first step is to separate out weak (and higher) scales with an operator product expansion, leading to an effective weak Hamiltonian for flavor-changing processes. This formalism applies for all flavor physics. For b quarks, one finds further simplifications, because $m_b \gg \Lambda_{\rm QCD}$. Two tools are used to separate these scales, heavy quark effective theory for hadronic matrix elements, and the heavy quark expansion for inclusive decay rates. Sec. 1.5 also includes a brief overview of lattice QCD, which is a promising numerical method to compute hadronic matrix elements of the electroweak Hamiltonian, when there is at most one hadron in the final state. In particular, we discuss how heavy quark effective theory can be used to control uncertainties in the numerical calculation.

A further predictive aspect of the CKM mechanism, with only one parameter to describe CP violation, is that observables in the B and B_s systems are connected to those in the kaon

system. Sec. 1.6 gives an overview of $K^0 - \overline{K}^0$ mixing using the same formalism as in our treatment of $B^0 - \overline{B}^0$ mixing in Sec. 1.3. This also gives us the opportunity to introduce the most important constraints from kaon physics: not only those currently available but also those that could be measured in the coming decade. Finally, Sec. 1.7 gives a summary of expectations for measurements of the unitarity triangle, based on global fits of kaon mixing and CP conserving observables in B physics.

1.2 CP Violation in the Standard Model

As mentioned in the introduction, in the Standard Model quark masses, flavor violation, and CP violation all arise from Yukawa interactions among the quark fields and the Higgs field. In this section we review how these phenomena appear, leading to the Cabibbo-Kobayashi-Maskawa (CKM) matrix. From a theoretical point of view, the CKM mechanism could, and probably does, exist along with other sources of CP violation. We therefore also discuss some of the important features of the CKM model, to provide a framework for testing it.

1.2.1 Yukawa interactions and the CKM matrix

Let us begin by recalling some of the most elementary aspects of particle physics. Experiments have demonstrated that there are several species, or flavors, of quarks and leptons. They are the down-type quarks (d, s, b), up-type quarks (u, c, t), charged leptons (e, μ, τ), and neutrinos (ν_e, ν_μ, ν_τ). They interact through the exchange of gauge bosons: the weak bosons $W^\pm$ and Z^0, the photon, and the gluons. These interactions are dictated by local gauge invariance, with gauge group $SU(3) \times SU(2) \times U(1)_Y$. With this gauge symmetry, and the observed quantum numbers of the fermions, at least one scalar field is needed to accommodate quark masses, and, in turns out, the couplings to this field can generate flavor and CP violation.

One of the most striking features of the charged-current weak interactions is that they do not couple solely to a vector current (as in QED and QCD) but to the linear combination of vector and axial vector currents $V - A$. As a consequence, the electroweak theory is a *chiral* gauge theory, which means that left- and right-handed fermions transform differently under the electroweak gauge group $SU(2) \times U(1)_Y$. The right-handed fermions do not couple to $W^\pm$, and they are singlets under $SU(2)$:

$$\begin{aligned} E_R &= (e_R, \mu_R, \tau_R)\,, \qquad & Y_E &= -1\,; \\ U_R &= (u_R, c_R, t_R)\,, \qquad & Y_U &= \frac{2}{3}\,; \\ D_R &= (d_R, s_R, b_R)\,, \qquad & Y_D &= -\frac{1}{3}\,; \end{aligned} \tag{1.1}$$

where the hypercharge Y is given. For convenience below, the three generations are grouped together. The gauge and kinetic interactions for G generations of these fields are

$$\mathcal{L}_R = \sum_{i=1}^{G} \bar{E}_R^i (i\partial\!\!\!/ - g_1 Y_E B\!\!\!/) E_R^i + \bar{D}_R^i (i\partial\!\!\!/ - g_1 Y_D B\!\!\!/) D_R^i + \bar{U}_R^i (i\partial\!\!\!/ - g_1 Y_U B\!\!\!/) U_R^i\,, \tag{1.2}$$

where B is the gauge boson of $U(1)_Y$, with coupling g_1, and D^μ is the covariant derivative of QCD: quarks are triplets under color $SU(3)$. On the other hand, the left-handed fermions do couple to $W^\pm$, so they are doublets under $SU(2)$:

$$\begin{aligned} L_L &= \left(\begin{pmatrix} \nu_e \\ e \end{pmatrix}_L, \begin{pmatrix} \nu_\mu \\ \mu \end{pmatrix}_L, \begin{pmatrix} \nu_\tau \\ \tau \end{pmatrix}_L \right), \qquad Y_L = -\frac{1}{2}; \\ Q_L &= \left(\begin{pmatrix} u \\ d \end{pmatrix}_L, \begin{pmatrix} c \\ s \end{pmatrix}_L, \begin{pmatrix} t \\ b \end{pmatrix}_L \right), \qquad Y_Q = \frac{1}{6}. \end{aligned} \tag{1.3}$$

The $SU(2)$ quantum number is called weak isospin, and the third component I_3 distinguishes upper and lower entries. The gauge and kinetic interactions for G generations of these fields are

$$\mathcal{L}_L = \sum_{i=1}^{G} \bar{L}_L^i (i\partial\!\!\!/ - g_1 Y_L B\!\!\!/ - g_2 W\!\!\!/) L_L^i + \bar{Q}_L^i (i\partial\!\!\!/ - g_1 Y_Q B\!\!\!/ - g_2 W\!\!\!/) Q_L^i \,, \tag{1.4}$$

where $W = W^a \sigma_a/2$ are the gauge bosons of $SU(2)$, with gauge coupling g_2. Note that as far as gauge interactions are concerned, the generations are simply copies of each other, and $\mathcal{L}_R + \mathcal{L}_L$ possesses a large global flavor symmetry. For G generations, the symmetry group is $U(G)^5$, that is, a $U(G)$ symmetry for each of E_R, U_R, D_R, L_L, and Q_L.

The assignments of $SU(2)$ and $U(1)_Y$ quantum numbers follow from simple, experimentally determined properties of weak decays. For example, by the mid-1980s measurements of decays of b-flavored hadrons had shown the weak isospin of b_L to be $-\frac{1}{2}$ [9]. Consequently, its isopartner t_L had to exist, for symmetry reasons, although several years passed before the top quark was observed at the Tevatron. In contrast, gauge symmetry does not motivate the inclusion of right-handed neutrinos, which would be neutral under all three gauge groups. For this reason, they are usually omitted from the "standard" model.

With only gauge fields and fermions, the model is incomplete. In particular, it does not accommodate the observed non-zero masses of the quarks, charged leptons, and weak gauge bosons $W^\pm$ and Z^0. For example, masses for the charged fermions[2] normally would come from interactions that couple the left- and right-handed components of the field, such as

$$\mathcal{L}_m = -m \left(\bar{\psi}_R \psi_L + \bar{\psi}_L \psi_R \right), \tag{1.5}$$

where, in the case at hand, $\psi \in \{e, \mu, \tau, d, s, b, u, c, t\}$. With the fields introduced above, one would have to combine a component of a doublet with a singlet, which would violate $SU(2)$. Any pairing of left- and right-handed fields with the listed hypercharges would violate $U(1)_Y$ as well.

To construct gauge invariant interactions coupling left- and right-handed fermions, at least one additional field is necessary. For simplicity, let us begin with only the first generation leptons. Consider

$$\mathcal{L}_Y = -y e^{i\delta}\, \bar{l}_L \phi\, e_R - y e^{-i\delta}\, \bar{e}_R\, \phi^\dagger l_L, \tag{1.6}$$

[2]Because it is completely neutral, a right-handed neutrino may have a so-called Majorana mass term, coupling neutrino to neutrino, instead of—or in addition to—a Dirac mass term, coupling neutrino to antineutrino. For this reason neutrino masses are even more perplexing than quark and charged lepton masses.

where $\bar{l}_L = (\bar{\nu}_L,\ \bar{e}_L)$, and y is real. If the quantum numbers of ϕ are chosen suitably, then the interaction $\mathcal{L}_I$ would be gauge (and Lorentz) invariant. To preserve Lorentz invariance, ϕ must have spin 0. To preserve invariance under $U(1)_Y$, the hypercharge of ϕ must be $Y_\phi = Y_L - Y_E = +\frac{1}{2}$. To preserve invariance under $SU(2)$ ϕ, must be a doublet,

$$\phi = \begin{pmatrix} \phi^+ \\ \phi^0 \end{pmatrix}. \tag{1.7}$$

The superscripts denote the electric charge $Q = Y + I_3$. An interaction similar to $\mathcal{L}_Y$ was first introduced by Yukawa to describe the decay $\pi^+ \to \mu^+\nu_\mu$, so it is called a Yukawa interaction, and the coupling y is called a Yukawa coupling.

At first glance, the interaction in Eq. (1.6) appears to violate CP, with a strength proportional to $y \sin\delta$. One may, however, remove δ, by exploiting the invariance of $\mathcal{L}_R + \mathcal{L}_L$ under independent changes in the phases of e_R and l_L. Thus, the one-generation Yukawa interaction has only one real parameter, y, and it conserves CP.

Since it is charged under $SU(2) \times U(1)_Y$, the field ϕ has gauge interactions, which are dictated by symmetry. The scalar field may also have self-interactions, which are not dictated by symmetry. If one limits one's attention to renormalizable interactions

$$V(\phi) = -\lambda v^2 \phi^\dagger\phi + \lambda(\phi^\dagger\phi)^2, \tag{1.8}$$

with two new parameters, v and λ. The state with no propagating particles, called the vacuum, is realized when ϕ minimizes $V(\phi)$. The quartic coupling λ must be positive; otherwise the potential energy would be unbounded from below, and the vacuum would be unstable. If $v^2 < 0$, then there is a single minimum of the potential, with vacuum expectation value $\langle\phi\rangle = 0$; this possibility does not interest us here. If $v^2 > 0$, then $V(\phi)$ takes the shape of a sombrero with a three-dimensional family of minima:

$$\langle\phi\rangle = e^{i\langle\xi^a\rangle\sigma_a/2v} \begin{pmatrix} 0 \\ v/\sqrt{2} \end{pmatrix}, \tag{1.9}$$

parametrized by $\langle\xi^a\rangle$. Through an x-independent $SU(2)$ transformation, one can set $\langle\xi^a\rangle = 0$. Although the Lagrangian fully respects local $SU(2)\times U(1)_Y$ gauge symmetry, the vacuum solution of the equations of motion given in Eq. (1.9) does not: this is called spontaneous (as opposed to explicit) symmetry breaking.

Physical particles arise from fluctuations around the solution of the equations of motion, so one writes

$$\phi(x) = e^{i\xi^a(x)\sigma_a/2v} \begin{pmatrix} 0 \\ [v + h(x)]/\sqrt{2} \end{pmatrix}. \tag{1.10}$$

The vacuum expectation values of the fluctuation fields are $\langle\xi^a\rangle = \langle h\rangle = 0$. Masses of the physical particles are found by inserting Eq. (1.10) into the expressions for the interactions in the Lagrangian and examining the quadratic terms. By comparing the $\bar{e}_R e_L$ terms in $\mathcal{L}_Y$ and $\mathcal{L}_m$, one sees that the electron mass in this model is $m_e = yv/\sqrt{2}$. Similarly, from $V(\phi)$ the field h is seen to have a (squared) mass $m_h^2 = 2\lambda v^2$, and from the kinetic energy of the scalar field non-zero masses for three of the gauge bosons arise: $m_{W^\pm}^2 = \frac{1}{4}g_2^2 v^2$ and $m_{Z^0}^2 = \frac{1}{4}(g_1^2 + g_2^2)v^2$, where Z^0 is the massive linear combination of W^3 and B. (The

orthogonal combination is the massless photon γ.) The amplitude for muon decay is, to excellent approximation, proportional to g_2^2/m_W^2. Therefore, one can obtain the vacuum expectation value from the Fermi decay constant, finding $v = 246$ GeV.

Repeating this construction with $(\bar{u}_L,\ \bar{d}_L)$ and d_R requires a doublet with hypercharge $Y_Q - Y_D = +\frac{1}{2}$. The Standard Model uses the same doublet as for leptons. Repeating it with $(\bar{u}_L,\ \bar{d}_L)$ and u_R requires a doublet with hypercharge $Y_Q - Y_U = -\frac{1}{2}$. The Standard Model uses the charge-conjugate

$$\tilde{\phi} \equiv i\sigma_2\phi^* = \begin{pmatrix} \overline{\phi^0} \\ -\phi^- \end{pmatrix} \tag{1.11}$$

of the doublet used for leptons. In the one-generation case, three real Yukawa couplings are introduced, leading to masses for the electron, down quark, and up quark.

With G generations the full set of Yukawa interactions is complicated. It is instructive to leave G arbitrary for now, and to compare the physics for $G = 2$, 3, 4, later on. The generations may interact with each other as in

$$\mathcal{L}_Y = -\sum_{i,j=1}^{G} \left[\hat{y}^e_{ij}\bar{L}^i_L\phi\, E^j_R + \hat{y}^d_{ij}\bar{Q}^i_L\phi\, D^j_R + \hat{y}^u_{ij}\bar{Q}^i_L\tilde{\phi}\, U^j_R + \text{h.c.}\right], \tag{1.12}$$

because no symmetry would enforce a simpler structure. For G generations, the Yukawa matrices are complex $G\times G$ matrices. At first glance, each matrix $\hat{y}^a$ seems to introduce $2G^2$ parameters: G^2 that are real and CP-conserving, and another G^2 that are imaginary and CP violating. But, as in the one-generation case, one must think carefully about physically equivalent matrices before understanding how many physical parameters there really are.

Let us consider the leptons first. As mentioned above, the non-Yukawa part of the Lagrangian is invariant under the following transformation of generations

$$\begin{aligned} E_R &\mapsto RE_R\,, \qquad & \bar{E}_R &\mapsto \bar{E}_R R^\dagger, \\ L_L &\mapsto SL_L\,, \qquad & \bar{L}_L &\mapsto \bar{L}_L S^\dagger, \end{aligned} \tag{1.13}$$

where $R \in U(G)_{E_R}$ and $S \in U(G)_{L_L}$. That means that the Yukawa matrix $\hat{y}^e$ is equivalent to $y^e = S\hat{y}^e R^\dagger$. By suitable choice, y^e can be made diagonal, real, and non-negative. The leptons' Yukawa interactions now read

$$\mathcal{L}_{Yl} = -\sum_{i=1}^{G} \left[y^e_i\bar{L}^i_L\phi\, E^i_R + \text{h.c.}\right]. \tag{1.14}$$

Note that if S and R achieve this structure, so do $S' = DS$ and $R' = DR$, where $D = \text{diag}\,(e^{i\varphi_1}, \ldots, e^{i\varphi_G})$. Thus, part of the transformation from $\hat{y}^e$ to y^e is redundant and must not be counted twice. (The freedom to choose these phases leads to global conservation of lepton flavor.) Hence, the transformation removes $2G^2 - G$ parameters, leaving G independent entries in y^e. Since all are real, there is no CP violation.

For the quarks the reasoning is the same but the algebra is trickier. There are now three distinct $U(G)$ symmetries, and the non-Yukawa Lagrangian is invariant under

$$\begin{aligned} D_R &\mapsto R_d D_R\,, & \bar{D}_R &\mapsto \bar{D}_R R_d^\dagger\,, \\ U_R &\mapsto R_u U_R\,, & \bar{U}_R &\mapsto \bar{U}_R R_u^\dagger\,, \\ Q_L &\mapsto S_u Q_L\,, & \bar{Q}_L &\mapsto \bar{Q}_L S_u^\dagger\,. \end{aligned} \tag{1.15}$$

One may again exploit S_u and R_u to transform $\hat{y}^u$ into the diagonal, real, non-negative form y^u. Then the transform of $\hat{y}^d$ is, in general, neither real nor diagonal. Instead

$$S_u \hat{y}^d R_d^\dagger = V y^d\,, \tag{1.16}$$

where $y^d = S_d \hat{y}^d R_d^\dagger$ *is* diagonal, real, and non-negative, and

$$V = S_u S_d^\dagger \tag{1.17}$$

is the Cabibbo-Kobayashi-Maskawa (CKM) matrix [10,11]. By construction, V is a $G \times G$ unitary matrix. The quarks' Yukawa interactions now read

$$\mathcal{L}_{Yq} = -\sum_{i,j=1}^{G} \left[y_j^d \bar{Q}_L^i \phi\, V_{ij} D_R^j + \text{h.c.} \right] - \sum_{i=1}^{G} \left[y_i^u \bar{Q}_L^i \tilde{\phi}\, U_R^i + \text{h.c.} \right]. \tag{1.18}$$

If S_u, R_u, and R_d achieve this structure, so do $e^{i\varphi} S_u$, $e^{i\varphi} R_u$, and $e^{i\varphi} R_d$. (The freedom to choose this phase leads to global conservation of total baryon number.) Thus, the manipulations remove $3G^2 - 1$ parameters from the $4G^2$ in two arbitrary $G \times G$ matrices, leaving $G^2 + 1$. Of these, $2G$ are in y^u and y^d, and the other $(G-1)^2$ are in the CKM matrix V. One can also count separately the real and imaginary parameters. Since a $G \times G$ unitary matrix has $\frac{1}{2}G(G-1)$ real and $\frac{1}{2}G(G+1)$ imaginary components, one finds that the CKM matrix has $\frac{1}{2}G(G-1)$ real, CP-conserving parameters, and $\frac{1}{2}(G-1)(G-2)$ imaginary, CP violating parameters. For example, the case $G = 2$ has no CP violation from this mechanism, $G = 3$ has a single CP violating parameter, and $G = 4$ has three.

The CKM matrix V arises from the misalignment of the matrices S_u and S_d. Under circumstances that preserve some of the flavor symmetry, they can be partially aligned, and then V contains even fewer physical parameters. In an example with three generations, if two entries either in y^u or in y^d are equal, partial re-alignment removes one real angle and one phase. Therefore, the CKM mechanism leads to CP violation only if like-charged quarks all have distinct masses.

Substituting Eq. (1.10) into $\mathcal{L}_Y$ and keeping quadratic terms shows that the masses are

$$m_k^a = \frac{v}{\sqrt{2}}\, y_k^a\,, \tag{1.19}$$

for $k = 1, 2, 3$, and $a = e, d, u$. For quarks this is easiest to see if one sets

$$Q_L = \begin{pmatrix} U_L \\ V D_L \end{pmatrix}, \tag{1.20}$$

which diagonalizes the mass terms for the down-like quarks in Eq. (1.18). In this basis the CKM matrix migrates to the charged-current vertex:

$$\mathcal{L}_{\bar{U}WD} = -\frac{g_2}{\sqrt{2}} \left[\bar{U}_L \not{W}^+ V D_L + \bar{D}_L V^\dagger \not{W}^- U_L \right], \tag{1.21}$$

where $W^{\pm} = (W^1 \mp iW^2)/\sqrt{2}$. The basis in (1.20), with diagonal mass matrices and the CKM matrix in the charged currents of quarks, is usually adopted in phenomenology.

Note that the neutral current interactions are unaffected by writing V in (1.20). Thus, there are no flavor-changing neutral currents (FCNC) at the tree level in the Standard Model. This is known as the Glashow-Iliopoulus-Maiani (GIM) effect [12]. Even at the loop level, where the FCNCs do arise, the GIM mechanism can suppress processes by a factor m_q^2/m_W^2, which is very small, except in the case of the top quark. GIM suppression and Cabibbo suppression (i.e., factors of λ) both imply near-null predictions for several processes. Observation of any of these would constitute a clear signal of non-standard physics.

Note that quark and lepton masses arise from the same microscopic interactions as CKM flavor violation. In Nature, the quark and lepton masses vary over orders of magnitude. Thus, the large flavor symmetry that would arise in the absence of Yukawa interactions is severely broken. In the Standard Model, the Yukawa couplings are simply chosen to contrive the observed masses. This is unsatisfactory, but we lack the detailed experimental information needed to develop a deeper theory of flavor.

1.2.2 General models

The foregoing discussion makes clear that the unitary CKM matrix arises in an algebraic way. Therefore, the mechanism can survive in models with a more complicated Higgs sector. The Standard Model is a model of economy: a single doublet generates mass for the gauge bosons, charged leptons, down-like quarks, and up-like quarks. In models with two doublets (and three or more generations), the CKM source of CP violations remains, but there can be additional CP violation in the Higgs sector [13].

To emphasize this point, let us consider an extreme example with

$$\mathcal{L}_Y = \bar{L}_L^i \Phi_{ij}^e E_R^j + \bar{Q}_L^i \Phi_{ij}^d D_R^j + \bar{Q}_L^i \tilde{\Phi}_{ij}^u U_R^j + \text{h.c.}, \tag{1.22}$$

where i, j run over generations, and we take the basis in which gauge interactions do not change generations. The tilde on $\tilde{\Phi}_u$ is introduced so that, with $\tilde{\Phi}^u = i\sigma_2 \Phi^{u*}$, all Φ^a are (matrix) fields with hypercharge $+\frac{1}{2}$. Here the Yukawa couplings are absorbed into the fields—Eq. (1.22) is hideous enough as it is. Since all Φ^a are doublets under $SU(2)$, they all would participate in electroweak symmetry breaking.

Suppose the Higgs potential, now a complicated function of all the scalar fields, leads to vacuum expectation values of the form

$$\langle \Phi_{ij}^a \rangle = \begin{pmatrix} 0 \\ \hat{m}_{ij}^a \end{pmatrix}. \tag{1.23}$$

Then the $\hat{m}_{ij}^a$ are mass matrices, and the algebra leading to the real, physical masses m_k^a and the CKM matrix is just as above. The CKM matrix, V, survives and should lead to CP violation, because there is no good reason for the phase in V to be small. There would, however, almost certainly be new sources of CP violation from the Higgs sector.

1.2.3 CP violation from a unitary CKM matrix

In the standard, one-doublet, model, we see that flavor and CP violation arise solely through the CKM matrix. Furthermore, in more general settings, the CKM matrix can still arise, but there may be other sources of CP violation as well. If the CKM matrix is the only source of CP violation, there are many relations between CP-conserving and CP violating observables that arise from the fact that V is a unitary matrix. This section outlines a framework for testing whether these constraints are, in fact, realized.

A useful way [14] of gauging the size of CP violation starts with the commutator of the mass matrices, $C = [\hat{m}^u \hat{m}^{u\dagger}, \hat{m}^d \hat{m}^{d\dagger}]$, which can be re-written

$$C = S_u^\dagger \left[(m^u)^2,\, V (m^d)^2\, V^\dagger \right] S_u \,, \tag{1.24}$$

to show that $\det C$ depends on the physical masses and V. After some algebra one finds

$$\det C = -2i F_u F_d J \,, \tag{1.25}$$

where

$$F_u = (m_u^2 - m_c^2)(m_c^2 - m_t^2)(m_t^2 - m_u^2) \,, \tag{1.26}$$
$$F_d = (m_d^2 - m_s^2)(m_s^2 - m_b^2)(m_b^2 - m_d^2) \,, \tag{1.27}$$
$$J = \mathrm{Im}\,[V_{11} V_{21}^*\, V_{22} V_{12}^*] \,. \tag{1.28}$$

To arrive at Eq. (1.25) one makes repeated use of the property $V V^\dagger = \mathbb{1}$, especially that

$$J = \mathrm{Im}\,[V_{ij} V_{kj}^*\, V_{kl} V_{il}^*] \sum_m \varepsilon_{ikm} \sum_n \varepsilon_{jln} \,, \tag{1.29}$$

for all combinations of i, j, k, and l. The determinant $\det C$ captures several essential features of CP violation from the CKM mechanism. It is imaginary, reminding us that CP violation stems from a complex coupling. More significantly, there is no CP violation unless F_u, F_d, and J are all different from zero. Non-vanishing F_u and F_d codify the requirements on the quark masses given above. Non-vanishing J codifies requirements on V, which are clearest after choosing a specific parameterization. The key point, however, is that the value taken by J is independent of the parameterization, by construction of $\det C$.

To emphasize the physical transitions associated with the CKM matrix, it is usually written

$$V = \begin{pmatrix} V_{ud} & V_{us} & V_{ub} \\ V_{cd} & V_{cs} & V_{cb} \\ V_{td} & V_{ts} & V_{tb} \end{pmatrix} , \tag{1.30}$$

so that the entries are labeled by the quark flavors. From Eq. (1.21), the vertex at which a b quark decays to a W^- and c quark is proportional to V_{cb}; similarly, the vertex at which a c quark decays to a W^+ and s quark is proportional to V_{cs}^*. Because V is unitary, $|V_{ud}|^2 + |V_{us}|^2 + |V_{ub}|^2 = 1$, and similarly for all other rows and columns. These constraints give information on unmeasured (or poorly measured) elements of V. For example, because

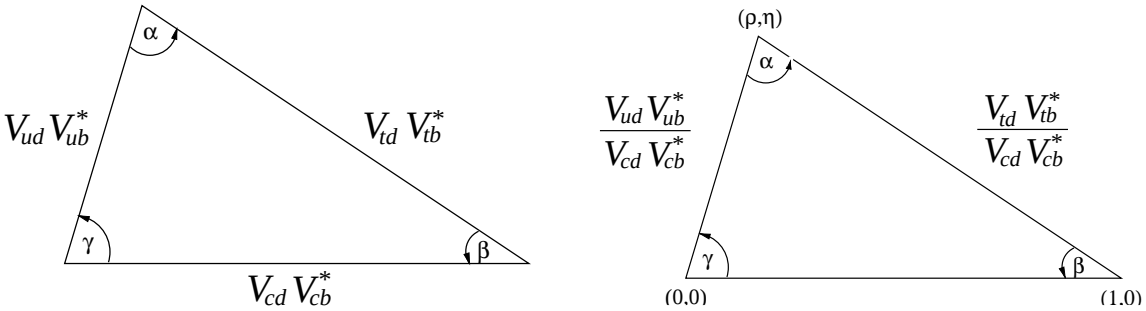

Figure 1.1: The unitarity triangle. The version on the left directly expresses Eq. (1.31). The rescaled version shows the definition of $(\bar{\rho}, \bar{\eta})$.

$|V_{cb}|$ and $|V_{ub}|$ are known to be small, $|V_{tb}|$ should be very close to 1—if, indeed, there are only three generations. Furthermore, $|V_{ts}|$ and $|V_{td}|$ must also be small.

Even more interesting constraints come from the orthogonality of columns (or rows) of a unitary matrix. Taking the first and third columns of V, one has

$$V_{ud}V_{ub}^* + V_{cd}V_{cb}^* + V_{td}V_{tb}^* = 0\,. \tag{1.31}$$

Equation (1.31) says that the three terms in the sum trace out a triangle on the complex plane. Because it is a consequence of the unitarity property of V, this triangle is called the "unitarity triangle," shown in Fig. 1.1. The lengths of the sides are simply $|V_{ud}V_{ub}^*|$, etc., and the angles are

$$\alpha = \arg\left[-\frac{V_{td}V_{tb}^*}{V_{ud}V_{ub}^*}\right], \qquad \beta = \arg\left[-\frac{V_{cd}V_{cb}^*}{V_{td}V_{tb}^*}\right], \qquad \gamma = \arg\left[-\frac{V_{ud}V_{ub}^*}{V_{cd}V_{cb}^*}\right]. \tag{1.32}$$

The notation $\beta \equiv \phi_1$, $\alpha \equiv \phi_2$, $\gamma \equiv \phi_3$ is also used. By construction $\alpha + \beta + \gamma = \pi$. The area of the triangle is $|J|/2$ and the terms trace out the triangle in a counter-clockwise (clockwise) sense if J is positive (negative). In fact, there are five more unitarity triangles, all with area $|J|/2$ and orientation linked to the sign of J.

The unitarity triangle(s) are useful because they provide a simple, vivid summary of the CKM mechanism. Separate measurements of lengths, through decay and mixing rates, and angles, through CP asymmetries, should fit together. Furthermore, when one combines measurements—from the B, B_s, K, and D systems, as well as from hadronic W decays—all triangles should have the same area and orientation. If there are non-CKM contributions to flavor or CP violation, however, the interpretation of rates and asymmetries as measurements of the sides and angles no longer holds. The triangle built from experimentally defined sides and angles will not fit with the CKM picture.

In the parameterization favored by the Particle Data Book [15]

$$V = \begin{pmatrix} c_{12}c_{13} & s_{12}c_{13} & s_{13}e^{-i\delta_{13}} \\ -s_{12}c_{23} - c_{12}s_{23}s_{13}e^{i\delta_{13}} & c_{12}c_{23} - s_{12}s_{23}s_{13}e^{i\delta_{13}} & s_{23}c_{13} \\ s_{12}s_{23} - c_{12}c_{23}s_{13}e^{i\delta_{13}} & -c_{12}s_{23} - s_{12}c_{23}s_{13}e^{i\delta_{13}} & c_{23}c_{13} \end{pmatrix}, \tag{1.33}$$

where $c_{ij} = \cos\theta_{ij}$ and $s_{ij} = \sin\theta_{ij}$. The real angles θ_{ij} may be chosen so that $0 \le \theta_{ij} \le \pi/2$, and the phase δ_{13} so that $0 \le \delta_{13} < 2\pi$. With Eq. (1.33) the Jarlskog invariant becomes

$$J = c_{12}c_{23}c_{13}^2 s_{12}s_{23}s_{13}\sin\delta_{13}\,. \tag{1.34}$$

The parameters must satisfy

$$\delta_{13} \neq 0,\ \pi\,; \qquad \theta_{ij} \neq 0,\ \pi/2\,; \tag{1.35}$$

otherwise J vanishes. Since CP violation is proportional to J, the CKM matrix must not only have complex entries, but also non-trivial mixing; otherwise the KM phase δ_{13} can be removed.

A convenient parameterization of the CKM matrix is due to Wolfenstein [16]. It stems from the observation that the measured matrix obeys a hierarchy, with diagonal elements close to 1, and progressively smaller elements away from the diagonal. This hierarchy can be formalized by defining λ, A, ρ, and η via

$$\lambda \equiv s_{12}\,, \qquad A \equiv s_{23}/\lambda^2\,, \qquad \rho + i\eta \equiv s_{13}e^{i\delta_{13}}/A\lambda^3\,. \tag{1.36}$$

From experiment $\lambda \approx 0.22$, $A \approx 0.8$, and $\sqrt{\rho^2+\eta^2} \approx 0.4$, so it is phenomenologically useful to expand V in powers of λ:

$$V = \begin{pmatrix} 1-\frac{1}{2}\lambda^2 & \lambda & A\lambda^3(\rho - i\eta) \\ -\lambda & 1-\frac{1}{2}\lambda^2 & A\lambda^2 \\ A\lambda^3(1-\rho-i\eta) & -A\lambda^2 & 1 \end{pmatrix} + \mathcal{O}(\lambda^4)\,. \tag{1.37}$$

The most interesting correction at $\mathcal{O}(\lambda^4)$ for our purposes is $\mathrm{Im}\,V_{ts} = -A\lambda^4\eta$. The Jarlskog invariant can now be expressed $J = A^2\lambda^6\eta \approx (7\times10^{-5})\eta$. One sees that CKM CP violation is small not because δ_{13} is small but because flavor violation must also occur, and flavor violation is suppressed, empirically, by powers of λ.

The unitarity triangle in Eq. (1.31) is special, because its three sides are all of order $A\lambda^3$. The triangle formed from the orthogonality of the first and third rows also has this property, but it is not accessible, because the top quark decays before the mesons needed to measure the angles are bound. The other triangles are all long and thin, with sides $(\lambda, \lambda, A\lambda^5)$ (e.g., for the kaon) or $(\lambda^2, \lambda^2, A\lambda^4)$ (e.g., for the B_s meson).

It is customary to rescale Eq. (1.31) by the common factor $A\lambda^3$, to focus on the less well-determined parameters (ρ, η). In the context of the Wolfenstein parameterization, there are many ways to do this. Since we anticipate precision in experimental measurements, and also in theoretical calculations of some important hadronic transition amplitudes, it is useful to choose an exact rescaling. We choose to divide all three terms in Eq. (1.31) by $V_{cd}V_{cb}^*$ and define[3]

$$\bar\rho + i\bar\eta \equiv -\frac{V_{ud}V_{ub}^*}{V_{cd}V_{cb}^*}. \tag{1.38}$$

[3]This definition differs at $\mathcal{O}(\lambda^4)$ from the original one in Ref. [17].

Then the rescaled triangle, also shown in Fig. 1.1, has its apex in the complex plane at $(\bar{\rho}, \bar{\eta})$. The angles of the triangle are easily expressed

$$\alpha = \tan^{-1}\left(\frac{\bar{\eta}}{\bar{\eta}^2 + \bar{\rho}(\bar{\rho}-1)}\right), \quad \beta = \tan^{-1}\left(\frac{\bar{\eta}}{1-\bar{\rho}}\right), \quad \gamma = \tan^{-1}\left(\frac{\bar{\eta}}{\bar{\rho}}\right), \tag{1.39}$$

Since $\bar{\eta}$, $\bar{\rho}$, and $1-\bar{\rho}$ could easily be of comparable size, the angles and, thus, the corresponding CP asymmetries could be large.

At the Tevatron there is also copious production of B_s mesons. The corresponding unitarity triangle is

$$V_{us}V_{ub}^* + V_{cs}V_{cb}^* + V_{ts}V_{tb}^* = 0\,, \tag{1.40}$$

replacing the d quark with s. In Eq. (1.40) the first side is much shorter than the other two. Therefore, the opposing angle

$$\beta_s = \arg\left[-\frac{V_{ts}V_{tb}^*}{V_{cs}V_{cb}^*}\right] = \lambda^2\eta + \mathcal{O}(\lambda^4) \tag{1.41}$$

is small, of order one degree. Therefore, the asymmetries in $B_s \to \psi\eta^{(\prime)}$ and $B_s \to \psi\phi$ are much smaller than in the corresponding B decays. On the other hand, this asymmetry is sensitive to new physics in $B_s^0 - \overline{B}_s^0$ mixing. In the standard model, as discussed below, mixing is induced by loop processes. When, as here, there is also Cabibbo suppression, it is easy for the non-standard phenomena to compete. Thus, in the short term a measurement of β_s represents a search for new physics, whereas in the long term it would be a verification of the CKM picture.

The unitarity triangle for the D system comes from the orthogonality of the top two rows of the CKM matrix. It is even longer and thinner than the one for the B_s system. Consequently, a non-zero measurement of the CP asymmetry associated with the small angle is a clear sign of new physics. It seems that experiments to measure the D-system unitarity triangle are not yet feasible.

1.2.4 Hadronic uncertainties and clean measurements

At a superficial level, the way to test the CKM picture is to measure rates and asymmetries that are sensitive to the sides and angles (of all triangles), in as many ways as possible. A serious obstacle, however, is that the quarks are confined in hadrons. Consequently, most relations between experimental observables and Lagrangian-level couplings, like the CKM matrix, involve hadronic matrix elements. In this subsection, we summarize briefly how to treat the matrix elements, with an eye toward identifying processes that are relatively free of hadronic uncertainty.

There are several approaches for treating the hadronic matrix elements, none of which is universally useful. In Sec. 1.5 we introduce some of the essential tools in greater detail. Here we illustrate the possibilities with examples.

- Perfect (or essentially perfect) symmetries of QCD, such as C or CP: When a single CKM factor dominates a process, the QCD part of the amplitude cancels in ratios such as the CP asymmetry in interference between decays with and without mixing. The two best examples are in the asymmetries for[4] $B \to \psi K_S$ and $B_s \to D_s^{\pm} K^{\mp}$. Assuming that CP violation comes only from the CKM matrix, the first class of modes cleanly yields $\sin 2\beta$, and the other pair of modes cleanly yields $\sin(\gamma - 2\beta_s)$.

- Approximate symmetries, such as isospin, flavor $SU(3)$, chiral symmetry, or heavy quark symmetry: The best-known examples are when the symmetry restricts a form factor for semileptonic decays. Isospin and $n \to pe\bar{\nu}_e$ give $|V_{ud}|$; flavor $SU(3)$ and $K \to \pi e\bar{\nu}_e$ give $|V_{us}|$; and heavy quark symmetry and $B \to D^* \ell \bar{\nu}_\ell$ give $|V_{cb}|$. The hadronic uncertainty is now in the deviation from the symmetry limit. An even more intriguing use of isospin is to relate the form factor of $K^0 \to \pi^+ e\bar{\nu}_e$ to that of $K^{0,\pm} \to \pi^{0,\pm}\nu\bar{\nu}$. The rare $\nu\bar{\nu}$ decays are, thus, essentially free of hadronic uncertainties.[5]

- Lattice QCD: This computational method is sound, in principle, for hadronic matrix elements with at most one final-state hadron. Limitations in computer power have led to an approximation, called the quenched approximation, whose error is difficult to quantify. With increases in computer resources, lattice results should, in the future, play a more important role in determining the sides of the unitarity triangles. For more details, see Sec.1.5.4.

- Perturbative QCD for exclusive processes: It may be possible to calculate the strong phases of certain nonleptonic B decays using perturbative QCD. This is in some ways analogous to computing cross sections in hadronic collisions, and the nonperturbative information is captured in light-cone distribution amplitudes [20]. There are, at present, two different approaches [21,22], whose practical relevance remains an open question.

- QCD sum rules: Like lattice and perturbative QCD, sum rules are based on QCD and field theory. Uncertainty estimates are usually semi-quantitative and it is difficult to reduce them in a controlled manner.

- Models of QCD, such as quark models, naive factorization, etc: These techniques can be applied for back-of-the-envelope estimates. There is no prospect for providing a quotable error and, thus, should not be used in quantitative work.

In summary, at the present time the cleanest observables are the CP asymmetries in $\overline{B}{}_d^0$ decays to charmonium+kaon and in $\overline{B}{}_s^0$ decays to $D_s^{\pm} K^{\mp}$. The rare decay $K_L \to \pi^0 \nu\bar{\nu}$ is free of theoretical uncertainties at a similar level, but presents a big experimental challenge. Semileptonic decays restricted by symmetries as well as $K^{\pm} \to \pi^{\pm}\nu\bar{\nu}$ are a step down, but still good. With enough computer power to overcome the quenched approximation, lattice QCD could yield, during the course of Run II, controlled uncertainty estimates for neutral-meson mixing and leptonic and semileptonic decays of a few percent.

[4] Here, and in the rest of this chapter, ψ stands for any charmonium state, J/ψ, ψ', χ_c, etc.

[5] In the charged mode there is an uncertainty stemming from the uncertainty in the charmed quark mass. It has been estimated to be around 5% in $|V_{ts}V_{td}|$ [18]. Power suppressed corrections to $K \to \pi\nu\bar{\nu}$ have also been estimated and found to be small [19].

1.3 General Formalism for Mixing and CP Violation

This section is devoted to the general formalism for meson mixing and CP violation. Much of the material can also be found in other review articles and reports [4,5,8], but some topics require a different viewpoint in the light of the B physics program at a hadron collider: unlike the B factories the Tevatron will be able to study B_s^0 mesons. The two mass eigenstates in the B_s^0 system may involve a sizable width difference $\Delta\Gamma$, which must be included in the formulae for the B_s^0 time evolution. We consequently present these formulae including all effects from a non-vanishing $\Delta\Gamma$.

Many details of the formalism depend on conventions, particularly in the choice of the complex phases that unavoidably appear in any CP violating physical system. We would like to discourage the reader from combining formulae from different sources, so we try to give a comprehensive and self-contained presentation of the subject. We start by introducing the discrete transformation C, P and T in Sec. 1.3.1. Experimentally we know that C, P and T are symmetries of the electromagnetic and strong interactions, so the corresponding quantum numbers can be used to classify the hadron states. The description in Sec. 1.3.2 of the time evolution of the neutral B meson system is applicable to both the B_d^0 and the B_s^0 meson systems. Sec. 1.3.3 deals with untagged B^0 decays and Sec. 1.3.4 presents the formulae for CP asymmetries. Finally, in Sec. 1.3.4 we discuss phase conventions and rephasing invariant quantities.

1.3.1 Discrete transformations

In this section we introduce the parity, P, time reversal, T, and charge conjugation, C, transformations. P and T are defined through their action on coordinate vectors $x = (x^0, x^1, x^2, x^3)$: P flips the sign of the spatial coordinates x^1,x^2,x^3 and T changes the time component $t = x^0$ into $-t$. Adopting the convention $g_{\mu\nu} = \mathrm{diag}(1, -1, -1, -1)$ for the Lorentz metric, one can compactly express the transformations in terms of $x_\mu = g_{\mu\nu}x^\nu$:

$$\begin{aligned} P: &\quad x^\mu \to x_\mu\,, \\ T: &\quad x^\mu \to -x_\mu\,. \end{aligned} \tag{1.42}$$

The definition (1.42) implies that the derivative operator $\partial^\mu = \partial/\partial x_\mu$ and the momentum p^μ transform under P and T in the same way as x^μ. Finally, C interchanges particles and anti-particles. Apart from the weak interactions, these transformations are symmetries of the Standard Model. It is therefore convenient to classify hadronic states by their C, P and T quantum numbers, which are multiplicative and take the values ± 1.

The Lagrangian of the Standard Model and its possible extensions contain bilinear currents of the quark fields, to which gauge bosons and scalar fields couple. For example, as discussed in Sec. 1.2, the W boson field W^μ couples to the chiral vector current $\overline{b}_L\gamma_\mu c_L$. Quark bilinears also appear in composite operators which represent the Standard Model interactions in low energy effective Hamiltonians, cf., Sec. 1.5.1. To understand how these interactions work, it is helpful to list the transformation of the quark bilinears under C, P,

current	$\overline{b}_R\, d_L\,(x^\rho)$	$\overline{b}_L\,\gamma_\mu\, d_L\,(x^\rho)$	$\overline{b}_R\,\sigma_{\mu\nu} d_L\,(x^\rho)$
C	$\overline{d}_R\, b_L\,(x^\rho)\,\eta_C$	$-\overline{d}_R\,\gamma_\mu\, b_R(x^\rho)\,\eta_C$	$-\overline{d}_R\,\sigma_{\mu\nu}\, b_L(x^\rho)$
P	$\overline{b}_L\, d_R\,(x_\rho)\,\eta_P$	$\overline{b}_R\,\gamma^\mu\, d_R\,(x_\rho)\,\eta_P$	$\overline{b}_L\,\sigma^{\mu\nu}\, d_R\,(x_\rho)\,\eta_P$
CP	$\overline{d}_L\, b_R\,(x_\rho)\,\eta_C\eta_P$	$-\overline{d}_L\,\gamma^\mu\, b_L\,(x_\rho)\,\eta_C\eta_P$	$-\overline{d}_L\,\sigma^{\mu\nu}\, b_R\,(x_\rho)\,\eta_C\eta_P$
T	$\overline{b}_R\, d_L\,(-x_\rho)\,\eta_T$	$\overline{b}_L\,\gamma^\mu\, d_L\,(-x_\rho)\,\eta_T$	$\overline{b}_R\,\sigma^{\mu\nu}\, d_L\,(-x_\rho)\,\eta_T$
CPT	$\overline{d}_L\, b_R\,(-x^\rho)\,\eta_C\eta_P\eta_T$	$-\overline{d}_L\,\gamma_\mu\, b_L\,(-x^\rho)\,\eta_C\eta_P\eta_T$	$\overline{d}_L\,\sigma_{\mu\nu}\, b_R\,(-x^\rho)\,\eta_C\eta_P\eta_T$

Table 1.1: C, P and T transformation properties of the chiral scalar, vector and magnetic currents. The coordinate x in parentheses is the argument of both quark fields.

T and the combined transformations CP and CPT. For illustration we specify to currents involving a b and a d field. The generic transformation under some discrete symmetry X is

$$X: \qquad \overline{b}\,\Gamma d \;\;\rightarrow\;\; X\,\overline{b}\,\Gamma d\,X^{-1}, \tag{1.43}$$

and Table 1.1 lists the transformation for the chiral scalar, vector and magnetic currents. Here $\sigma_{\mu\nu} = (i/2)[\gamma_\mu, \gamma_\nu]$. The transformation laws for the currents with opposite chirality are obtained by interchanging $L \leftrightarrow R$ in Table 1.1. The phase factors

$$\eta_X = \eta_X^{bd} = e^{i\left(\phi_X^d - \phi_X^b\right)}, \qquad X = C, P, T\,. \tag{1.44}$$

depend on the quark flavors, but for simplicity the flavor indices of the η_Xs have been omitted in Table 1.1. One can absorb these arbitrary phase factors $\exp(i\phi_X^q)$ into the definitions of the discrete transformations for every quark field in the theory. This feature originates from the freedom to redefine any quark field by a phase transformation

$$q \rightarrow q\, e^{i\phi^q}. \tag{1.45}$$

In the absence of flavor-changing couplings the change in (1.45) is a $U(1)$ symmetry transformation leaving the Lagrangian invariant. The corresponding conserved quantum number is the flavor of the quark q. After including the flavor-changing interactions, the phase transformations in (1.45) change the phases of the flavor-changing couplings. The flavor symmetry is broken and every phase transformation (1.45) leads to a different, but physically equivalent Lagrangian. In the case of the Standard Model these transform the Yukawa couplings and, hence, the CKM matrix from one phase convention into another.

The currents in Table 1.1 create and destroy the meson states with the appropriate quantum numbers. Since the QCD interaction, which binds the quarks into mesons, conserves C, P and T, the meson states transform like the corresponding currents in Table 1.1. For example, the B_d meson is pseudoscalar and transforms under CP as

$$\begin{aligned} CP\,|\overline{B}_d^0\,(P^\rho)\rangle &= -\eta_P^{bd}\,\eta_C^{bd}\,|B_d^0\,(P_\rho)\rangle\,, \\ CP\,|B_d^0\,(P^\rho)\rangle &= -\eta_P^{bd*}\eta_C^{bd*}\,|\overline{B}_d^0\,(P_\rho)\rangle\,. \end{aligned} \tag{1.46}$$

	photon, gluon, Z boson	W boson	Higgs
field	$V^\mu(x^\rho) = A^\mu(x^\rho), A^{\mu,a}(x^\rho), Z^\mu(x^\rho)$	$W^{\pm,\mu}(x^\rho)$	$H(x^\rho)$
C	$-V^\mu(x^\rho)$	$-W^{\mp,\mu}(x^\rho)$	$H(x^\rho)$
P	$V_\mu(x_\rho)$	$W^\pm_\mu(x_\rho)$	$H(x_\rho)$
CP	$-V_\mu(x_\rho)$	$-W^\mp_\mu(x_\rho)$	$H(x_\rho)$
T	$V_\mu(-x_\rho)$	$W^\pm_\mu(-x_\rho)$	$H(-x_\rho)$
CPT	$-V^\mu(-x^\rho)$	$-W^{\mp,\mu}(-x^\rho)$	$H(-x^\rho)$

Table 1.2: C, $P$and T transformation properties of bosons in the Standard Model.

The vacuum state $|0\rangle$ is invariant under C, P and T. Hence one finds, for example,

$$\langle 0|\,\overline{b}\gamma_\mu\gamma_5 d(x)\,|B^0_d(P)\rangle \stackrel{CP}{=} \langle 0|\,\overline{d}\gamma_\mu\gamma_5 b(x)\,|\overline{B}^0_d(P)\rangle = if_{B_d}P_\mu e^{-iP\cdot x}\,, \tag{1.47}$$

which is the definition of the B meson decay constant f_{B_d}. The phases $\eta^{bd}_P\eta^{bd}_C$ from the CP transformation of the pseudovector current $\overline{b}\gamma_\mu\gamma_5 d = \overline{b}_R\gamma_\mu d_R - \overline{b}_L\gamma_\mu d_L$ and $\eta^{bd*}_P\eta^{bd*}_C$ from (1.46) cancel in the first relation in (1.47). We can further multiply $|B^0_d(P)\rangle$ and $|\overline{B}^0_d(P)\rangle$ by another common phase factor (unrelated to CP) to choose f_{B_d} positive.

Although C and P are unitary transformations, T is anti-unitary (i.e., $T^\dagger T = 1$ and $\langle T\phi|T\psi\rangle = \langle\psi|\phi\rangle$). Thus, for example,

$$T\,|B^0_d(P^\rho)\rangle = \langle B^0_d(-P_\rho)|\,. \tag{1.48}$$

The anti-unitary property of T means also that c-numbers, such as the CKM matrix, are transformed into their complex conjugates.

Table 1.2 lists the transformation properties of the vector bosons and the scalar Higgs field H appearing in the Standard Model. The transformation properties of the photon and gluon field are deduced from the experimental observation that QED and QCD conserve C, P and Tquantum numbers. For the weak gauge bosons the absence of CP and T violation in the gauge sector fixes the transformation properties of $W^{\pm,\mu}$ and Z^μ under CP and T. The assignment of the C and P transformations to the weak gauge bosons and the Higgs in Table 1.2 is chosen such that the Standard Model conserves C and P in the absence of fermion fields. These assignments do not impose additional selection rules on the Standard Model interactions and therefore have no observable consequences.

From Table 1.1 one can see why the weak interaction in the Standard Model violates C and P. These transformations flip the chirality of the quark fields, but left- and right-handed fields belong to different representations of the $SU(2)$ gauge group. The combined transformation CP, however, maps the quark fields onto fields with the same chirality. Still, the currents and their CP conjugates (i.e., the first and fourth rows of Table 1.1) are not identical: instead they are Hermitian conjugates of each other. Since the Lagrangian of any quantm field theory is Hermitian, it contains for each coupling of a quark current to a vector field its Hermitian conjugate coupling as well. For example, the coupling of the W

to b and u quarks in the Standard Model is

$$\mathcal{L} = -\frac{g_2}{\sqrt{2}} \left[V_{ub}\, \overline{u}_L\, \gamma^\mu b_L\, W_\mu^+ + V_{ub}^*\, \overline{b}_L\, \gamma^\mu u_L\, W_\mu^- \right]. \tag{1.49}$$

From Tables 1.1 and 1.2 one derives the CP transformation

$$CP\, \mathcal{L}\, (CP)^{-1} = -\frac{g_2}{\sqrt{2}} \left[V_{ub}\, \overline{b}_L\, \gamma^\mu u_L\, W_\mu^- + V_{ub}^*\, \overline{u}_L\, \gamma^\mu b_L\, W_\mu^+ \right], \tag{1.50}$$

which is the same only if $V_{ub} = V_{ub}^*$. This illuminates why CP violation is related to complex phases in couplings. Yet complex couplings alone are not sufficient for a theory to violate CP. A phase rotation (1.45) of the quark fields in the CP transformed Lagrangian changes the phases of the couplings. If we can in this way rotate the phases in $CP\, \mathcal{L}\, (CP)^{-1}$ back into those in $\mathcal{L}$, then CP is conserved. In our example (1.49) the choice $\phi^b - \phi^u = 2 \arg V_{ub}$ would transform $CP\, \mathcal{L}\, (CP)^{-1}$ back into $\mathcal{L}$. As outlined in Sec. 1.2, Kobayashi and Maskawa realized that it is not possible to remove all the phases, once there are more than two quark generations [11].

It is also illustrative to apply the time reversal transformation to (1.49). It does not modify the currents, but, due to its anti-unitary character, it flips the phases of the couplings and thereby leads to the same result as the CP transformation. In our example we have disregarded the changes in the arguments x^ρ of the fields shown in (1.42). Since physical observables depend on the action, $S = \int \mathrm{d}^4x\, \mathcal{L}(x)$, rather than on $\mathcal{L}$, the sign of x^ρ can be absorbed into a change of the integration variables.

From Table 1.1 and Table 1.2 one can verify that the action of the Standard Model is invariant under the combined transformation CPT. The CPT transformation simply turns the currents and the vector fields into their Hermitian conjugates. Due to $\mathcal{L} = \mathcal{L}^\dagger$ one has

$$S = \int \mathrm{d}^4x\, \mathcal{L}(x) = \int \mathrm{d}^4x'\, \mathcal{L}(-x') = \int \mathrm{d}^4x'\, CPT\, \mathcal{L}(x')\, (CPT)^{-1} = CPT\, S\, (CPT)^{-1}. \tag{1.51}$$

This *CPT theorem* holds in any local Poincaré invariant quantum field theory [23]. It implies that particles and antiparticles have the same masses and total decay widths. In certain string theories CPT violation may be possible, and at low energies manifests itself in the violation of Poincaré invariance or of quantum mechanics [24]. In the standard framework of quantum field theory, however, the CPT theorem is built in from the very beginning. For example, the Feynman diagram for any decay or scattering process and its CPT conjugate diagram are simply related by complex conjugation and give the same result for the decay rate or cross section. Unless stated otherwise it is always assumed that CPT invariance holds in all the formulae in this report. In this context it is meaningless to distinguish CP violation and T violation.

1.3.2 Time evolution and mixing

In this section we list the necessary formulae to describe $B_d^0 - \overline{B}_d^0$ mixing and $B_s^0 - \overline{B}_s^0$ mixing. The formulae are general and apply to both B_d^0 and to B_s^0 mesons, although with different values of the parameters. Eqs. (1.52)–(1.62) are even correct for $K^0 - \overline{K}^0$ mixing

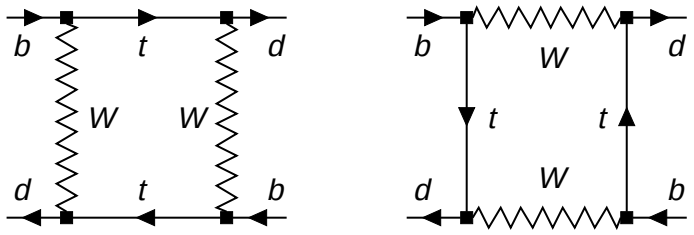

Figure 1.2: Standard Model box diagrams inducing $B^0_d - \overline{B}^0_d$ mixing.

and $D^0 - \overline{D}^0$ mixing. In the following, the notation B^0 represents either of the two neutral B meson species with the standard convention that B^0 ($\overline{B}^0$) contains a $\overline{b}$ antiquark (a b quark).

$B^0 - \overline{B}^0$ mixing refers to transitions between the two flavor eigenstates $|B^0\rangle$ and $|\overline{B}^0\rangle$. In the Standard Model $B^0 - \overline{B}^0$ mixing is caused by the fourth order flavor-changing weak interaction described by the box diagrams in Fig. 1.2. Such transitions are called $|\Delta B| = 2$ transitions, because they change the bottom quantum number by two units. In the Standard Model $|\Delta B| = 2$ amplitudes are small, so measurements of $B^0 - \overline{B}^0$ mixing could easily be sensitive to new physics.

$B^0 - \overline{B}^0$ mixing induces oscillations between B^0 and $\overline{B}^0$. An initially produced B^0 or $\overline{B}^0$ evolves in time into a superposition of B^0 and $\overline{B}^0$. Let $|B^0(t)\rangle$ denote the state vector of a B meson which is tagged as a B^0 at time $t = 0$, i.e., $|B^0(t=0)\rangle = |B^0\rangle$. Likewise $|\overline{B}^0(t)\rangle$ represents a B meson initially tagged as a $\overline{B}^0$. The time evolution of these states is governed by a Schrödinger equation:

$$i\,\frac{\mathrm{d}}{\mathrm{d}\,t}\left(\begin{array}{c}|B(t)\rangle\\ |\overline{B}(t)\rangle\end{array}\right) = \left(M - i\,\frac{\Gamma}{2}\right)\left(\begin{array}{c}|B(t)\rangle\\ |\overline{B}(t)\rangle\end{array}\right). \tag{1.52}$$

The *mass matrix* M and the *decay matrix* Γ are t-independent, Hermitian 2×2 matrices. CPT invariance implies that

$$M_{11} = M_{22}\,, \qquad\qquad \Gamma_{11} = \Gamma_{22}\,. \tag{1.53}$$

$|\Delta B| = 2$ transitions induce non-zero off-diagonal elements in (1.52), so that the mass eigenstates of the neutral B meson are different from the flavor eigenstates $|B^0\rangle$ and $|\overline{B}^0\rangle$. The mass eigenstates are defined as the eigenvectors of $M - i\,\Gamma/2$. We express them in terms of the flavor eigenstates as

$$\begin{aligned}\text{Lighter eigenstate:}\quad & |B_L\rangle = p|B^0\rangle + q|\overline{B}^0\rangle\,,\\ \text{Heavier eigenstate:}\quad & |B_H\rangle = p|B^0\rangle - q|\overline{B}^0\rangle\,,\end{aligned} \tag{1.54}$$

with $|p|^2 + |q|^2 = 1$. Note that, in general, $|B_L\rangle$ and $|B_H\rangle$ are not orthogonal to each other.

The time evolution of the mass eigenstates is governed by the two eigenvalues $M_H - i\,\Gamma_H/2$ and $M_L - i\,\Gamma_L/2$:

$$|B_{H,L}(t)\rangle = e^{-(iM_{H,L}+\Gamma_{H,L}/2)t}\,|B_{H,L}\rangle\,, \tag{1.55}$$

where $|B_{H,L}\rangle$ (without the time argument) denotes the mass eigenstates at time $t = 0$: $|B_{H,L}\rangle = |B_{H,L}(t=0)\rangle$. We adopt the following definitions for the average mass and width and the mass and width differences of the B meson eigenstates:

$$\begin{aligned} m &= \frac{M_H + M_L}{2} = M_{11}\,, & \Gamma &= \frac{\Gamma_L + \Gamma_H}{2} = \Gamma_{11}\,, \\ \Delta m &= M_H - M_L\,, & \Delta\Gamma &= \Gamma_L - \Gamma_H\,. \end{aligned} \tag{1.56}$$

Δm is positive by definition. Note that the sign convention for $\Delta\Gamma$ is opposite to the one used in Refs. [4–6,8]. In our convention the Standard Model prediction for $\Delta\Gamma$ is positive.

We can find the time evolution of $|B(t)\rangle$ and $|\overline{B}(t)\rangle$ as follows. We first invert (1.54) to express $|B^0\rangle$ and $|\overline{B}^0\rangle$ in terms of the mass eigenstates and using their time evolution in (1.55):

$$\begin{aligned} |B^0(t)\rangle &= \frac{1}{2p}\left[e^{-iM_L t-\Gamma_L t/2}\,|B_L\rangle \;+\; e^{-iM_H t-\Gamma_H t/2}\,|B_H\rangle\right], \\ |\overline{B}^0(t)\rangle &= \frac{1}{2q}\left[e^{-iM_L t-\Gamma_L t/2}\,|B_L\rangle \;-\; e^{-iM_H t-\Gamma_H t/2}\,|B_H\rangle\right]. \end{aligned} \tag{1.57}$$

These expressions will be very useful in the discussion of B_s mixing.[6] With (1.54) we next eliminate the mass eigenstates in (1.57) in favor of the flavor eigenstates:

$$\begin{aligned} |B^0(t)\rangle &= \quad g_+(t)\,|B^0\rangle + \frac{q}{p}\,g_-(t)\,|\overline{B}^0\rangle\,, \\ |\overline{B}^0(t)\rangle &= \frac{p}{q}\,g_-(t)\,|B^0\rangle + \quad g_+(t)\,|\overline{B}^0\rangle\,, \end{aligned} \tag{1.58}$$

where

$$\begin{aligned} g_+(t) &= e^{-imt}\,e^{-\Gamma t/2}\left[\quad \cosh\frac{\Delta\Gamma\, t}{4}\,\cos\frac{\Delta m\, t}{2} - i\sinh\frac{\Delta\Gamma\, t}{4}\,\sin\frac{\Delta m\, t}{2}\right], \\ g_-(t) &= e^{-imt}\,e^{-\Gamma t/2}\left[-\sinh\frac{\Delta\Gamma\, t}{4}\,\cos\frac{\Delta m\, t}{2} + i\cosh\frac{\Delta\Gamma\, t}{4}\,\sin\frac{\Delta m\, t}{2}\right]. \end{aligned} \tag{1.59}$$

Note that—owing to $\Delta\Gamma \neq 0$—the coefficient $g_+(t)$ has no zeros, and $g_-(t)$ vanishes only at $t = 0$. Hence an initially produced B^0 will never turn into a pure $\overline{B}^0$ or back into a pure B^0. The coefficients in (1.59) will enter the formulae for the decay asymmetries in the combinations

$$\begin{aligned} |g_\pm(t)|^2 &= \frac{e^{-\Gamma t}}{2}\left[\cosh\frac{\Delta\Gamma\, t}{2} \pm \cos\left(\Delta m\, t\right)\right], \\ g_+^*(t)\,g_-(t) &= \frac{e^{-\Gamma t}}{2}\left[-\sinh\frac{\Delta\Gamma\, t}{2} + i\sin\left(\Delta m\, t\right)\right]. \end{aligned} \tag{1.60}$$

[6] The Schrödinger equation, (1.52), is not exactly valid, but the result of the so-called *Wigner-Weisskopf approximation* [25] to the decay problem. In general, there are tiny corrections to the exponential decay laws in (1.57) at very short and very large times [26]. These corrections are irrelevant for the mixing and CP studies at Run II, but they must be taken into account in high precision searches for CPT violation [27].

In a given theory, such as the Standard Model, one can calculate the off-diagonal elements M_{12} and Γ_{12} entering (1.52) from $|\Delta B|=2$ diagrams. In order to exploit the formulae (1.57)–(1.59) for the time evolution we still need to express Δm, $\Delta\Gamma$ and q/p in terms of M_{12} and Γ_{12}. By solving for the eigenvalues and eigenvectors of $M - i\,\Gamma/2$ one finds

$$(\Delta m)^2 - \frac{1}{4}\,(\Delta\Gamma)^2 \;= 4\,|M_{12}|^2 - |\Gamma_{12}|^2\;, \tag{1.61a}$$

$$\Delta m\,\Delta\Gamma = -4\,\mathrm{Re}\,(M_{12}\Gamma_{12}^*)\,, \tag{1.61b}$$

$$\frac{q}{p} = -\frac{\Delta m + i\,\Delta\Gamma/2}{2M_{12} - i\,\Gamma_{12}} = -\frac{2M_{12}^* - i\,\Gamma_{12}^*}{\Delta m + i\,\Delta\Gamma/2}\,. \tag{1.61c}$$

The relative phase between M_{12} and Γ_{12} appears in many observables related to B mixing. We introduce

$$\phi = \arg\left(-\frac{M_{12}}{\Gamma_{12}}\right). \tag{1.62}$$

Now one can solve (1.61) for Δm and $\Delta\Gamma$ in terms of $|M_{12}|$, $|\Gamma_{12}|$ and ϕ.

The general solution is not illuminating, but a simple, approximate solution may be derived when

$$|\Gamma_{12}| \ll |M_{12}|\;, \qquad \text{and} \qquad \Delta\Gamma \ll \Delta m\,. \tag{1.63}$$

These inequalities hold (empirically) for both B^0 systems. We first note that $|\Gamma_{12}| \le \Gamma$ always, because Γ_{12} stems from the decays into final states common to B^0 and $\overline{B}^0$. For the B_s^0 meson the lower bound on Δm_{B_s} establishes experimentally that $\Gamma_{B_s} \ll \Delta m_{B_s}$. Hence $\Gamma_{12}^s \ll \Delta m_{B_s}$, and Eqs. (1.61a) and (1.61b) imply $\Delta m_{B_s} \approx 2|M_{12}^s|$ and $|\Delta\Gamma_{B_s}| \le 2|\Gamma_{12}^s|$, so that (1.63) holds. For the B_d^0 meson the experiments give $\Delta m_{B_d} \approx 0.75\,\Gamma_{B_d}$. The Standard Model predicts $|\Gamma_{12}^d|/\Gamma_{B_d} = \mathcal{O}(1\%)$, but Γ_{12}^d stems solely from CKM-suppressed decay channels (common to B_d^0 and $\overline{B}_d^0$) and could therefore be affected by new physics. New decay channels would, however, also increase Γ_{B_d} and potentially conflict with the precisely measured semileptonic branching ratio. A conservative estimate is $|\Gamma_{12}^d|/\Gamma_{B_d} < 10\%$. Hence for both the B_s^0 and B_d^0 system an expansion in Γ_{12}/M_{12} and $\Delta\Gamma/\Delta m$ is a good approximation, and we easily find

$$\Delta m = 2\,|M_{12}|\left[1 + \mathcal{O}\left(\left|\frac{\Gamma_{12}}{M_{12}}\right|^2\right)\right], \tag{1.64a}$$

$$\Delta\Gamma = 2\,|\Gamma_{12}|\cos\phi\left[1 + \mathcal{O}\left(\left|\frac{\Gamma_{12}}{M_{12}}\right|^2\right)\right]. \tag{1.64b}$$

We also need an approximate expression for q/p in (1.61). It is convenient to define a small parameter

$$a = \mathrm{Im}\,\frac{\Gamma_{12}}{M_{12}} = \left|\frac{\Gamma_{12}}{M_{12}}\right|\sin\phi\,, \tag{1.65}$$

because occasionally we need to keep terms of order a. Then q/p becomes

$$\frac{q}{p} = -e^{-i\phi_M}\left[1 - \frac{a}{2}\right] + \mathcal{O}\left(\left|\frac{\Gamma_{12}}{M_{12}}\right|^2\right), \tag{1.66}$$

where ϕ_M is the phase of M_{12},

$$M_{12} = |M_{12}|\, e^{i\phi_M}\,. \tag{1.67}$$

Note that (1.66) and the normalization condition $|p|^2 + |q|^2 = 1$ imply

$$|p| = \frac{1}{\sqrt{2}}\left(1 + \frac{a}{4}\right) + \mathcal{O}\left(\left|\frac{\Gamma_{12}}{M_{12}}\right|^2\right), \qquad |q| = \frac{1}{\sqrt{2}}\left(1 - \frac{a}{4}\right) + \mathcal{O}\left(\left|\frac{\Gamma_{12}}{M_{12}}\right|^2\right). \tag{1.68}$$

We are now prepared to exhibit the time-dependent decay rate $\Gamma(B^0(t) \to f)$ of an initially tagged B^0 into some final state f. It is defined as

$$\Gamma(B^0(t) \to f) = \frac{1}{N_B}\,\frac{\mathrm{d}N(B^0(t) \to f)}{\mathrm{d}t}\,, \tag{1.69}$$

where $\mathrm{d}N(B^0(t) \to f)$ denotes the number of decays of a B meson tagged as a B^0 at $t = 0$ into the final state f occurring within the time interval between t and $t + \mathrm{d}t$. N_B is the total number of B^0's produced at time $t = 0$. An analogous definition holds for $\Gamma(\overline{B}^0(t) \to f)$. One has

$$\Gamma(B^0(t) \to f) = \mathcal{N}_f \left|\langle f|B^0(t)\rangle\right|^2, \qquad \Gamma(\overline{B}^0(t) \to f) = \mathcal{N}_f \left|\langle f|\overline{B}^0(t)\rangle\right|^2. \tag{1.70}$$

Here $\mathcal{N}_f$ is a time-independent normalization factor. To calculate $\Gamma(B^0(t) \to f)$ we introduce the two decay amplitudes

$$A_f = \langle f|B^0\rangle\,, \qquad\qquad \overline{A}_f = \langle f|\overline{B}^0\rangle\,, \tag{1.71}$$

and the quantity

$$\lambda_f = \frac{q}{p}\,\frac{\overline{A}_f}{A_f} \simeq -e^{-i\phi_M}\,\frac{\overline{A}_f}{A_f}\,\left[1 - \frac{a}{2}\right]. \tag{1.72}$$

We will see in the following sections that λ_f plays the pivotal role in CP asymmetries and other observables in B mixing. Finally with (1.58), (1.60) and $|p/q|^2 = (1 + a)$ we find the desired formulae for the decay rates:

$$\begin{aligned}\Gamma(B^0(t) \to f) = \mathcal{N}_f\,|A_f|^2\, e^{-\Gamma t}\Bigg\{&\frac{1 + |\lambda_f|^2}{2}\,\cosh\frac{\Delta\Gamma\, t}{2} + \frac{1 - |\lambda_f|^2}{2}\,\cos(\Delta m\, t)\\ &-\mathrm{Re}\,\lambda_f\,\sinh\frac{\Delta\Gamma\, t}{2} - \mathrm{Im}\,\lambda_f\,\sin(\Delta m\, t)\Bigg\},\end{aligned} \tag{1.73}$$

$$\begin{aligned}\Gamma(\overline{B}^0(t) \to f) = \mathcal{N}_f\,|A_f|^2\,(1 + a)\, e^{-\Gamma t}\Bigg\{&\frac{1 + |\lambda_f|^2}{2}\,\cosh\frac{\Delta\Gamma\, t}{2} - \frac{1 - |\lambda_f|^2}{2}\,\cos(\Delta m\, t)\\ &-\mathrm{Re}\,\lambda_f\,\sinh\frac{\Delta\Gamma\, t}{2} + \mathrm{Im}\,\lambda_f\,\sin(\Delta m\, t)\Bigg\}.\end{aligned} \tag{1.74}$$

Next we consider the decay into $\overline{f}$, which denotes the CP conjugate state to f,

$$|\overline{f}\rangle = CP\,|f\rangle\,. \tag{1.75}$$

For example, for $f = D_s^- \pi^+$ the CP conjugate state is $\overline{f} = D_s^+ \pi^-$. The decay rate into $\overline{f}$ can be obtained from (1.73) and (1.74) by simply replacing f with $\overline{f}$. Yet $|A_{\overline{f}}|$ and $|A_f|$ are unrelated, unless f is a CP eigenstate, fulfilling $|\overline{f}\rangle = \pm|f\rangle$. On the other hand the CP transformation relates $|\overline{A}_{\overline{f}}|$ to $|A_f|$, so it is more useful to factor out $|\overline{A}_{\overline{f}}|$,

$$\Gamma(B^0(t) \to \overline{f}) = \mathcal{N}_f \left|\overline{A}_{\overline{f}}\right|^2 e^{-\Gamma t} (1-a) \left\{ \frac{1+|\lambda_{\overline{f}}|^{-2}}{2} \cosh\frac{\Delta\Gamma\, t}{2} - \frac{1-|\lambda_{\overline{f}}|^{-2}}{2} \cos(\Delta m\, t) \right.$$
$$\left. -\mathrm{Re}\,\frac{1}{\lambda_{\overline{f}}} \sinh\frac{\Delta\Gamma\, t}{2} + \mathrm{Im}\,\frac{1}{\lambda_{\overline{f}}} \sin(\Delta m\, t) \right\}, \tag{1.76}$$

$$\Gamma(\overline{B}^0(t) \to \overline{f}) = \mathcal{N}_f \left|\overline{A}_{\overline{f}}\right|^2 e^{-\Gamma t} \left\{ \frac{1+|\lambda_{\overline{f}}|^{-2}}{2} \cosh\frac{\Delta\Gamma\, t}{2} + \frac{1-|\lambda_{\overline{f}}|^{-2}}{2} \cos(\Delta m\, t) \right.$$
$$\left. -\mathrm{Re}\,\frac{1}{\lambda_{\overline{f}}} \sinh\frac{\Delta\Gamma\, t}{2} - \mathrm{Im}\,\frac{1}{\lambda_{\overline{f}}} \sin(\Delta m\, t) \right\}. \tag{1.77}$$

Here we set $\mathcal{N}_{\overline{f}} = \mathcal{N}_f$, because these normalization factors arise from kinematics. In Eqs. (1.73)–(1.77) we consistently keep terms of order a, which appear explicitly in the prefactor in (1.74), (1.76) and are implicit in λ_f through (1.72).[7]

We now apply the derived formalism to the decay rate into a *flavor-specific* final state f meaning that a B^0 can decay into f, while $\overline{B}^0$ cannot. Examples are $f = D_s^- \pi^+$ (from B_s^0) and $f = X\ell^+\nu_\ell$. In such decays $\overline{A}_f = A_{\overline{f}} = 0$ by definition and, hence, $\lambda_f = 1/\lambda_{\overline{f}} = 0$. Therefore,

$$\Gamma(B^0(t) \to f) = \mathcal{N}_f\ |A_f|^2\ e^{-\Gamma t}\, \frac{1}{2} \left[\cosh\frac{\Delta\Gamma\, t}{2} + \cos(\Delta m\, t)\right] \qquad \text{for } \overline{A}_f = 0\,, \tag{1.78}$$

$$\Gamma(B^0(t) \to \overline{f}) = \mathcal{N}_f\ \left|\overline{A}_{\overline{f}}\right|^2\ (1-a)\, e^{-\Gamma t}\, \frac{1}{2} \left[\cosh\frac{\Delta\Gamma\, t}{2} - \cos(\Delta m\, t)\right] \quad \text{for } A_{\overline{f}} = 0\,. \tag{1.79}$$

Flavor-specific decays can be used to measure Δm via the asymmetry in decays from mixed and unmixed Bs:

$$\mathcal{A}_0(t) = \frac{\Gamma(B^0(t) \to f) - \Gamma(B^0(t) \to \overline{f})}{\Gamma(B^0(t) \to f) + \Gamma(B^0(t) \to \overline{f})}\,. \tag{1.80}$$

The amplitudes A_f and $\overline{A}_{\overline{f}}$ are related to each other by CP conjugation. If there is no CP violation in the decay amplitude (i.e., no *direct CP violation*), $|A_f|$ and $|\overline{A}_{\overline{f}}|$ are equal. This is the case for decays like $B_s \to D_s^- \pi^+$ and $B \to X\ell^+\nu_\ell$ conventionally used to measure Δm. Then the mixing asymmetry in (1.80) reads

$$\mathcal{A}_0(t) = \frac{\cos(\Delta m\, t)}{\cosh(\Delta\Gamma\, t/2)} + \frac{a}{2} \left[1 - \frac{\cos^2(\Delta m\, t)}{\cosh^2(\Delta\Gamma\, t/2)}\right], \tag{1.81}$$

where we have allowed for a non-zero width difference.

[7] We have omitted terms of order $|\Gamma_{12}/M_{12}|^2$ in Eqs. (1.72)–(1.77) and will do this throughout the report. In most applications one can set a to zero and often also $\Delta\Gamma$ can be neglected, so that the expressions in Eqs. (1.73)–(1.77) simplify considerably.

1.3.3 Time evolution of untagged B^0 mesons

Since B^0's and $\overline{B}^0$'s are produced in equal numbers at the Tevatron, the untagged decay rate for the decay $\stackrel{(}{B}\stackrel{)}{\to} f$ reads

$$\begin{aligned}\Gamma[f,t] &= \Gamma(B^0(t)\to f) + \Gamma(\overline{B}^0(t)\to f) \\ &= \mathcal{N}_f\,|A_f|^2\left(1+|\lambda_f|^2\right)e^{-\Gamma t}\left[\cosh\frac{\Delta\Gamma\, t}{2} + \sinh\frac{\Delta\Gamma t}{2}\,A_{\Delta\Gamma}\right] + \mathcal{O}(a)\end{aligned} \tag{1.82}$$

with

$$A_{\Delta\Gamma} = -\frac{2\,\mathrm{Re}\,\lambda_f}{1+|\lambda_f|^2}\,. \tag{1.83}$$

From this equation one realizes that untagged samples are interesting for the determination of $\Delta\Gamma$. The fit of an untagged decay distribution to (1.82) involves the overall normalization factor $\mathcal{N}_f\,|A_f|^2\,(1+|\lambda_f|^2)$. From (1.69) one realizes that by integrating $\Gamma[f,t]$ over all times one obtains the branching ratio for the decay of an untagged B^0 into the final state f:

$$\begin{aligned}\mathcal{B}(\stackrel{(}{B}\stackrel{)}{\to} f\,) = \frac{1}{2}\int_0^\infty \mathrm{d}t\,\Gamma[f,t] \;&= \frac{\mathcal{N}_f}{2}\,|A_f|^2\,\frac{\Gamma\,(1+|\lambda_f|^2) - \Delta\Gamma\,\mathrm{Re}\,\lambda_f}{\Gamma^2-(\Delta\Gamma/2)^2} + \mathcal{O}(a) \\ &= \frac{\mathcal{N}_f}{2}\,|A_f|^2\left(1+|\lambda_f|^2\right)\frac{1}{\Gamma}\left[1+\frac{\Delta\Gamma}{2\Gamma}\,A_{\Delta\Gamma} + \mathcal{O}\left(\frac{(\Delta\Gamma)^2}{\Gamma^2}\right)\right].\end{aligned} \tag{1.84}$$

Relation (1.84) allows to eliminate $\mathcal{N}_f\,|A_f|^2\,[1+|\lambda_f|^2]$ from (1.82), if the branching ratio is known. If both $\mathcal{B}\,(\stackrel{(}{B}\stackrel{)}{\to} f)$ and $\Delta\Gamma$ are known, a one-parameter fit to the measured untagged time evolution (1.82) allows to determine $A_{\Delta\Gamma}$, which is of key interest for CP studies.

Finally we write down a more intuitive expression for $\Gamma[f,t]$. From (1.70) and (1.57) one immediately finds

$$\Gamma[f,t] = \mathcal{N}_f\left[e^{-\Gamma_L t}\,|\langle f|B_L\rangle|^2 + e^{-\Gamma_H t}\,|\langle f|B_H\rangle|^2\right] + \mathcal{O}(a)\,. \tag{1.85}$$

With (1.54) one recovers (1.82) from (1.85). Now (1.85) nicely shows that the decay of the untagged sample into some final state f is governed by two exponentials. If B_s mixing is correctly described by the Standard Model, the mass eigenstates $|B_L\rangle$ and $|B_H\rangle$ are to a high precision also CP eigenstates and (1.85) proves useful for the description of decays into CP eigenstates.

1.3.4 Time-dependent and time-integrated CP asymmetries

The CP asymmetry for the decay of a charged B into the final state f reads

$$a_f = \frac{\Gamma(B^-\to f) - \Gamma(B^+\to \overline{f})}{\Gamma(B^-\to f) + \Gamma(B^+\to \overline{f})} \qquad \text{with } \; |\overline{f}\rangle = CP\,|f\rangle. \tag{1.86}$$

Defining

$$A_f = \langle f|B^+\rangle \qquad \text{and} \qquad \overline{A}_{\overline{f}} = \langle \overline{f}|B^-\rangle \tag{1.87}$$

in analogy to (1.71) one finds

$$a_f = -\frac{1-\left|\overline{A}_{\overline{f}}/A_f\right|^2}{1+\left|\overline{A}_{\overline{f}}/A_f\right|^2}\,. \tag{1.88}$$

Since charged B mesons cannot mix, a non-zero a_f can only occur through CP violation in the $|\Delta B|=1$ matrix elements A_f and $\overline{A}_{\overline{f}}$. This is called *direct* CP violation and stems from $|A_f| \neq |\overline{A}_{\overline{f}}|$.

Next we consider the decay of a neutral B meson into a CP eigenstate $f = f_{CP} = \eta_f \overline{f}$. Here $\eta_f = \pm 1$ is the CP quantum number of f. An example for this situation is the decay $B_s^0 \to D_s^+ D_s^-$, where $\eta_f = +1$. We define the time-dependent CP asymmetry as

$$a_f(t) = \frac{\Gamma(\overline{B}^0(t)\to f) - \Gamma(B^0(t)\to f)}{\Gamma(\overline{B}^0(t)\to f) + \Gamma(B^0(t)\to f)}\,. \tag{1.89}$$

Using (1.73) and (1.74) one finds

$$a_f(t) = -\frac{A_{CP}^{\rm dir}\cos(\Delta m\, t) + A_{CP}^{\rm mix}\sin(\Delta m\, t)}{\cosh(\Delta\Gamma\, t/2) + A_{\Delta\Gamma}\sinh(\Delta\Gamma\, t/2)} + \mathcal{O}(a)\,, \tag{1.90}$$

where $A_{\Delta\Gamma}$ is defined in (1.83), and the *direct* and *mixing-induced* (or *interference type*) CP asymmetries are

$$A_{CP}^{\rm dir} = \frac{1-|\lambda_f|^2}{1+|\lambda_f|^2}\,, \qquad A_{CP}^{\rm mix} = -\frac{2\,{\rm Im}\,\lambda_f}{1+|\lambda_f|^2}\,, \tag{1.91}$$

$A_{CP}^{\rm mix}$ stems from the interference of the decay amplitudes of the unmixed and the mixed B, i.e., of $\overline{B}^0 \to f$ and $B^0 \to f$. It is discussed in more detail in Sec. 1.4.1. Note that the quantities in (1.91) and (1.83) are not independent, $|A_{CP}^{\rm dir}|^2 + |A_{CP}^{\rm mix}|^2 + |A_{\Delta\Gamma}|^2 = 1$.

The time integrated asymmetry reads[8]

$$a_f^{\rm int} = \frac{\int_0^\infty {\rm d}t\left[\Gamma(\overline{B}^0(t)\to f) - \Gamma(B^0(t)\to f)\right]}{\int_0^\infty {\rm d}t\left[\Gamma(\overline{B}^0(t)\to f) + \Gamma(B^0(t)\to f)\right]} = -\frac{1+y^2}{1+x^2}\,\frac{A_{CP}^{\rm dir} + A_{CP}^{\rm mix}\, x}{1+A_{\Delta\Gamma}\, y}\,. \tag{1.92}$$

Here the quantities x and y are defined as

$$x = \frac{\Delta m}{\Gamma}\,, \qquad y = \frac{\Delta\Gamma}{2\,\Gamma}\,. \tag{1.93}$$

Thus, even without following the time evolution, a measurement of $a_f^{\rm int}$ puts constraints on Δm and $\Delta\Gamma$.

[8] Our sign conventions for the CP asymmetries in (1.86) and (1.89) are opposite to those in [8]. Our definitions of $A_{CP}^{\rm dir}$, $A_{CP}^{\rm mix}$ and $A_{\Delta\Gamma}$ are the same as in [8], taking into account that the quantity $\xi_f^{(q)}$ of [8] equals $-\lambda_f$.

1.3.5 Phase conventions

In Sec. 1.3.1 we learned that there is no unique way to define the CP transformation, because it involves an arbitrary phase factor $\eta_{CP} \equiv \eta_C \eta_P$ (see Table 1.1 and Eq. (1.44)). This arbitrariness stems from the fact that phases of quark fields are unobservable and phase redefinitions as in (1.45) transform the Lagrangian into a physically equivalent one. This feature implies that the phases of the flavor-changing couplings in our Lagrangian are not fixed and the phase rotation (1.45) transforms one phase convention for these couplings into another one. Of course, physical observables are independent of these phase conventions. Hence it is worth noting which of the quantities defined in the previous sections are invariant, when η_{CP} or the phases of the quark fields are changed. It is also important to identify the quantities that do depend on phase conventions to avoid mistakes when combining convention dependent quantities into an invariant observable.

The phases of

$$M_{12}\,,\ \Gamma_{12}\,,\ \frac{q}{p}\,,\ \text{and}\ \frac{\overline{A}_f}{A_f}\,. \tag{1.94}$$

depend on the phase convention of the CP transformation or the phase convention of the CP violating couplings. In particular, the phase ϕ_M of the mixing amplitude M_{12} (defined in (1.67)) is convention dependent. When speaking informally, one often says that a given process, such as $B_d^0 \to \psi K_S$, measures the phase of the $|\Delta B|=2$ amplitude, i.e., ϕ_M. Such statements refer to a specific phase convention, in which the decay amplitude of the process has a vanishing (or negligible) phase. The following quantities are independent of phase conventions:

$$\left|\frac{q}{p}\right|\,,\ \left|\frac{\overline{A}_f}{A_f}\right|\,,\ a\,,\ \phi\,,\ \Delta m\,,\ \Delta\Gamma\,,\ \text{and}\ \lambda_f\,. \tag{1.95}$$

The only complex quantity here is λ_f. Its phase is a physical observable.

We have shown that the arbitrary phases accompanying the CP transformation stem from the freedom to rephase the quark fields, see (1.45). The corresponding phase factors η_{CP} in the CP transformed quark bilinears are sufficient to parameterize this arbitrariness and likewise appear in the CP transformations of the mesons and the quantities in (1.94). In some discussions of this issue authors allow for phases different from η_{CP} accompanying the CP transformation (1.46) of the meson states. This is simply equivalent to using our transformation (1.46) followed by a multiplication of $|B_d^0\rangle$ and $|\overline{B}_d^0\rangle$ with extra phase factors (unrelated to CP), which do not affect observables. This would further introduce an extra inconvenient phase into (1.47). The quantities in (1.95) are still invariant under such an extra rephasing and no new information is gained from this generalization. Unless stated otherwise, we will use the phase convention $\eta_{CP} = 1$, i.e.,

$$CP\,|\overline{B}^0(P^\rho)\rangle = -|B^0(P_\rho)\rangle\,, \qquad CP\,|B^0(P^\rho)\rangle = -|\overline{B}^0(P_\rho)\rangle\,. \tag{1.96}$$

For the phases of the CKM elements we use the convention of the Particle Data Group, (1.33).

1.4 Aspects of CP Violation

1.4.1 The three types of CP violation

As discussed in Sec. 1.3.5, there are three phase convention independent physical CP violating observables

$$\left|\frac{q}{p}\right|, \qquad \left|\frac{\overline{A}_{\overline{f}}}{A_f}\right|, \qquad \lambda_f = \frac{q}{p}\frac{\overline{A}_f}{A_f}\,. \tag{1.97}$$

If any one of these quantities is not equal to 1 (or -1 for λ_f), then CP is violated in the particular decay. In fact, there are decays where only one of these types of CP violations occur (to a very good approximation).

CP violation in mixing ($|q/p| \neq 1$)

It follows from Eq. (1.61c) that

$$\left|\frac{q}{p}\right|^2 = \left|\frac{2M_{12}^* - i\,\Gamma_{12}^*}{2M_{12} - i\,\Gamma_{12}}\right|. \tag{1.98}$$

If CP were conserved, then the relative phase between M_{12} and Γ_{12} would vanish, and so $|q/p| = 1$. If $|q/p| \neq 1$, then CP is violated. This is called CP violation in mixing, because it results from the mass eigenstates being different from the CP eigenstates. It follows from Eq. (1.54) that $\langle B_H|B_L\rangle = |p|^2 - |q|^2$, and so the two physical states are orthogonal if and only if CP is conserved in $|\Delta B| = 2$ amplitudes.

The simplest example of this type of CP violation is the neutral meson semileptonic decay asymmetry to "wrong sign" leptons

$$\begin{aligned} a_{\rm sl}(t) &= \frac{\Gamma(\overline{B}^0(t) \to \ell^+\nu X) - \Gamma(B^0(t) \to \ell^-\bar{\nu} X)}{\Gamma(\overline{B}^0(t) \to \ell^+\nu X) + \Gamma(B^0(t) \to \ell^-\bar{\nu} X)} \\ &= \frac{|p/q|^2 - |q/p|^2}{|p/q|^2 + |q/p|^2} = \frac{1 - |q/p|^4}{1 + |q/p|^4} = a + \mathcal{O}(a^2)\,. \end{aligned} \tag{1.99}$$

The second line follows from Eq. (1.58). In B meson decay such an asymmetry is expected to be $\mathcal{O}(10^{-2})$. The calculation of $|q/p| - 1$ involves $\mathrm{Im}\,(\Gamma_{12}/M_{12})$, which suffers from hadronic uncertainties. Thus, it would be difficult to relate the observation of such an asymmetry to CKM parameters. This type of CP violation can also be observed in any decay for which $A_f \gg A_{\overline{f}}$, such as decays to flavor specific final states (for which $A_{\overline{f}} = 0$), e.g., $B_{(s)} \to D^-_{(s)}\pi^+$. In kaon decays this asymmetry was recently measured by CPLEAR [28] in agreement with the expectation that it should be equal to $4\,\mathrm{Re}\,\epsilon_K$.

CP violation in decay ($|\overline{A}_{\overline{f}}/A_f| \neq 1$)

For any final state f, the quantity $|\overline{A}_{\overline{f}}/A_f|$ is a phase convention independent physical observable. There are two types of complex phases which can appear in $\overline{A}_{\overline{f}}$ and A_f defined

in Eq. (1.71). Complex parameters in the Lagrangian which enter a decay amplitude also enter the CP conjugate amplitude but in complex conjugate form. In the Standard Model such parameters only occur in the CKM matrix. These so-called weak phases enter $\overline{A}_{\overline{f}}$ and A_f with opposite signs. Another type of phase can arise even when the Lagrangian is real, from absorptive parts of decay amplitudes. These correspond to on-shell intermediate states rescattering into the desired final state. Such rescattering is usually dominated by strong interactions, and give rise to CP conserving strong phases, which enter $\overline{A}_{\overline{f}}$ and A_f with the same signs. Thus one can write $\overline{A}_{\overline{f}}$ and A_f as

$$A_f = \sum_k A_k \, e^{i(\delta_k + \phi_k)} , \qquad \overline{A}_{\overline{f}} = \sum_k A_k \, e^{i(\delta_k - \phi_k)} , \tag{1.100}$$

where k label the separate contributions to the amplitudes, A_k are the magnitudes of each term, δ_k are the strong phases, and ϕ_k are the weak phases. The individual phases δ_k and ϕ_k are convention dependent, but the phase differences between different terms, $\delta_i - \delta_j$ and $\phi_i - \phi_j$, are physical.

Clearly, if $|\overline{A}_{\overline{f}}/A_f| \neq 1$ then CP is violated. This is called CP violation in decay, or direct CP violation. It occurs due to interference between various terms in the decay amplitude, and requires that at least two terms differ both in their strong and in their weak phases. The simplest example of this is direct CP violation in charged B decays

$$\frac{\Gamma(B^- \to f) - \Gamma(B^+ \to \overline{f})}{\Gamma(B^- \to f) + \Gamma(B^+ \to \overline{f})} = -\frac{1 - |\overline{A}_{\overline{f}}/A_f|^2}{1 + |\overline{A}_{\overline{f}}/A_f|^2} . \tag{1.101}$$

To extract the interesting weak phases from such CP violating observables, one needs to know the amplitudes A_k and their strong phases δ_k. The problem is that theorists do not know how to compute these from first principles, and most estimates are unreliable. The only experimental observation of direct CP violation so far is $\mathrm{Re}\,\epsilon'_K$ in kaon decays.

This type of CP violation can also occur in neutral B decays in conjunction with the others. In such cases direct CP violation is rarely beneficial, and is typically a source of hadronic uncertainties that are hard to control.

CP violation in the interference between decay and mixing ($\lambda_f \neq \pm 1$)

Another type of CP violation is possible in neutral B decay into a CP eigenstate final state, f_{CP}. If CP is conserved, then not only $|q/p| = 1$ and $|\overline{A}_f/A_f| = 1$, but the relative phase between q/p and $\overline{A}_f/A_f$ also vanishes. In this case it is convenient to rewrite

$$\lambda_{f_{CP}} = \frac{q}{p}\frac{\overline{A}_{f_{CP}}}{A_{f_{CP}}} = \eta_{f_{CP}} \frac{q}{p}\frac{\overline{A}_{\overline{f}_{CP}}}{A_{f_{CP}}} , \tag{1.102}$$

where $\eta_{f_{CP}} = \pm 1$ is the CP eigenvalue of f_{CP}. This form of $\lambda_{f_{CP}}$ is useful for calculations, because $A_{f_{CP}}$ and $\overline{A}_{\overline{f}_{CP}}$ are related by CP as discussed in the previous subsection. If $\lambda_{f_{CP}} \neq \pm 1$ then CP is violated. This is called CP violation in the interference between

decays with and without mixing, because it results from the CP violating interference between $B^0 \to f_{CP}$ and $B^0 \to \overline{B}^0 \to f_{CP}$.

As derived in Eq. (1.90), the time dependent asymmetry is

$$\begin{aligned} a_f(t) &= \frac{\Gamma(\overline{B}^0(t) \to f) - \Gamma(B^0(t) \to f)}{\Gamma(\overline{B}^0(t) \to f) + \Gamma(B^0(t) \to f)} \\ &= -\frac{(1-|\lambda_f|^2)\cos(\Delta m\, t) - 2\,\mathrm{Im}\,\lambda_f \sin(\Delta m\, t)}{(1+|\lambda_f|^2)\cosh(\Delta\Gamma\, t/2) - 2\,\mathrm{Re}\,\lambda_f \sinh(\Delta\Gamma\, t/2)} + \mathcal{O}(a)\,. \end{aligned} \tag{1.103}$$

This asymmetry is non-zero if any type of CP violation occurs. In particular, it is possible that $\mathrm{Im}\,\lambda_f \neq 0$, but $|\lambda_f| = 1$ to a good approximation, because $|q/p| \simeq 1$ and $|\overline{A}_f/A_f| \simeq 1$. In both the B_d and B_s systems $|q/p| - 1 \lesssim \mathcal{O}(10^{-2})$. Furthermore, if only one amplitude contributes to a decay, then $|\overline{A}_f/A_f| = 1$ automatically. These modes are "clean", because in such cases A_f drops out and

$$a_f(t) = \frac{\mathrm{Im}\,\lambda_f \sin(\Delta m\, t)}{\cosh(\Delta\Gamma\, t/2) - \mathrm{Re}\,\lambda_f \sinh(\Delta\Gamma\, t/2)}\,, \tag{1.104}$$

measures $\mathrm{Im}\,\lambda_f$, which is given by a weak phase. In addition, if $\Delta\Gamma$ can be neglected then $a_f(t)$ further simplifies to $a_f(t) = \mathrm{Im}\,\lambda_f \sin(\Delta m\, t)$.

The best known example of this type of CP violation (and also the one where $|\lambda_f| = 1$ holds to a very good accuracy) is the asymmetry in $B \to \psi K_S$, where ψ denotes any charmonium state. The decay is dominated by the tree level $b \to c\bar{c}s$ transition and its CP conjugate. In the phase convention (1.96) one finds

$$\frac{\overline{A}_{\psi K_S}}{A_{\psi K_S}} = \left(\frac{V_{cb}V_{cs}^*}{V_{cb}^*V_{cs}}\right)\left(\frac{V_{cs}V_{cd}^*}{V_{cs}^*V_{cd}}\right). \tag{1.105}$$

The overall plus sign arises from (1.96) and because ψK_S is CP odd, $\eta_{\psi K_S} = -1$, and the last factor is $(q/p)^*$ in $K^0 - \overline{K}^0$ mixing. This is crucial, because in the absence of $K^0 - \overline{K}^0$ mixing there could be no interference between $\overline{B}^0 \to \psi\overline{K}^0$ and $B^0 \to \psi K^0$. There are also penguin contributions to this decay, which have different weak and strong phases. These are discussed in detail in Chapter 6, where they are shown to give rise to hadronic uncertainties suppressed by λ^2. Then one finds

$$\lambda_{\psi K_S} = -\left(\frac{V_{tb}^*V_{td}}{V_{tb}V_{td}^*}\right)\left(\frac{V_{cb}V_{cs}^*}{V_{cb}^*V_{cs}}\right)\left(\frac{V_{cs}V_{cd}^*}{V_{cs}^*V_{cd}}\right) = -e^{-2i\beta}\,, \tag{1.106}$$

where the first factor is the Standard Model value of q/p in B_d mixing. Thus, $a_{\psi K_S}(t)$ measures $\mathrm{Im}\,\lambda_{\psi K_S} = \sin 2\beta$ cleanly.

Of significant interest are some final states which are not pure CP eigenstates, but have CP self conjugate particle content and can be decomposed in CP even and odd partial waves. In some cases an angular analysis can separate the various components, and may provide theoretically clean information. An example is $B_s \to \psi\,\phi$ discussed in Chapters 6 and 8. There are many cases when CP violation in decay occurs in addition to CP violation

in the interference between mixing and decay. Then the asymmetry in Eq. (1.103) depends on the ratio of different decay amplitudes and their strong phases, which introduce hadronic uncertainties. In some cases it is possible to remove (or reduce) these by measuring several rates related by isospin symmetry. An example is $B_d \to \rho\,\pi$ (or $\pi\,\pi$) discussed in Chapter 6.

1.4.2 Decays to non-CP eigenstates

In certain decays to final states which are not CP eigenstates, it is still possible to extract weak phases model independently from the interference between mixing and decay. This occurs if both B^0 and $\overline{B}^0$ can decay into a particular final state and its CP conjugate, but there is only one contribution to each of these decay amplitudes. In this case no assumptions about hadronic physics are needed, even though $|\overline{A}_f/A_f| \neq 1$ and $|\overline{A}_{\overline{f}}/A_{\overline{f}}| \neq 1$.

The most important example is $B_s \to D_s^{\pm} K^{\mp}$, which allows a model independent determination of γ [29]. Both $\overline{B}_s^0$ and B_s^0 can decay to $D_s^+ K^-$ and $D_s^- K^+$, but the only decay processes are the tree level $b \to c\bar{u}s$ and $b \to u\bar{c}s$ transitions, and their CP conjugates. One can easily see that

$$\frac{\overline{A}_{D_s^+ K^-}}{A_{D_s^+ K^-}} = \frac{A_1}{A_2}\left(\frac{V_{cb}V_{us}^*}{V_{ub}^*V_{cs}}\right), \qquad \frac{\overline{A}_{D_s^- K^+}}{A_{D_s^- K^+}} = \frac{A_2}{A_1}\left(\frac{V_{ub}V_{cs}^*}{V_{cb}^*V_{us}}\right), \tag{1.107}$$

where the ratio of amplitudes, A_1/A_2, includes the strong phases, and is an unknown complex number of order unity. It is important for the utility of this method that $|V_{cb}V_{us}|$ and $|V_{ub}V_{cs}|$ are comparable in magnitude, since both are of order λ^3 in the Wolfenstein parameterization. Eqs. (1.73) and (1.74) show that measuring the four time dependent decay rates determine both $\lambda_{D_s^+ K^-}$ and $\lambda_{D_s^- K^+}$. The unknown A_1/A_2 ratio drops out from their product

$$\lambda_{D_s^+ K^-}\,\lambda_{D_s^- K^+} = \left(\frac{V_{tb}^*V_{ts}}{V_{tb}V_{ts}^*}\right)^2\left(\frac{V_{cb}V_{us}^*}{V_{ub}^*V_{cs}}\right)\left(\frac{V_{ub}V_{cs}^*}{V_{cb}^*V_{us}}\right) = e^{-2i(\gamma-2\beta_s-\beta_K)}\,. \tag{1.108}$$

The first factor is the Standard Model value of q/p in B_s mixing. The angles β_s and β_K occur in "squashed" unitarity triangles; β_s defined in Eq. (1.41) is of order λ^2 and $\beta_K = \arg(-V_{cs}V_{cd}^*/V_{us}V_{ud}^*)$ is of order λ^4. Thus, this mode can provide a precise determination of γ (or $\gamma - 2\beta_s$); the determination of β_s is discussed in Chapter 6, e.g., from $B_s \to \psi\,\eta^{(\prime)}$.

In exact analogy to the above, the $B_d \to D^{(*)\pm}\pi^{\mp}$ decays can determine $\gamma + 2\beta$, since $\lambda_{D^+\pi^-}\,\lambda_{D^-\pi^+} = \exp\left[-2i(\gamma+2\beta)\right]$. In this case, however, the two decay amplitudes differ in magnitude by order λ^2, and therefore the CP asymmetries are expected to be much smaller, at the percent level.

1.4.3 $\Delta F = 2$ vs. $\Delta F = 1$ CP violation

At low energies flavor-changing transitions are described by effective Hamiltonians, which are discussed in detail in Sec. 1.5.1. Decays are mediated by the $\Delta F = 1$ Hamiltonian

$H^{|\Delta F|=1}$, whereas mixing is induced by the $\Delta F = 2$ Hamiltonian. The changing flavor is $F = B$ for B decays and $F = S$ for K decays. In kaon physics it is customary to distinguish $\Delta F = 1$ CP violation, which is often called *direct* CP violation, from $\Delta F = 2$ CP violation, called *indirect* CP violation. Here we compare this classification with the three types of CP violation in B decays discussed in Sec. 1.4.1.

If we can find phase transformations of the quark fields in (1.45) which leave the Hamiltonian invariant, $CP\,H^{|\Delta F|=1}(CP)^{-1} = H^{|\Delta F|=1}$, then we conclude that the $|\Delta F| = 1$ interaction conserves CP. Analogously we could define CP violation and CP conservation in $H^{|\Delta F|=2}$, but a B physics experiment probes only one matrix element of $H^{|\Delta F|=2}$, namely M_{12}. One can always find a phase transformation which renders M_{12} real and thereby shifts the CP violation from $H^{|\Delta F|=2}$ completely into $H^{|\Delta F|=1}$. The converse is not true, since one can explore the different couplings in $H^{|\Delta F|=1}$ by studying different decay modes. This leaves three scenarios to be experimentally distinguished:

i) With rephasing of the quark fields one can achieve $CP\,H(CP)^{-1} = H$ for both $H^{|\Delta F|=2}$ and $H^{|\Delta F|=1}$: The theory conserves CP.

ii) One can rephase the quark fields such that $CP\,H^{|\Delta F|=1}(CP)^{-1} = H^{|\Delta F|=1}$, but for this phase transformation $CP\,H^{|\Delta F|=2}(CP)^{-1} \neq H^{|\Delta F|=2}$. This scenario is called *superweak* [30].

iii) $CP\,H^{|\Delta F|=1}(CP)^{-1} \neq H^{|\Delta F|=1}$ for any phase convention of the quark fields. This scenario is realized in the CKM mechanism of the Standard Model.

Historically, after the discovery of CP violation in 1964 [31], it was of prime interest to distinguish the second from the third scenario in kaon physics. The recent establishment of $\epsilon'_K \neq 0$ has shown that possibility iii) is realized in kaon physics.

It is difficult (but possible) to build a viable theory with $\epsilon'_K \neq 0$ in which CP violation in the B system is of the superweak type. Still we can play the rules of the kaon game and ask, what must be measured to rule out the superweak scenario. Clearly, CP violation in decay unambiguously proves $|\Delta F| = 1$ CP violation. CP violation in mixing purely measures CP violation in the $|\Delta F| = 2$ transition. It measures the relative phase between M_{12} and the decay matrix Γ_{12}. Γ_{12} arises at second order in the $|\Delta F| = 1$ interaction, from $\sum_f A_f^* \overline{A}_f$, where A_f and $\overline{A}_f$ are the $|\Delta F| = 1$ decay amplitudes introduced in (1.87). M_{12} receives contributions at first order in $H^{|\Delta F|=2}$ and at second order in $H^{|\Delta F|=1}$. Interference type CP violation measures the difference between the mixing phase $\phi_M = \arg M_{12}$ and twice the weak phase ϕ_f of some decay amplitude $\overline{A}_f$. Both types of CP violations are therefore sensitive to relative phases between $H^{|\Delta F|=2}$ and $H^{|\Delta F|=1}$. Yet the measurement of a single CP violating observable of either type is not sufficient to rule out the superweak scenario, because we can always rephase Γ_{12} or A_f to be real. However, the measurement of interference type CP violation in two different decay modes with different results would prove that two weak phases in $H^{|\Delta F|=1}$ are different. Since $\phi_{f_1} - \phi_{f_2}$ is a rephasing invariant observable, no field transformation in (1.45) can render $H^{|\Delta F|=1}$ real and $|\Delta F| = 1$ CP violation is established. Hence for example the measurement of different CP asymmetries in $B_d \to J/\psi K_S$ and $B_d \to \pi^+\pi^-$ is sufficient to rule out the superweak scenario. Interestingly,

ϵ'_K contains both of the discussed types of $\Delta S = 1$ CP violation: CP violation in decay and the difference of two interference type CP violating phases. Since in both K- and B physics the dominant decay modes have the same weak phases, essentially no new information is gained by comparing CP violation in mixing with interference type CP violation in a dominant decay mode. We will see this in Sec. 1.6 when comparing ϵ_K with the semileptonic CP asymmetry in K_L decays.

1.5 Theoretical Tools

This section provides a brief review of the tools used to derive theoretical predictions for B mixing and decays. The theory of b production and fragmentation is discussed in Chapter 9.

The principal aim of B physics is to learn about the short distance dynamics of nature. Short distance physics couples to b quarks, while experiments detect b-flavored hadrons. One therefore needs to connect the properties of these hadrons in terms of the underlying b quark dynamics. Except for a few special cases, this requires an understanding of the long distance, nonperturbative properties of QCD. It is then useful to separate long distance physics from short distance using an operator product expansion (OPE) or an effective field theory. The basic idea is that interactions at higher scales give rise to local operators at lower scales. This allows us to think about the short distance phenomena responsible for the flavor structure in nature independent of the complications due to hadronic physics, which can then be attacked separately. This strategy can lead to very practical results: the hadronic part of an interesting process may be related by exact or approximate symmetries to the hadronic part of a less interesting or more easily measured process.

In the description of B decays several short distances arise. CP and flavor violation stem from the weak scale and, probably, even shorter distances. These scales are separated from the scale m_B with an OPE, leading to an effective Hamiltonian for flavor changing processes. This is reviewed in Sec. 1.5.1. Furthermore, the b and (to a lesser extent) the c quark masses are much larger than $\Lambda_{\rm QCD}$. In the limit $\Lambda_{\rm QCD}/m_Q \to 0$, the bound state dynamics simplify. Implications for exclusive processes are discussed in Sec. 1.5.2. For inclusive decays one can apply an OPE again, the so-called heavy quark expansion, reviewed in Sec. 1.5.3. Despite the simplifications, these expansions still require hadronic matrix elements, so we briefly review lattice QCD in Sec. 1.5.4.

1.5.1 Effective Hamiltonians

To predict the decay rate of a B meson into some final state f, one must calculate the transition amplitude $\mathcal{M}$ for $B \to f$. In general there are many contributions to $\mathcal{M}$, each of which is, at the quark level, pictorially represented by Feynman diagrams such as those in Fig. 1.3.

Quark diagrams are a poor description for the decay amplitude of a B meson. The quarks feel the strong interaction, whose nature changes drastically over the distances at which it is probed: At short distances much smaller than $1/\Lambda_{\rm QCD}$ the strong interaction can

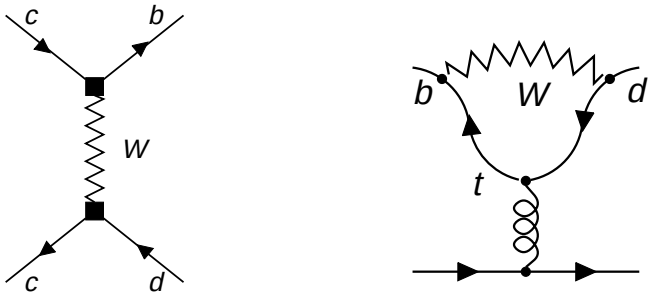

Figure 1.3: Standard Model W exchange diagram and penguin diagram with internal top quark for the decay $b \to c\bar{c}d$.

be described perturbatively by dressing the lowest order diagrams in Fig. 1.3 with gluons. When traveling over a distance of order $1/\Lambda_{\rm QCD}$, however, quarks and gluons hadronize and QCD becomes nonperturbative. Therefore the physics from different length scales, or, equivalently, from different energy scales must be treated differently. One theoretical tool for this is the *operator product expansion* (OPE) [32]. Schematically the decay amplitude $\mathcal{M}$ is expressed as

$$\mathcal{M} = -\frac{4\,G_F}{\sqrt{2}}\,V_{\rm CKM}\sum_j C_j(\mu)\,\langle f|O_j(\mu)|B\rangle\left[1+\mathcal{O}\left(\frac{m_b^2}{M_W^2}\right)\right], \tag{1.109}$$

where μ is a renormalization scale. Physics from distances shorter than μ^{-1} is contained in the Wilson coefficients C_j, and physics from distances longer than μ^{-1} is accounted for by the hadronic matrix elements $\langle f|O_j|B\rangle$ of the local operators O_j. In principle, there are infinitely many terms in the OPE, but higher dimension operators yield contributions suppressed by powers of m_b^2/m_W^2. From a practical point of view, therefore, the sum in (1.109) ranges over operators of dimension five and six.

All dependence on heavy masses $M \gg \mu$ such as m_t, M_W or the masses of new undiscovered heavy particles is contained in C_j. By convention one factors out $4\,G_F/\sqrt{2}$ and the CKM factors, which are denoted by $V_{\rm CKM}$ in (1.109). On the other hand, the matrix element $\langle f|O_j|B\rangle$ of the $B \to f$ transition contains information from scales, such as $\Lambda_{\rm QCD}$, that are below μ. Therefore, they can only be evaluated using nonperturbative methods such as lattice calculations (cf., Sec. 1.5.4), QCD sum rules, or by using related processes to obtain them from experiment.

An important feature of the OPE in (1.109) is the universality of the coefficients C_j; they are independent of the external states, i.e., their numerical value is the same for all final states f in (1.109). Therefore one can view the C_j's as effective coupling constants and the O_j's as the corresponding interaction vertices. Thus one can introduce the *effective Hamiltonian*

$$H^{|\Delta{\rm B}|=1} = \frac{4\,G_F}{\sqrt{2}}\,V_{\rm CKM}\sum_j C_j\,O_j + {\rm h.c.} \tag{1.110}$$

An amplitude calculated from $H^{|\Delta{\rm B}|=1}$ defined at a scale of order m_b, reproduces the corresponding Standard Model result up to corrections of order m_b^2/M_W^2 as indicated in

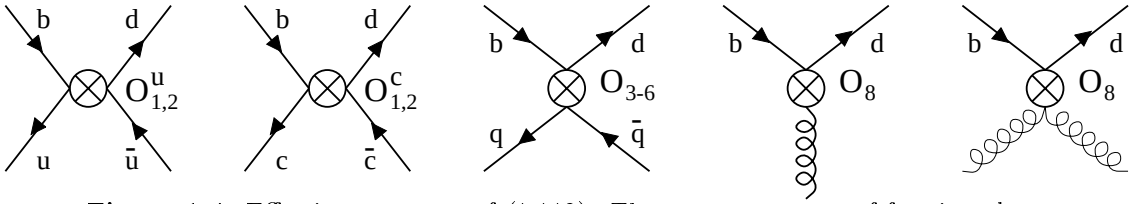

Figure 1.4: Effective operators of (1.112). There are two types of fermion-gluon couplings associated with the chromomagnetic operator O_8.

(1.109). Hard QCD effects can be included perturbatively in the Wilson coefficients, i.e., by calculating Feynman diagrams with quarks and gluons.

The set of operators O_j needed in (1.110) depends on the flavor structure of the physical process under consideration. Pictorially the operators are obtained by contracting the lines corresponding to heavy particles in the Feynman diagrams to a point. The tree level diagram involving the W boson in Fig. 1.3 generates the operator O_2^c shown in Fig. 1.4. In the Standard Model only two operators occur for $b \to c\overline{u}d$ transitions,

$$O_1 = \bar{b}_L^\alpha \gamma_\mu c_L^\beta \, \bar{u}_L^\beta \gamma^\mu d_L^\alpha \,, \qquad O_2 = \bar{b}_L^\alpha \gamma_\mu c_L^\alpha \, \bar{u}_L^\beta \gamma^\mu d_L^\beta \,, \tag{1.111}$$

where α and β are color indices. These arise from W exchange shown in Fig. 1.3, and QCD corrections to it. Operators and Wilson coefficients at different scales μ_1 and μ_2 are related by a renormalization group transformation. $C_{1,2}(\mu_1)$ is not just a function of $C_{1,2}(\mu_2)$, but a linear combination of both $C_1(\mu_2)$ and $C_2(\mu_2)$. This feature is called operator mixing. It is convenient to introduce the linear combinations $O_\pm = (O_2 \pm O_1)/2$, which do not mix with each other. Their coefficients can be more easily calculated and are related to C_1 and C_2 by $C_\pm = C_2 \pm C_1$.

The Hamiltonian for $\Delta B = 1$ and $\Delta C = \Delta S = 0$ transitions consists of more operators, because it must also accommodate for the so-called penguin diagram with an internal top quark, shown in Fig. 1.3. The corresponding operator basis reads

$$\begin{aligned}
O_1^c &= \bar{d}_L^\alpha \gamma_\mu c_L^\beta \, \bar{c}_L^\beta \gamma^\mu b_L^\alpha \,, & O_1^u &= \bar{d}_L^\alpha \gamma_\mu u_L^\beta \, \bar{u}_L^\beta \gamma^\mu b_L^\alpha \,, \\
O_2^c &= \bar{d}_L^\alpha \gamma_\mu c_L^\alpha \, \bar{c}_L^\beta \gamma^\mu b_L^\beta \,, & O_2^u &= \bar{d}_L^\alpha \gamma_\mu u_L^\alpha \, \bar{u}_L^\beta \gamma^\mu b_L^\beta \,, \\
O_3 &= \sum_{q=u,d,s,c,b} \bar{d}_L^\alpha \gamma_\mu b_L^\alpha \, \bar{q}_L^\beta \gamma^\mu q_L^\beta \,, & O_4 &= \sum_{q=u,d,s,c,b} \bar{d}_L^\alpha \gamma_\mu b_L^\beta \, \bar{q}_L^\beta \gamma^\mu q_L^\alpha \,, \\
O_5 &= \sum_{q=u,d,s,c,b} \bar{d}_L^\alpha \gamma_\mu b_L^\alpha \, \bar{q}_R^\beta \gamma^\mu q_R^\beta \,, & O_6 &= \sum_{q=u,d,s,c,b} \bar{d}_L^\alpha \gamma_\mu b_L^\beta \, \bar{q}_R^\beta \gamma^\mu q_R^\alpha \,, \\
O_8 &= -\frac{g}{16\pi^2} \, m_b \, \bar{d}_L \sigma^{\mu\nu} G^a_{\mu\nu} T^a b_R \,.
\end{aligned} \tag{1.112}$$

These operators are also depicted in Fig. 1.4. In O_8, $G^a_{\mu\nu}$ is the chromomagnetic field strength tensor. The operators are grouped into classes, based on their origin: O_1 and O_2 are called *current-current operators*, O_3 through O_6 are called *four-quark penguin operators*, and O_8 is called the *chromomagnetic penguin operator.*[9]

[9] In the literature one also finds O_7 and O_8 with the opposite signs. In QCD and QED the sign of the

The operators in (1.112) arise from the lowest order in the electroweak interaction, i.e., diagrams involving a single W bosons plus QCD corrections to it. In some cases, especially when isospin breaking plays a role, one also needs to consider penguin diagrams which are of higher order in the electroweak fine structure constant α_{ew}. They give rise to the *electroweak penguin operators*:

$$\begin{aligned}
O_7 &= -\frac{e}{16\pi^2}\, m_b\, \bar{d}_L^\alpha\, \sigma^{\mu\nu} F_{\mu\nu}\, b_R^\alpha\,, \\
O_7^{\rm ew} &= \frac{3}{2} \sum_{q=u,d,s,c,b} e_q\, \bar{d}_L^\alpha \gamma_\mu b_L^\alpha\, \bar{q}_R^\beta \gamma^\mu q_R^\beta\,, \qquad O_8^{\rm ew} = \frac{3}{2} \sum_{q=u,d,s,c,b} e_q\, \bar{d}_L^\alpha \gamma_\mu b_L^\beta\, \bar{q}_R^\beta \gamma^\mu q_R^\alpha\,, \\
O_9^{\rm ew} &= \frac{3}{2} \sum_{q=u,d,s,c,b} e_q\, \bar{d}_L^\alpha \gamma_\mu b_L^\alpha\, \bar{q}_L^\beta \gamma^\mu q_L^\beta\,, \qquad O_{10}^{\rm ew} = \frac{3}{2} \sum_{q=u,d,s,c,b} e_q\, \bar{d}_L^\alpha \gamma_\mu b_L^\beta\, \bar{q}_L^\beta \gamma^\mu q_L^\alpha\,.
\end{aligned} \tag{1.113}$$

Here $F^{\mu\nu}$ is the electromagnetic field strength tensor, and e_q denotes the charge of quark q. The magnetic (penguin) operator O_7 is also of key importance for the radiative decay $b \to d\gamma$. Eqs. (1.112) and (1.113) reveal that there is no consensus yet on how to number the operators consecutively.

For semileptonic decays the following additional operators occur

$$\begin{aligned}
O_9 &= \frac{e^2}{16\pi^2}\, \bar{d}_L\, \gamma_\mu\, b_L\, \bar{\ell}\, \gamma^\mu\, \ell\,, \qquad O_{10} = \frac{e^2}{16\pi^2}\, \bar{d}_L\, \gamma_\mu\, b_L\, \bar{\ell}\, \gamma^\mu \gamma_5\, \ell\,, \\
O_{11} &= \frac{e^2}{32\pi^2 \sin^2\theta_W}\, \bar{d}_L\, \gamma_\mu\, b_L\, \bar{\nu}_L\, \gamma^\mu\, \nu_L\,,
\end{aligned} \tag{1.114}$$

and the counterparts of these with $\bar{d}_L$ replaced by $\bar{s}_L$.

Hence the $\Delta B = 1$ and $\Delta C = \Delta S = 0$ Hamiltonian reads:

$$H^{|\Delta \mathrm{B}|=1} = \frac{4\, G_F}{\sqrt{2}} \left\{ \sum_{j=1}^{2} C_j \left(\xi_c O_j^c + \xi_u O_j^u \right) - \xi_t \sum_{j=3}^{11} C_j\, O_j - \xi_t \sum_{j=7}^{10} C_j^{\rm ew}\, O_j \right\} + \text{h.c.}\,, \tag{1.115}$$

where

$$\xi_q = V_{qb}^* V_{qd}\,. \tag{1.116}$$

Note that $\xi_u + \xi_c + \xi_t = 0$ by unitarity of the CKM matrix. The corresponding operator basis for $b \to s$ transitions is obtained by simply exchanging d with s in (1.112), (1.113) and (1.114) and changing ξ_i accordingly.

The operators introduced above are sufficient to describe nonleptonic transitions in the Standard Model to order G_F. In extensions of the Standard Model, on the other hand, the short distance structure can be very different. Additional operators with new Dirac structures, whose standard Wilson coefficients vanish, could enter the effective Hamiltonian. A list of these operators, including their RG evolution, can be found in [33].

In general the QCD corrections to the transition amplitude $\mathcal{M}(B \to f)$ contain large logarithms such as $\ln(m_b/M_W)$ which need to be resummed to all orders in α_s. The OPE

gauge coupling is convention dependent, and (1.112) is consistent with the values for C_8 in Table 1.3, if the Feynman rule for the quark-gluon coupling is chosen as $+ig$.

splits these logarithms as $\ln(m_b/M_W) = \ln(\mu/M_W) - \ln(\mu/m_b)$. The former term resides in the Wilson coefficients, the latter logarithm is contained in the matrix element. Such large logarithms can be summed to all orders by solving *renormalization group* (RG) equations for the C_j's. These RG-improved perturbation series are well-behaved. The minimal way to include QCD corrections is the *leading logarithmic approximation*. The corresponding *leading order* (LO) Wilson coefficients comprise $[\alpha_s \ln(m_b/M_W)]^n$ to all orders $n = 0, 1, 2, \ldots$ in perturbation theory. This approximation has certain conceptual deficits and is too crude for the precision of the experiments and the accuracy of present day lattice calculations of the hadronic matrix elements. The *next-to-leading order* (NLO) results for the C_j's comprises in addition terms of order $\alpha_s\,[\alpha_s \ln(m_b/M_W)]^n, n = 0, 1, 2, \ldots$. The Wilson coefficients depend on the unphysical scale μ at which the OPE is performed. Starting from the NLO the C_j's further depend on the *renormalization scheme*, which is related to the way one treats divergent loops in Feynman diagrams. In an exact calculation both the scale and scheme dependence cancels between the coefficients and the matrix elements, but in practice the calculation of matrix elements with the correct scale and scheme dependence can be a non-trivial task. The appearance of the scale and scheme dependence in the coefficients is inevitable. The OPE enforces the short distance physics involving heavy masses like M_W and m_t to belong to the C_j's, while the long distance physics is contained in the matrix elements. But a constant number can be attributed to either of them. Switching from one scheme to another or changing the scale μ just shuffles constant terms between the Wilson coefficients and the matrix elements. There is no unique definition of "scheme independent" Wilson coefficients.

The numerical values for the renormalization group improved Wilson coefficients can be found in Table 1.3. The NLO coefficients are listed for two popular schemes, the *naive dimensional regularization* (NDR) scheme and the *'t Hooft-Veltman* (HV) scheme. These results have been independently obtained by the Rome and Munich groups [34]. The situation with C_8 is special: To obtain the LO values for C_{1-6} in Table 1.3 one must calculate one-loop diagrams. The calculation of C_8, however, already involves two-loop diagrams in the leading order. This implies that even the LO expression for C_8 is scheme dependent. The tabulated value corresponds to the commonly used "effective" coefficient C_8 introduced in [36], which is defined in a scheme independent way. To know the NLO value for C_8 one must calculate three-loop diagrams. The operator basis in (1.112) is badly suited for this calculation and hence a different one has been used [37]. For the basis in (1.112) the NLO value for C_8 is not known, we therefore leave the corresponding rows open. In Table 1.3 small corrections proportional to α_{ew} have been omitted. For the Wilson coefficients of the electroweak penguin operators in (1.113) and the semileptonic operators in (1.114) we refer the reader to [35].

We can derive an effective Hamiltonian for the $|\Delta B| = 2$ transition, which induces B^0_d–$\overline{B}^0_d$ mixing, just in the same way as discussed above for $|\Delta B| = 1$. In the Standard Model only a single operator Q arises:[10]

$$H^{|\Delta B|=2} = \frac{G_F^2}{4\pi^2}\,(V_{tb}V_{td}^*)^2\,C^{|\Delta B|=2}(m_t, M_W, \mu)\,Q(\mu) + h.c. \qquad (1.117)$$

[10] Once again in (1.117), new short distance physics can generate Wilson coefficients for additional operators.

$\alpha_s(M_Z)$	scheme	μ (GeV)	C_1	C_2	C_3	C_4	C_5	C_6	C_8
0.112	LO	4.8	−0.229	1.097	0.010	−0.024	0.007	−0.029	−0.146
		2.4	−0.325	1.149	0.015	−0.033	0.009	−0.043	−0.161
		9.6	−0.155	1.062	0.007	−0.016	0.005	−0.019	−0.133
	NDR	4.8	−0.160	1.066	0.011	−0.031	0.008	−0.035	
		2.4	−0.245	1.110	0.017	−0.043	0.009	−0.052	
		9.6	−0.093	1.036	0.008	−0.021	0.006	−0.023	
	HV	4.8	−0.177	0.993	0.009	−0.024	0.007	−0.026	
		2.4	−0.260	1.020	0.014	−0.033	0.010	−0.038	
		9.6	−0.111	0.975	0.006	−0.015	0.005	−0.017	
0.118	*LO*	4.8	−0.249	1.108	0.011	−0.026	0.008	−0.031	−0.149
		2.4	−0.361	1.169	0.017	−0.036	0.010	−0.048	−0.166
		9.6	−0.167	1.067	0.007	−0.018	0.005	−0.020	−0.135
	NDR	4.8	−0.174	1.073	0.013	−0.034	0.009	−0.038	
		2.4	−0.272	1.124	0.020	−0.047	0.010	−0.060	
		9.6	−0.100	1.039	0.008	−0.024	0.006	−0.025	
	HV	4.8	−0.192	0.993	0.010	−0.026	0.008	−0.028	
		2.4	−0.286	1.022	0.016	−0.036	0.011	−0.042	
		9.6	−0.120	0.972	0.006	−0.017	0.005	−0.018	
0.124	*LO*	4.8	−0.272	1.120	0.012	−0.028	0.008	−0.035	−0.153
		2.4	−0.403	1.194	0.019	−0.040	0.011	−0.055	−0.172
		9.6	−0.180	1.073	0.008	−0.019	0.006	−0.022	−0.138
	NDR	4.8	−0.190	1.082	0.014	−0.037	0.009	−0.043	
		2.4	−0.303	1.142	0.022	−0.054	0.011	−0.069	
		9.6	−0.108	1.042	0.009	−0.025	0.007	−0.028	
	HV	4.8	−0.208	0.993	0.011	−0.028	0.008	−0.031	
		2.4	−0.316	1.025	0.018	−0.040	0.012	−0.048	
		9.6	−0.129	0.970	0.007	−0.018	0.006	−0.019	

Table 1.3: QCD Wilson coefficients in the leading and next-to-leading order. The NLO running of α_s has been used in both the LO and NLO coefficients. $\alpha_s(M_Z) = 0.112,\ 0.118,\ 0.124$ implies $\alpha_s(4.8\,\mathrm{GeV}) = 0.196,\ 0.216,\ 0.238$. The corresponding values of the five-flavor QCD scale parameter $\Lambda_{\overline{\mathrm{MS}}}$ are 159, 226 and 312 MeV. The dependence on $m_t(m_t)$, here taken as 168 GeV, is negligible. The NLO coefficients are listed for the NDR and HV scheme. There are two different conventions for the HV scheme, here we use the one adopted in [34]. The HV coefficients tabulated in [35] are related to our C_j^{HV}'s by $C_j^{HV}([35]) = [1 + 16/3 \cdot \alpha_s(\mu)/(4\pi)]C_j^{HV}$. Small QED corrections have been omitted.

with

$$Q = \overline{d}_L \gamma_\nu b_L \, \overline{d}_L \gamma^\nu b_L. \tag{1.118}$$

The Wilson coefficient is

$$C^{|\Delta B|=2}(m_t, M_W, \mu) = M_W^2 \, S\left(\frac{m_t^2}{M_W^2}\right) \eta_B \, b_B(\mu) \,. \tag{1.119}$$

It contains the *Inami-Lim function* [38]

$$S(x) = x \left[\frac{1}{4} + \frac{9}{4}\frac{1}{1-x} - \frac{3}{2}\frac{1}{(1-x)^2}\right] - \frac{3}{2}\left[\frac{x}{1-x}\right]^3 \ln x \,, \tag{1.120}$$

which is calculated from the box diagram in Fig. 1.2. The coefficients η_B and b_B in (1.119) account for short distance QCD corrections. In the next-to-leading order of QCD one finds $\eta_B = 0.55$ [39]. b_B depends on the renormalization scale $\mu = \mathcal{O}(m_b)$, at which the matrix element $\langle B_d^0 | Q | \overline{B}_d^0 \rangle$ is calculated. $b_B(\mu)$ equals $[\alpha_s(\mu)]^{-6/23}$ in the LO. The μ-dependence of $b_B(\mu)$ cancels the μ-dependence of the matrix element to the calculated order. The same remark applies to the dependence of $b_B(\mu)$ on the renormalization scheme in which the calculation is carried out. One parameterizes the hadronic matrix elements as

$$\langle B^0 | Q(\mu) | \overline{B}^0 \rangle = \frac{2}{3} f_B^2 m_B^2 \frac{\widehat{B}_B}{b_B(\mu)}, \tag{1.121}$$

so that $\widehat{B}_B$ is scale and scheme independent. The effective Hamiltonian for $B_s^0 - \overline{B}_s^0$ mixing is obtained as usual by replacing d with s in (1.117) and (1.118). The Wilson coefficient in (1.119) does not depend on the light quark flavor.

1.5.2 Heavy quark effective theory

In hadrons composed of a heavy quark and light degrees of freedom (light quarks, antiquarks, and gluons), the binding energy, which is of order $\Lambda_{\rm QCD}$, is small compared to the heavy quark mass m_Q. In the limit $m_Q \gg \Lambda_{\rm QCD}$, the heavy quark acts approximately as a static color-triplet source,[11] and its spin and flavor do not affect the light degrees of freedom. This is analogous to atomic physics, where isotopes with different nuclei have nearly the same properties. Thus, the properties of heavy-light hadrons are related by a symmetry, called heavy quark symmetry (HQS) [40–47]. In practice, only the b and c quarks have masses large enough for HQS to be useful.[12] This results in an $SU(2N_h)$ spin-flavor symmetry, where $N_h = 1$ or 2, depending on the problem at hand.

The heavy quark spin-flavor symmetries are helpful for understanding many aspects of the spectroscopy and decays of heavy hadrons from first principles. For example, in the infinite mass limit, mass splittings between b-flavored hadrons can be related to those between charmed hadrons, and many semileptonic and radiative decay form factors can

[11] For the same reason, heavy quark symmetries also apply to hadrons composed of two heavy and a light quark, because the color quantum numbers of the two heavy quarks combine to an antitriplet.

[12] The top quark also satisfies $m_t \gg \Lambda_{\rm QCD}$, but it decays before it hadronizes.

be related to one another. There are corrections to the HQS limit from long distances and from short distances. The former are suppressed by powers of $\Lambda_{\rm QCD}/m_Q$. They must be calculated by nonperturbative methods, but HQS again imposes relations among these terms. The latter arise from the exchange of hard virtual gluons, so they can be calculated accurately in a perturbation series in $\alpha_s(m_Q)$. The heavy quark effective theory (HQET) provides a convenient framework for treating these effects [45–51]. In leading order the effective theory reproduces the model independent predictions of HQS, and both series of symmetry breaking corrections are developed in a systematic, consistent way.

To see how the heavy quark symmetries arise, it is instructive to look at the infinite-mass limit of the Feynman rules. For momentum $p = m_Q v + k$, with $v^2 = 1$ and $k \ll m_Q$, the propagator of a heavy quark becomes

$$\frac{i}{\not p - m_Q} = \frac{i(\not p + m_Q)}{p^2 - m_Q^2} = \frac{i(m_Q \not v + \not k + m_Q)}{2 m_Q\, v\cdot k + k^2} = \frac{i}{v\cdot k}\,\frac{1+\not v}{2} + \ldots\,. \tag{1.122}$$

As $m_Q \to \infty$ it is independent of its mass, and in this way heavy quark *flavor* symmetry emerges. In a Feynman diagram, the quark-gluon vertex appears between two propagators and, hence, for $m_Q \to \infty$, sandwiched between the projection operator

$$P_+(v) = \frac{1+\not v}{2}\,. \tag{1.123}$$

Consequently the gamma matrix at the vertex becomes

$$P_+ \gamma^\mu P_+ = v^\mu\, P_+\,. \tag{1.124}$$

Thus, both the vertex and the propagator depend on gamma matrices only through P_+. Since $P_+^2 = P_+$, all these factors reduce to a single one, and in this way heavy quark *spin* symmetry emerges.

The construction of HQET [40] starts by removing the mass-dependent piece of the momentum operator by a field redefinition. One introduces a field $h_v(x)$, which annihilates a heavy quark with velocity v [47],

$$h_v(x) = e^{i m_Q v\cdot x}\, P_+(v)\, Q(x)\,, \tag{1.125}$$

where $Q(x)$ denotes the quark field in full QCD. Here the physical interpretation of the projection operator P_+ is that h_v represents just the heavy quark (rather than antiquark) components of Q. If p is the total momentum of the heavy quark, then the field h_v carries the residual momentum $k = p - m_Q v$. Inside a hadron, the residual momentum $k \sim \mathcal{O}(\Lambda_{\rm QCD})$. Since the phase factor in Eq. (1.125) effectively removes the mass of the heavy quark from the states, it is the mass difference

$$\bar\Lambda = m_H - m_Q\,, \tag{1.126}$$

where m_H is the hadron mass, that determines the x-dependence of hadronic matrix elements in HQET [51]. It is also this parameter that sets the characteristic scale of the $1/m_Q$ expansion. Because of heavy quark flavor symmetry $\bar\Lambda = m_B - m_b = m_D - m_c$, and

because of heavy quark spin symmetry $\bar{\Lambda} = m_{B^*} - m_b$, in both cases up to $\mathcal{O}(\Lambda^2_{\rm QCD}/m_Q)$ corrections. Other heavy hadrons, for example heavy-flavored baryons, have a distinct "$\bar{\Lambda}$", but the flavor symmetry implies $m_{\Lambda_b} - m_b = m_{\Lambda_c} - m_c$, up to $\mathcal{O}(\Lambda^2_{\rm QCD}/m_Q)$.

The HQET Lagrangian is constructed from the field h_v. Including the leading $1/m_Q$ corrections, it is [45,47,48]

$$\mathcal{L}_{\rm HQET} = \bar{h}_v \, iv\cdot D \, h_v + \frac{1}{2m_Q}\Big[O_{\rm kin} + C_{\rm mag}(\mu)\, O_{\rm mag}(\mu)\Big] + \mathcal{O}(1/m_Q^2)\,, \tag{1.127}$$

where $D^\mu = \partial^\mu - ig_s T_a A^\mu_a$ is the color $SU(3)$ covariant derivative. The leading term respects both the spin and flavor symmetries, and reproduces the heavy quark propagator derived above. The symmetry breaking operators appearing at order $1/m_Q$ are

$$O_{\rm kin} = \bar{h}_v \, (iD)^2 \, h_v\,, \qquad O_{\rm mag} = \frac{g_s}{2}\, \bar{h}_v \, \sigma_{\mu\nu}\, G^{\mu\nu}\, h_v\,. \tag{1.128}$$

Here $G^{\mu\nu}$ is the gluon field strength tensor defined by $[iD^\mu, iD^\nu] = ig_s G^{\mu\nu}$. In the rest frame of the hadron, $O_{\rm kin}$ describes the kinetic energy resulting from the residual motion of the heavy quark, whereas $O_{\rm mag}$ corresponds to the chromomagnetic coupling of the heavy quark spin to the gluon field. While $O_{\rm kin}$ violates only the heavy quark flavor symmetry, $O_{\rm mag}$ violates the spin symmetry as well.

In the operators of the electroweak Hamiltonian, the QCD field Q must also be replaced with h_v and a series of higher-dimension operators to describe $1/m_Q$ effects. The short distance behavior can be matched using perturbation theory. The matrix elements of the HQET operators still cannot be calculated in perturbatively, but HQS restricts their form. The best known example is in exclusive semileptonic $b \to c$ corrections. In $B \to D^{(*)}\ell\nu$ and $\Lambda_b \to \Lambda_c \ell\nu$, let v (v') be the velocity of the initial (final) heavy-light hadron. HQS requires that the mesonic decays are described by a set of heavy quark spin- and mass-independent functions of the kinematic variable $w = v\cdot v'$. The baryonic decay is described by another function of w. When $v = v'$ the symmetry becomes larger—from $SU(2)_v \times SU(2)_{v'}$ to $SU(4)$—so there are further restrictions. One is that symmetry limit of the form factor is completely determined by symmetry (at $w = 1$). Furthermore, HQS also requires that the $1/m_Q$ corrections to $B \to D^*\ell\nu$ and $\Lambda_b \to \Lambda_c\ell\nu$ vanish for $w = 1$.

The utility of HQET is not limited to exclusive decays. Matrix elements of the effective Lagrangian play an important role in inclusive semileptonic and radiative decays. One defines

$$\begin{aligned} \lambda_1 &= \frac{1}{2\,m_M}\,\langle M(v)|\, O_{\rm kin}\,|M(v)\rangle\,, \\ d_M\,\lambda_2 &= \frac{1}{2\,m_M}\,\langle M(v)|\, O_{\rm mag}\,|M(v)\rangle\,, \end{aligned} \tag{1.129}$$

where M denotes a B or B^* meson, and $d_M = 3, -1$ for B and B^*, respectively. Strictly speaking, both λ_1 and λ_2 depend on the renormalization scale μ. For λ_1, however, there is no μ dependence if $O_{\rm kin}$ is renormalized in the $\overline{\rm MS}$ scheme. For λ_2, the μ dependence is canceled by the coefficient $C_{\rm mag}(\mu)$ in (1.127).

HQET provides an expansion of the heavy meson masses in terms of the heavy quark masses,

$$m_B = m_b + \bar{\Lambda} - \frac{\lambda_1 + 3\lambda_2}{2m_b} + \dots , \qquad m_{B^*} = m_b + \bar{\Lambda} - \frac{\lambda_1 - \lambda_2}{2m_b} + \dots . \tag{1.130}$$

Consequently, the value of λ_2 is related to the mass splitting between the vector and the pseudoscalar mesons,

$$\lambda_2 = \frac{m_{B^*}^2 - m_B^2}{4} + \mathcal{O}\Big(\Lambda_{\rm QCD}^3/m_b\Big) , \tag{1.131}$$

taking $\mu = m_b$ and $C_{\rm mag}(m_b) = 1$. From the measured B and B^* masses one finds $\lambda_2(m_b) \simeq 0.12$ GeV^2. These formulae will play an important role in the description of both inclusive and exclusive heavy meson decays in the following chapters.

It was only recognized recently that HQS also yields important simplifications in the description of heavy-to-light radiative and semileptonic decays in the region of large recoil (small q^2) [52]. In the infinite mass limit, the three form factors which parameterize the vector and tensor current matrix elements in $B \to K\ell^+\ell^-$ are related to a single function of q^2, and the seven form factors which occur in $B \to K^*\ell^+\ell^-$ are related to only two functions of q^2. In contrast to the predictions of HQS in the region of small recoil, in this case it is not known yet how to formulate the subleading corrections suppressed by powers of $\Lambda_{\rm QCD}/m_Q$. Nevertheless, these relations play a very important role in Chapter 7, where they will be discussed in detail.

1.5.3 Heavy quark expansion

In inclusive B decays, when many final states are summed over, certain model independent formulae can be derived. In this section we examine how the large b quark mass, $m_b \gg \Lambda_{\rm QCD}$, allows one to extract reliable information about such decays. In most of the phase space the energy release, which can be as large as $\mathcal{O}(m_b)$, is much larger than the typical scale of hadronic interactions. The large energy release implies a short distance, and we can use the same tools as before—an operator product expansion [53–55] (though not the same OPE as in Sec. 1.5.1) and HQET—to separate short and long distances. In this way, inclusive decay rates can be described with a double series in $\Lambda_{\rm QCD}/m_b$ and $\alpha_s(m_b)$.

Inclusive decay widths are given by the sum over all final states. Schematically, the width is given by

$$\Gamma \sim \sum_X \langle B|O^\dagger|X\rangle \, \langle X|O|B\rangle . \tag{1.132}$$

where X is any final state. One can also limit X to X_c or X_u, i.e., to final states with or without a charmed quark, respectively. From Sec. 1.5.1, we see that inclusive semileptonic B decays are mediated by operators of the form

$$O_\ell \sim \bar{q}_L \gamma^\mu b_L \, \bar{\ell}_{L1} \gamma_\mu \ell_{L2} , \tag{1.133}$$

and nonleptonic decays are mediated by four-quark operators of the form

$$O_h \sim \bar{q}_L \gamma^\mu b_L \, \bar{q}_{L1} \gamma_\mu q_{L2} . \tag{1.134}$$

Although these operators are superficially similar, we shall see that they have to be treated differently, because in O_h hard gluons can be exchanged among all four quark fields. We start by showing in detail how the OPE and HQET are used to describe inclusive semileptonic B decays. We then explain what restrictions arise for nonleptonic decay rates and lifetimes. Finally, we treat the width difference in the B_s system, which is of special interest to Tevatron experiments.

1.5.3.1 Inclusive semileptonic B decays

In semileptonic decays, one may factorize the matrix element of the four-fermion operator

$$\langle X\ell\,\bar\nu_\ell|\,O_\ell\,|B\rangle = \langle X|\,\bar q\,\gamma^\mu P_L\,b\,|B\rangle\,\langle\ell\,\bar\nu_\ell|\,\bar\ell\,\gamma_\mu P_L\,\nu_\ell\,|0\rangle\,, \tag{1.135}$$

neglecting electroweak loop corrections. Then the decay rate can be written in the form

$$\frac{\mathrm{d}^2\Gamma}{\mathrm{d}y\,\mathrm{d}q^2} \sim \int \mathrm{d}(q\cdot v)\,L_{\mu\nu}(p_\ell,p_{\bar\nu})\,W^{\mu\nu}(q\cdot v,q^2)\,, \tag{1.136}$$

where $L_{\mu\nu}$ is the lepton tensor and $W^{\mu\nu}$ is the hadron tensor. The momentum of the decaying b quark is written as $p_b^\mu = m_b v^\mu$, $q^\mu = p_\ell^\mu + p_{\bar\nu}^\mu$, and we have introduced the dimensionless variable $y = 2E_\ell/m_b$. Since the antineutrino is not detected, its energy or, equivalently, $q\cdot v = E_\ell + E_{\bar\nu}$ is integrated over. The lepton tensor $L^{\mu\rho} = 2(p_\ell^\mu p_{\bar\nu}^\rho + p_\ell^\rho p_{\bar\nu}^\mu - g^{\mu\rho}p_\ell\cdot p_{\bar\nu} - i\varepsilon^{\mu\rho\alpha\beta}p_{\ell\alpha}p_{\bar\nu\beta})$. The hadron tensor $W^{\mu\nu}$ contains all strong interaction physics relevant for the semileptonic decay, and it can be expressed as

$$W^{\mu\nu} = \sum_X (2\pi)^3\,\delta^4(p_B - q - p_X)\,\frac{\langle\overline{B}|\,J^{\mu\dagger}\,|X\rangle\,\langle X|\,J^\nu\,|\overline{B}\rangle}{2m_B}\,, \tag{1.137}$$

where $J^\mu = \bar q\,\gamma^\mu P_L\,b$.

The optical theorem can be used to relate $W^{\mu\nu}$ to the discontinuity across a cut of the forward scattering matrix element of a time ordered product

$$T^{\mu\nu} = -i\int \mathrm{d}^4x\,e^{-iq\cdot x}\,\frac{\langle\overline{B}|\,T\{J^{\mu\dagger}(x)\,J^\nu(0)\}|\overline{B}\rangle}{2m_B}\,. \tag{1.138}$$

To show that

$$W^{\mu\nu} = -\frac{1}{\pi}\,\mathrm{Im}\,T^{\mu\nu}\,, \tag{1.139}$$

one inserts a complete set of states between the currents in the two possible time orderings in $T^{\mu\nu}$. Using $\langle A|J(x)|B\rangle = \langle A|J(0)|B\rangle\,e^{i(p_A-p_B)\cdot x}$ and the identity $\theta(x^0) = i/(2\pi)\int_{-\infty}^{+\infty}\mathrm{d}\omega\,[e^{-i\omega x^0}/(\omega+i\varepsilon)]$, the d^4x integration gives (in the B rest frame, so $q\cdot v = q^0$)

$$\begin{aligned} T^{\mu\nu} = &\sum_{X_q}\frac{\langle\overline{B}|\,J^{\mu\dagger}\,|X_q\rangle\,\langle X_q|\,J^\nu\,|\overline{B}\rangle}{2m_B\,(m_B - E_X - q^0 + i\varepsilon)}\,(2\pi)^3\,\delta^3(\boldsymbol{q}+\boldsymbol{p}_X) \\ &- \sum_{X_{\bar q bb}}\frac{\langle\overline{B}|\,J^{\nu}\,|X_{\bar q bb}\rangle\,\langle X_{\bar q bb}|\,J^{\mu\dagger}\,|\overline{B}\rangle}{2m_B\,(E_X - m_B - q^0 - i\varepsilon)}\,(2\pi)^3\,\delta^3(\boldsymbol{q}-\boldsymbol{p}_X)\,. \end{aligned} \tag{1.140}$$

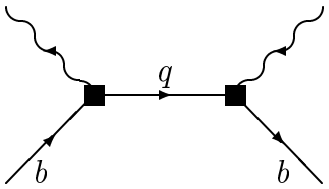

Figure 1.5: OPE diagram for semileptonic and radiative B decays.

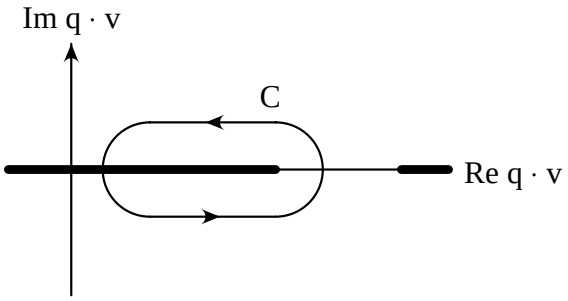

Figure 1.6: The analytic structure of $T^{\mu\nu}$ in the $q \cdot v$ plane, with q^2 fixed. The cuts corresponding to B decay (left) and to an unphysical process (right) are both shown, together with the integration contour for computing the decay rate.

This form shows that, for fixed q^2, $T^{\mu\nu}$ has cuts in the complex q^0 plane corresponding to physical processes. The first sum in Eq. (1.140) corresponds to B decay shown in Fig. 1.5, with intermediate states containing a q quark (and arbitrary number of gluons and light quark-antiquark pairs). It leads to a cut for $q^0 = q \cdot v < (m_B^2 + q^2 - m_{X_q^{\rm min}}^2)/2m_B$, towards the left in Fig. 1.6. For charmed final states $m_{X_q^{\rm min}}^2 = m_D^2$ and for charmless final states $m_{X_q^{\rm min}}^2 = m_\pi^2$. The second sum in Eq. (1.140) corresponds to an unphysical process with a $\bar{q}$ and two b quarks in the intermediate state. It leads to another cut for $q^0 = q \cdot v > (m_{X_{\bar{q}bb}^{\rm min}}^2 - m_B^2 - q^2)/2m_B$, towards the right in Fig. 1.6. The imaginary part can be read off using $\mathrm{Im}\,(A + i\varepsilon)^{-1} = -\pi\delta(A)$, and (1.139) follows immediately, because the kinematics of the decay process allow only the first sum to contribute.

Because $W^{\mu\nu}$ is the discontinuity across the left cut in Fig. 1.6, the integral in (1.136) can be replaced with a contour integral of $L_{\mu\nu}T^{\mu\nu}$. The two cuts are well separated (unless $m_q \to 0$ and $q^2 \to m_b^2$), so one may deform the contour away from the cuts [56], as shown in Fig. 1.6. The equivalence of the sum over hadronic states with a contour ranging far from the physical region is called "global duality". This procedure is advantageous, because $T^{\mu\nu}$ can be reliably described by an operator product expansion (OPE) far (compared to $\Lambda_{\rm QCD}$) from its singularities in the complex $q \cdot v$ plane [53–55]. One simply replaces the time ordered product

$$-i \int \mathrm{d}^4x\, e^{-iq\cdot x}\, T\{J^{\mu\dagger}(x)\, J^\nu(0)\}\,, \tag{1.141}$$

appearing in Eq. (1.138), with a series of local operators multiplied with Wilson coefficients. The Wilson coefficients of this OPE can again be evaluated in a perturbation series in $\alpha_s(m_b)$. Higher dimension operators in the OPE incorporate higher powers of $\Lambda_{\rm QCD}/m_b$.

Unfortunately, the contour C must still approach the cut near the low $q \cdot v$ endpoint of the integration. Using the OPE directly in the physical region is an assumption called "local duality". It introduces an uncertainty to the calculation, which can be argued to be small. First, in semileptonic and radiative decays the fraction of the contour which has to be within order $\Lambda_{\rm QCD}$ from the cut scales as $\Lambda_{\rm QCD}/m_b$. Second, since the energy release to the hadronic final state is large compared to $\Lambda_{\rm QCD}$, the imaginary part of $T^{\mu\nu}$ is dominated by multiparticle states, so it is expected to be a smooth function. In the end, the violation of local duality is believed to be exponentially suppressed in the $m_Q \to \infty$ limit, but it is not well understood how well it works at the scale of the b quark mass. In semileptonic decay the agreement between the inclusive and exclusive determinations of $|V_{cb}|$ suggests that duality violation is at most a few percent. But there is no known relation between the size of duality violation in semileptonic and nonleptonic B decays [57], or between these processes and others, such as $e^+e^- \to$ hadrons.

At lowest order in $\Lambda_{\rm QCD}/m_b$ the OPE leads to operators of the form $\bar b \Gamma b$ occur, where Γ is any Dirac matrix. For $\Gamma = \gamma^\mu$ or $\gamma^\mu\gamma_5$ their matrix elements are known to all orders in $\Lambda_{\rm QCD}/m_B$

$$\begin{aligned} \langle \overline{B}(p_B)|\, \bar b\, \gamma^\mu b\, |\overline{B}(p_B)\rangle &= 2p_B^\mu = 2m_B\, v^\mu\,, \\ \langle \overline{B}(p_B)|\, \bar b\, \gamma^\mu\gamma_5\, b\, |\overline{B}(p_B)\rangle &= 0\,. \end{aligned} \tag{1.142}$$

by conservation of the b quark number current and parity invariance of strong interactions, respectively. The matrix elements for other gamma matrices can be related by heavy quark symmetry to these plus order $\Lambda_{\rm QCD}^2/m_b^2$ corrections. Consequently, at the leading order in $\Lambda_{\rm QCD}/m_b$ inclusive decay rates are given by the rate for b quark decay, multiplied with a Wilson coefficient that does not depend on the decaying hadron.

To compute subleading corrections in $\Lambda_{\rm QCD}/m_b$, it is convenient to use HQET. There are no order $\Lambda_{\rm QCD}/m_b$ corrections because the matrix element of any gauge invariant dimension-4 two-quark operator vanishes,

$$\langle \overline{B}(v)|\, \bar h_v^{(b)}\, iD_\alpha \Gamma\, h_v^{(b)}\, |\overline{B}(v)\rangle = 0\,, \tag{1.143}$$

because contracting the left-hand side by v^α gives zero due to the equation of motion following from (1.127). Thus, the leading nonperturbative corrections to b quark decay occur at order $\Lambda_{\rm QCD}^2/m_b^2$. The operators that appear are again $O_{\rm kin}$ and $O_{\rm mag}$ so the same hadronic elements λ_1 and λ_2, defined in Eq. (1.129), appear again.

Combining the matrix elements from Eqs. (1.142), (1.143) and (1.129) with the Wilson coefficients leads to expressions of the form

$$\begin{aligned} \frac{{\rm d}^2\Gamma}{{\rm d}y\,{\rm d}q^2} = \begin{pmatrix} b \text{ quark} \\ \text{decay} \end{pmatrix} \times \Bigg\{ 1 + \frac{\alpha_s}{\pi}\, A_1 + \frac{\alpha_s^2}{\pi^2}\, A_2 + \ldots + \frac{f(\lambda_1,\lambda_2)}{m_B^2} \Big[1 + \mathcal{O}(\alpha_s) + \ldots \Big] \\ + \mathcal{O}(\Lambda_{\rm QCD}^3/m_B^3) + \ldots \Bigg\}\,. \end{aligned} \tag{1.144}$$

The differential rate may be integrated to obtain the full rate. The description in (1.144) is model independent, although λ_1 must be determined either from data [58] or from lattice

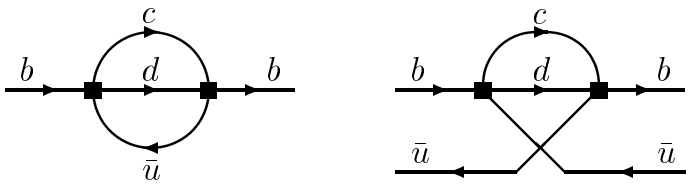

Figure 1.7: OPE diagrams for nonleptonic B decays. The left one is the leading contribution, while the "Pauli interference" diagram on the right corresponds to a dimension-6 contribution of order $16\pi^2\,(\Lambda_{\rm QCD}^3/m_B^3)$.

QCD [59]. For most quantities of interest the functions f, A_1, and the part of A_2 proportional to β_0, the first coefficient of the β-function, are known. Corrections to the $m_b \to \infty$ limit are expected to be under control in parts of the $\overline{B} \to X_q\,\ell\,\bar\nu$ phase space where several hadronic final states are allowed (but not required) to contribute with invariant mass and energy satisfying $m_X^2 \gg m_q^2 + \Lambda_{\rm QCD} E_X$.

1.5.3.2 Inclusive nonleptonic B decays

Inclusive nonleptonic decays can also be studied using the OPE, and much of the discussion in Sec. 1.5.3.1 applies here also. In this case, however, there are no "external" variables, such as q^2 and $q\cdot v$, since all particles in the final state interact strongly. For this reason, only the fully integrated inclusive width can be treated with the OPE, term-by-term in the weak Hamiltonian. For example, the B decay width corresponding to the $b\to c\bar u d$ effective Hamiltonian in (1.110)–(1.111) is given by

$$\begin{aligned}\Gamma &= \frac{1}{2m_B}\sum_X (2\pi)^4\,\delta^4(p_B - p_X)\,\Big|\langle X(p_X)|\,H^{|\Delta B|=1}(0)\,|\overline{B}(p_B)\rangle\Big|^2 \\ &= \frac{1}{2m_B}\,{\rm Im}\,\langle\overline{B}|\,i\int {\rm d}^4x\,T\left\{H^{|\Delta B|=1}(x)\,H^{|\Delta B|=1}(0)\right\}|\overline{B}\rangle\,. \end{aligned} \tag{1.145}$$

Because one has to use the OPE directly in the physical region, the results are more sensitive to violations of local duality than in the case of semileptonic and radiative decays. The leading term in the OPE corresponds to the left diagram in Fig. 1.7, whose imaginary part gives the total nonleptonic width.

The result is again of the form shown in Eq. (1.144). An important new ingredient at order $\Lambda_{\rm QCD}^3/m_B^3$ are certain contributions due to four-quark operators involving the spectator quark. They are usually called "weak annihilation", "W exchange", and "Pauli interference" contributions. (The last is sketched on the right in Fig. 1.7). They contain one less loop than the diagram on the left, so they are enhanced by a relative factor of $16\pi^2$. They are expected to be more important than the dimension-5 contributions proportional to λ_1 and λ_2. The matrix elements of the resulting four-quark operators are poorly known. Such contributions are expected to explain the $D^\pm - D^0$ lifetime difference.

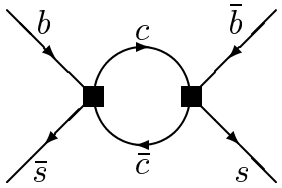

Figure 1.8: OPE diagram for the B_s width difference.

1.5.3.3 B_s width difference, $\Delta\Gamma$

Another important application, especially for the Tevatron, is for the B_s width difference. The off-diagonal element of the width matrix (cf., Sec. 1.3.2) is given by

$$\begin{aligned}\Gamma_{12} &= \frac{1}{2m_{B_s}} \sum_X (2\pi)^4\, \delta^4(p_{B_s} - p_X)\, \langle B_s |\, H^{|\Delta B|=1}\, |X\rangle\, \langle X|\, H^{|\Delta B|=1}\, |\overline{B}_s\rangle \\ &= \frac{1}{2m_{B_s}} \mathrm{Im}\, \langle B_s |\, i \int \mathrm{d}^4x\, T\left\{ H^{|\Delta B|=1}(x)\, H^{|\Delta B|=1}(0)\right\} |\overline{B}_s\rangle\,. \end{aligned} \tag{1.146}$$

The first line defines Γ_{12}, and the second line can be verified by inserting a complete set of intermediate states. The corresponding diagram is shown in Fig. 1.8. Γ_{12} arises from final states X which are common to both B_s and $\overline{B}_s$ decay. Therefore, the spectator quark is involved, and Eq. (1.146) is dominated by the $b \to c\bar{c}s$ part of the weak Hamiltonian, O_1 and O_2 in Eq. (1.112), with the others, O_3 through O_6, making very small contributions.

Thus, the naive estimate of the B_s width difference is $\Delta\Gamma_{B_s}/\Gamma_{B_s} = 2\,|\Gamma_{12}|\cos\phi/\Gamma_{B_s} \sim 16\pi^2(\Lambda^3_{\rm QCD}/m^3_B) \sim 0.1$. In the B_d system the common decay modes of B^0 and $\overline{B}^0$ are suppressed relative to the leading ones by the Cabibbo angle, and therefore the naive estimate is $\Delta\Gamma_{B_d}/\Gamma_{B_d} \lesssim 1\%$. See the discussion following (1.63) and Chapter 8 for more details.

1.5.4 Lattice QCD

If one considers the long term goal of "measuring" the Wilson coefficients of the electroweak Hamiltonian, as outlined elsewhere, then it is clear that it will be important to gain theoretical control over hadronic matrix elements. Since QCD is a completely well-defined quantum field theory, the calculation of hadronic matrix elements should be, in principle, possible. The main difficulty is that hadronic wavefunctions are sensitive mostly to the long distances where QCD becomes nonperturbative.

The difficulties of the bound-state problem in QCD led Wilson [60] to formulate gauge field theory on a discrete spacetime, or lattice. The basic idea starts with the functional integral for correlation functions in QCD

$$\langle O_1 \cdots O_n\rangle = \frac{1}{Z}\int \prod_{x,\mu} dA_\mu(x) \prod_x d\psi(x) d\bar{\psi}(x)\, O_1 \cdots O_n\, e^{-S_{\rm QCD}} \tag{1.147}$$

where Z is defined so that $\langle 1\rangle = 1$. For QCD A_μ is the gluon field, ψ and $\bar{\psi}$ are the quark and antiquark fields, and $S_{\rm QCD}$ is the QCD action. The O_i are operators for creating and

annihilating the hadrons of interest and also terms in the electroweak Hamiltonian. The continuous spacetime is then replaced with a discrete grid of points, or lattice. Then the quark variables live on sites; the gluons on links connecting the sites. With quarks on sites and gluons on links, it is possible to devise lattice actions that respect gauge symmetry. As in discrete approximations to partial differential equations, derivatives in the Lagrangian are replaced with difference operators.

The breakthrough of the lattice formulation is that it turns quantum field theory into a mathematically well-defined problem in statistical mechanics. Condensed matter theorists and mathematical physicists have devised a variety of methods for tackling such problems, only one of which is weak-coupling perturbation theory. In the years immediately following Wilson's work, many of these tools were tried, for example analytical strong coupling expansions. The strong coupling limit is especially appealing, because confinement emerges immediately [61].

Strong coupling is, however, not the whole story. Owing to asymptotic freedom, the continuum limit of lattice QCD is controlled by weak coupling. Unfortunately, strong coupling expansions do not converge quickly enough to reach into the weak-coupling regime, at least with the simple discretizations that have been used till now. Consequently, results from strong coupling expansions for hadron masses and matrix elements are not close enough to continuum QCD to apply to particle phenomenology.

Since such analytical methods have not borne out, the tool of choice now is to compute (the discrete version of) Eq. (1.147) numerically via Monte Carlo integration. This numerical method has, over the years, developed several specialized features, and corresponding jargon, that often make its results impenetrable to non-experts. Moreover, as with any numerical method, there are several sources of systematic uncertainty. Most of the systematic effects can, however, be controlled with effective field theories, i.e., with techniques like those explained in the previous sections. After reviewing the basic elements of the Monte Carlo method, we cover the systematic effects. First is the so-called quenched approximation, which is difficult to control, but also not a fundamental limitation. Other uncertainties, which can be controlled, are reviewed next, emphasizing the role of effective field theories. It is hoped that in this way non-experts can learn to make simple estimates of size systematic uncertainties, without repeating all the steps of the numerical analysis. We end with a comment on the (unsatisfactory) status of computing strong phase shifts for B decays.

1.5.4.1 Monte Carlo integration

This part of the method is well understood and, these days, rarely leads to controversy. For completeness, however, we include a short explanation, focusing on the points that limit the range of applicability of the method. A more thorough treatment aimed at experimenters can be found in Ref. [62].

The first salient observation is that there are very many variables. Continuum field theory has uncountably many degrees of freedom. Field theory on an infinite lattice still has an infinite number of degrees of freedom, but at least countably infinite. (This makes

the products over x in Eq. (1.147) well-defined.) To keep the number finite (for a computer with finite memory), one must also introduce a finite spacetime volume. This may seem alarming, but what one has done is simply to introduce an ultraviolet cutoff (the lattice) and an infrared cutoff (the finite volume). This is usual in quantum field theory, and field theoretic techniques can be used to understand how to extract cutoff-free quantities from numerically calculable cutoff quantities.

Even with a finite lattice, the number of integration variables is large. If one only demands a volume a few times the size of a hadron and also several grid points within a hadron's diameter, one already requires at least, say, 10 points along each direction. In four-dimensional spacetime this leads to $\sim 32 \times 10^4$ gluonic variables. With so many variables, the only feasible methods are based on Monte Carlo integration. The basic idea of Monte Carlo integration is simple: generate an ensemble of random variables and approximate the integrals in Eq. (1.147) by ensemble averages.

Quarks pose special problems, principally because, to implement Fermi statistics, fermionic variables are Grassmann numbers. In all cases of interest, the quark action can be written

$$S_F = \sum_{\alpha\beta} \bar{\psi}_\alpha M_{\alpha\beta} \psi_\beta, \tag{1.148}$$

where α and β are multi-indices for (discrete) spacetime, spin and internal quantum numbers. The matrix $M_{\alpha\beta}$ is some discretization of the Dirac operator $\not{D} + m$. Note that it depends on the gauge field, but one may integrate over the gauge fields after integrating over the quark fields. Then, because the quark action is a quadratic form, the integral can be carried out exactly:

$$\int \prod_{\alpha\beta} d\bar{\psi}_\alpha d\psi_\beta \, e^{-\bar{\psi} M \psi} = \det M. \tag{1.149}$$

Similarly, products $\psi_\alpha \bar{\psi}_\beta$ in the integrand are replaced with quark propagators $[M^{-1}]_{\alpha\beta}$. The computation of M^{-1} is demanding, and the computation of $\det M$ (or, more precisely, changes in $\det M$ as the gauge field is changed) is very demanding.

With the quarks integrated analytically, it is the gluons that are subject to the Monte Carlo method. The factor with the action is now $\det M e^{-S}$, where S is now just the gluons' action. Both $\det M$ and e^{-S} are the exponential of a number that scales with the spacetime volume. In Minkowski spacetime the exponent is an imaginary number, so there are wild fluctuations for moderate changes in the gauge field. On the other hand, in Euclidean spacetime, with an imaginary time variable, S is real. In that case (assuming $\det M$ is positive definite) one can devise a Monte Carlo with *importance sampling*, which means that the random number generator creates gauges field weighted according to $\det M e^{-S}$. Because importance sampling is essential, only in Euclidean spacetime is lattice QCD numerically tractable.

Importance sampling works well if $\det M$ is positive. For pairs of equal-mass quarks, this is easy to achieve. As a result, most calculations of $\det M$ are for 2 or 4 flavors. Note that a physically desirable situation with three flavors, with the strange quark's mass different from that of two lighter quarks, must either cope with (occasional) non-positive weights, or find a (new) discretization with $\det M$ positive flavor by flavor.

The choice of imaginary time has an important practical advantage. Consider the two-point correlation function

$$C_2(t) = \langle 0|\Phi_B(t)\Phi_B^\dagger(0)|0\rangle, \tag{1.150}$$

where Φ_B is an operator with the quantum numbers of the B meson at rest. Inserting a complete set of states between B and $B^\dagger$

$$C_2(t) = \sum_n \frac{1}{2m_n}\langle 0|\Phi_B|B_n\rangle\langle B_n|\Phi_B^\dagger|0\rangle e^{im_n t}, \tag{1.151}$$

where m_n is the mass of $|B_n\rangle$, the nth radial excitation of the B meson. For real t it would be difficult to disentangle all these contributions. If, however, $t = ix_4$, with x_4 real and positive, then one has a sum of damped exponentials. For large x_4 the lowest-lying state dominates and

$$C_2(x_4) = (2m_B)^{-1}|\langle 0|\Phi_B|B\rangle|^2 e^{-m_B x_4} + \cdots, \tag{1.152}$$

where $|B\rangle$ is the lowest-lying state and m_B its mass. The omitted terms are exponentially suppressed. It is straightforward to test when the first term dominates a numerically computed correlation function, and then fit the exponential form to obtain the mass.

This technique for isolating the lowest-lying state is essential also for obtaining hadronic matrix elements. For $B^0 - \overline{B}^0$ mixing, for example, one must compute the matrix element $\langle B^0|Q|\overline{B}^0\rangle$, given in Eq. (1.118). One uses a three-point correlation function

$$C_Q(x_4, y_4) = \langle 0|\Phi_B(x_4 + y_4)Q(y_4)\Phi_B(0)|0\rangle, \tag{1.153}$$

where only the Euclidean times of the operators have been written out. Inserting complete sets of states and taking x_4 and y_4 large enough,

$$C_Q(x_4, y_4) = (2m_B)^{-1}(2m_{\overline{B}})^{-1}\langle 0|\Phi_B|B\rangle\langle B|Q|\overline{B}\rangle\langle\overline{B}|\Phi_B|0\rangle e^{-m_B x_4 - m_{\overline{B}} y_4}. \tag{1.154}$$

The amplitude ($\langle 0|\Phi_B|B\rangle = \langle\overline{B}|\Phi_B|0\rangle$) and mass ($m_B = m_{\overline{B}}$) are obtained from C_2, leaving $\langle B|Q|\overline{B}\rangle$ to be determined from C_Q. Similarly, to obtain amplitudes for B decays to a single hadron (plus leptons or photons), simply replace one of the Φ_B operators with one for the desired hadron and Q with the desired operator. To compute the purely leptonic decay, simply replace Φ_B in C_2 with the charged current.

These methods are conceptually clean and technically feasible for the calculation of masses and hadronic matrix elements with at most one hadron in the final state. The procedure for computing correlation functions is as follows. First generate an ensemble of lattice gluon fields with the appropriate weight. Next form the desired product $O_1 \cdots O_n$, with quark variables exactly integrated out to form propagators M^{-1}. Then take the average over the ensemble. Finally, fit the Euclidean time dependence of Eqs. (1.152) and (1.154). Note that since the same ensemble is used for many similar correlation functions, the statistical fluctuations within the ensemble are correlated. This is not a concern, as long as the correlations are propagated sensibly through the analysis.

1.5.4.2 Quenched approximation

Any perusal of the literature on lattice QCD quickly comes across something called the "quenched approximation." As mentioned above, the factor $\det M$ in Eq. (1.149) is difficult to incorporate. The determinant generates sea quarks inside a hadron. The quenched approximation replaces $\det M$ with 1 *and* compensates the corresponding omission of the sea quarks with shifts in the bare couplings. This is analogous to a dielectric approximation in electromagnetism, and it fails under similar circumstances. In particular, if one is interested in comparing two quantities that are sensitive to somewhat different energy scales, one cannot expect the same dielectric shift to suffice. Another name for the quenched approximation is the "valence" approximation, which makes clearer that the valence quarks (and gluons) in hadrons are treated fully, and the sea quarks merely modeled.

It is not easy to estimate quantitatively the effect of quenching. For α_s [63] and the quark masses [64] one can compute the short distance contribution to the quenching shift, but that is only a start. The quenched approximation can be cast as the first term in a systematic expansion [65], but it is about as difficult to compute the next term as to restore the fermion determinant. In the context of heavy quark physics one should note that the CP-PACS [66] and MILC [67] groups now have unquenched calculations of the heavy-light decay constants f_B, f_{B_s}, f_D, and f_{D_s}. Both have results at several lattice spacings, so they can study the a dependence. Their results are about 10–15% higher than the most mature estimates from the quenched approximation.

1.5.4.3 Controllable systematic uncertainties

By a controllable systematic uncertainty we mean an uncertainty that can be incrementally improved in a well-defined way. In lattice QCD they arise from the ultraviolet and infrared cutoffs, and also from the fact that quark masses are freely adjustable and, for technical reasons, not always adjusted to their physical values. Because these effects are subject to theoretical control, the errors they introduce can largely be reduced to a level that is essentially statistical, given enough computing.

One of the least troublesome systematic effects comes from the finite volume. Finite-volume effects can be understood separately from lattice-spacing effects with an effective massive quantum field theory [68]. In some cases adjusting the volume at will is, at least in principle, a boon, yielding valuable information, such as scattering lengths and resonance widths.

The computer algorithms for computing the quark propagator M^{-1} converge more quickly at masses near that of the strange quark than for lighter masses. Consequently, the Monte Carlo is run at a sequence of light quark masses typically in the range $0.2m_s \lesssim m_q \lesssim m_s$. (The up and down quark masses are far smaller still and not reached.) The dependence on m_q can be understood and controlled via the chiral Lagrangian [69], another effective field theory. A recent development is to show in detail how to extract physical information from results at practical values of the light quark masses [70].

A special difficulty with heavy quarks is the effect of non-zero lattice spacing. The

bottom and charmed quark masses are large in lattice units. For this reason it is frequently (but incorrectly) stated that heavy quarks cannot be directly accommodated by a lattice. From the inception of HQET and NRQCD, these effective field theories have been used to treat heavy quarks, and more recently it has been shown how to use these tools to understand the discretization effects of heavy quarks discretized with the original Wilson formulation [71].

Let us first recall how lattice-spacing effects are controlled for systems of light quarks. Long ago, Symanzik introduced a local effective Lagrangian (LE$\mathcal{L}$) to describe cutoff effects [72]. One writes

$$\mathcal{L}_{\rm lat} \doteq \mathcal{L}_{\rm cont} + \sum_i a^{s_{\mathcal{O}_i}} K_i(a;\mu)\mathcal{O}_i(\mu), \tag{1.155}$$

where $s_{\mathcal{O}_i} = \dim \mathcal{O}_i - 4$. The symbol $\doteq$ means "has the same (on-shell) matrix elements as". For operators such as Q, needed for mixing,

$$Q_{\rm lat} \doteq Z_Q^{-1}(a;\mu) Q_{\rm cont}(\mu) + \sum_i a^{s_{\mathcal{Q}_i}} C_i(a;\mu)\,\mathcal{Q}_i(\mu), \tag{1.156}$$

where now $s_{\mathcal{Q}_i} = \dim \mathcal{Q}_i - \dim Q$. The continuum operators $\mathcal{O}_i$, $Q_{\rm cont}$, and $\mathcal{Q}_i$ are defined in a mass-independent scheme at scale μ. They do not depend on the lattice spacing a. The coefficients K_i, Z_Q, and C_i account for short distance effects, so they do depend on a.

If a is small enough the higher terms can be treated as perturbations. So, the a dependence of $\langle B|Q_{\rm lat}|\overline{B}\rangle$ is

$$\langle B|Q_{\rm lat}|\overline{B}\rangle = Z_Q^{-1}\langle B|Q_{\rm cont}|\overline{B}\rangle + aK_{\sigma F}\langle B|T\,Q_{\rm cont}\int d^4x\,\bar\psi\sigma\cdot F\psi|\overline{B}\rangle + aC_1\langle B|\mathcal{Q}_1|\overline{B}\rangle, \tag{1.157}$$

keeping only contributions of order a. To reduce the unwanted terms one might try to reduce a greatly, but CPU time goes as $a^{-(5\text{ or }6)}$. It is more effective to use a sequence of lattice spacings and extrapolate, with Eq. (1.157) as a guide. It is even better to adjust things so $K_{\sigma F}$ and K_1 are $\mathcal{O}(\alpha_s^\ell)$ [73] or $\mathcal{O}(a)$ [74], which is called Symanzik improvement. For light hadrons, a combination of improvement and extrapolation is best. Note that one still has to adjust $Q_{\rm lat}$ so that $Z_Q = 1$. In some cases the needed adjustment can be made nonpertubatively, even though it is a short distance quantity. When that is possible, lattice QCD can provide results with no perturbative uncertainty, although perturbative uncertainty may reenter through the electroweak Hamiltonian.

The Symanzik theory, as usually applied, assumes $m_q a \ll 1$. The bottom and charmed quarks' masses in lattice units are at present large: $m_b a \sim$ 1–2 and $m_c a$ about a third of that. It will not be possible to reduce a enough to make $m_b a \ll 1$ for many, many years. So, other methods are needed to control the lattice spacing effects of heavy quarks. There are several alternatives:

1. static approximation [75]
2. lattice NRQCD [76]
3. extrapolation from $m_Q \lesssim m_c$ up to m_b

3′. combine 3 with 1

4. normalize systematically to HQET [77]

5. anisotropic lattices with temporal lattice spacing $a_t \ll a$ [78]

All but the last use the heavy quark expansion in some way. The first two discretize continuum HQET; method 1 stops at the leading term, and method 2 carries the heavy quark expansion out to the desired order. Methods 3 and 3′ keep the heavy quark mass artificially small and appeal to the $1/m_Q$ expansion to extrapolate back up to m_b. Method 4 uses the same lattice action as method 3, but uses the heavy quark expansion to normalize and improve it. Methods 2 and 4 are able to calculate matrix elements directly at the b-quark mass. Method 5 has only recently been applied to heavy-light mesons [79], and, like the other methods, it requires that spatial momenta are much less than m_Q.

The methods can be compared and contrasted by *describing* the lattice theories with HQET [80]. This is, in a sense, the opposite of *discretizing* HQET. One writes down a (continuum) effective Lagrangian

$$\mathcal{L}_{\rm lat} \doteq \sum_n \mathcal{C}^{(n)}_{\rm lat}(m_Q a;\mu) O^{(n)}_{\rm HQET}(\mu), \tag{1.158}$$

with the operators $O^{(n)}_{\rm HQET}$ defined exactly as in Sec. 1.5.2, so they do not depend on m_Q or a. As long as $m_Q \gg \Lambda_{\rm QCD}$ this description makes sense. There are two short distances, $1/m_Q$ and the lattice spacing a, so the short distance coefficients $\mathcal{C}^{(n)}_{\rm lat}$ depend on $m_Q a$. Since all dependence on $m_Q a$ is isolated into the coefficients, this description shows that heavy quark lattice artifacts arise only from the mismatch of the $\mathcal{C}^{(n)}_{\rm lat}$ and their continuum analogs $\mathcal{C}^{(n)}_{\rm cont}$.

For methods 1 and 2, Eq. (1.158) is just a Symanzik LE$\mathcal{L}$. For lattice NRQCD we recover the result that some of the coefficients $\mathcal{C}^{(n)}_{\rm lat}$ have power-law divergences as $a \to 0$ [76]. So, to obtain continuum (NR)QCD, one must add more and more terms to the action. (This is just a generic feature of effective field theories, namely, that accuracy is improved by adding more terms, rather than taking the cutoff too high.) The truncation leaves a systematic error, which, in practice, is usually accounted for conservatively.

Eq. (1.158) is more illuminating for methods 3–5, which use the same actions, but with different normalization conditions. The lattice quarks are Wilson fermions [71], which have the same degrees of freedom and heavy quark symmetries as continuum quarks. Thus, the HQET description is admissible for all $m_Q a$. Method 4 matches the coefficients of Eq. (1.158) term by term to Eq. (1.127), by adjusting the lattice action and operators. In practice, this is possible only to finite order, so there are errors $(\mathcal{C}^{(n)}_{\rm lat} - \mathcal{C}^{(n)}_{\rm cont})\langle O^{(n)}_{\rm HQET}\rangle$. The rough size of matrix element here is $\Lambda_{\rm QCD}^{\dim O-4}$. The coefficients balance the dimensions with a and $1/m_Q$. If $\mathcal{C}^{(n)}_{\rm lat}$ is matched to $\mathcal{C}^{(n)}_{\rm cont}$ in perturbation theory, the difference is of order α_s^ℓ. Method 3 artificially reduces $m_Q a$ until the mismatch is of order $(m_Q a)^2$. This would be fine if $m_Q a$ were small enough, but with currently available lattices, $m_Q a$ is small only if m_Q is reduced until the heavy quark expansion falls apart. In method 5 the temporal

lattice spacing a_t is smaller than the spatial lattice spacing. The behavior of the mismatch $\mathcal{C}^{(n)}_{\rm lat} - \mathcal{C}^{(n)}_{\rm cont}$ for practical values of m_Q and a_t is still an open question [81].

The non-expert can get a feel for which methods are most appropriate by asking himself what order in $\Lambda_{\rm QCD}/m_b$ is needed. For zeroth order, method 1 will do. Perhaps the only quantity where this is sufficiently accurate is the mass of the b quark, where the most advanced calculation [82] neglects the subleading term λ_1/m_b in Eq. (1.130). For matrix elements, the first non-trivial terms are those of Eq. (1.128), so the other methods must be used. With method 3 one should check that $m_Q/\Lambda_{\rm QCD}$ is large enough; so far, all work with this method is worrisome in this respect.

Most of the matrix elements that are of interest to B physics will soon be recalculated, like f_B [66,67] and m_b [82], with two flavors of sea quarks. It seems, therefore, not useful tabulate quenched results. One can consult recent reviews focusing on the status of matrix elements instead [83].

1.5.4.4 Strong phases of nonleptonic decays

In considering CP asymmetries one encounters strong phase shifts. It is therefore interesting to consider computing them in lattice QCD.

A short summary is that this is still an unsolved problem, at least for inelastic decays, such as B decays. This does not mean that it is an unsolvable problem, but at this time numerical lattice calculations are not helpful for computing scattering phases above the inelastic threshold.

Often an even bleaker picture is painted, based on a superficial understanding a theorem of Maiani and Testa [84]. The theorem assumes an infinite volume and is, thus, relevant only to extremely large volumes. In volumes of (2–6 fm)^3 it is possible to disentangle phase information, because the scattering phase shift enters into the finite-volume boundary conditions of the final-state two-body wave function [85]. This works, however, only in the kinematic region with two-body final states. This has been worked out explicitly for kaon decays [86], giving also references to earlier work.

1.6 Constraints from Kaon Physics

There are two strong reasons for the discussion of the neutral kaon system in a report on B physics. First, for more than 30 years the only observation of CP violation was in the neutral kaon system. Over these years the formalism used to describe CP violation has changed, partly because our theoretical understanding of the subject has improved. One example of this development is the present classification of three, rather than two, types of CP violation, as explained in Sec. 1.4.1. Second, the Standard Model expresses all CP violating quantities in terms of the same CKM phase. The consistency of the experiments in B physics with those in the kaon system therefore provides a stringent test of the Standard Model. In practice both B and K data are used to overconstrain the unitarity triangle: the indirect constraints on $\sin 2\beta$, in particular its sign, rely largely on ϵ_K. Any future

inconsistency in the overdetermined unitarity triangle indicates new physics either in the B or K system or in both.

Sec.1.6.1 describes the neutral kaon system with the modern formalism and makes contact with the formalism traditionally used for kaon physics. To show how kaon measurements shape our expectations for B physics, Sec. 1.6.2 discusses the already measured CP violating quantities ϵ_K and ϵ'_K. In a similar vein, Sec. 1.6.3 deals with the rare decays $K^+ \to \pi^+ \nu\bar{\nu}$ and $K_L \to \pi^0 \nu\bar{\nu}$, which are the target of new high-precision kaon experiments.

1.6.1 The neutral kaon system

CP violation in $K^0 - \overline{K}^0$ mixing was discovered in 1964 [31]. The quantity ϵ_K, which is discussed in Sec. 1.6.2, is of key importance to test the CKM mechanism of CP violation, because new physics enters K and B physics in different ways. We introduce the neutral kaon system using the same formalism as for the B-meson system as derived in Sec. 1.3 and translate it to the traditional notation.

The lighter mass eigenstate of the neutral kaon is $|K_S\rangle$ and the heavier one is $|K_L\rangle$, where the subscripts refer to their short and long lifetimes. They are

$$\begin{aligned} |K_S\rangle &= p\,|K^0\rangle + q\,|\overline{K}^0\rangle = \frac{(1+\overline{\epsilon})\,|K^0\rangle - (1-\overline{\epsilon})\,|\overline{K}^0\rangle}{\sqrt{2\,(1+|\overline{\epsilon}|^2)}}\,, \\ |K_L\rangle &= p\,|K^0\rangle - q\,|\overline{K}^0\rangle = \frac{(1+\overline{\epsilon})\,|K^0\rangle + (1-\overline{\epsilon})\,|\overline{K}^0\rangle}{\sqrt{2\,(1+|\overline{\epsilon}|^2)}}\,. \end{aligned} \tag{1.159}$$

The quantity

$$\overline{\epsilon} = \frac{1+q/p}{1-q/p} \tag{1.160}$$

depends on phase conventions. (The parameter $\overline{\epsilon}$ is not to be confused with the well-known parameter ϵ_K, defined in (1.169).)

CP conservation in $|\Delta S| = 2$ transitions corresponds to $\overline{\epsilon} = 0$, in which case $|K_S\rangle$ and $|K_L\rangle$ become the CP even and CP odd eigenstates. CP violation in mixing is well-established from the semileptonic CP asymmetry

$$\begin{aligned} \delta(\ell) &= \frac{\Gamma(K_L \to \ell^+ \nu\,\pi^-) - \Gamma(K_L \to \ell^- \bar{\nu}\,\pi^+)}{\Gamma(K_L \to \ell^+ \nu\,\pi^-) + \Gamma(K_L \to \ell^- \bar{\nu}\,\pi^+)} \\ &= \frac{1-|q/p|^2}{1+|q/p|^2} = \frac{2\,\mathrm{Re}\,\overline{\epsilon}}{1+|\overline{\epsilon}|^2} \;=\; (3.27 \pm 0.12) \times 10^{-3}\,. \end{aligned} \tag{1.161}$$

The quoted numerical value is the average for $\ell = e$ and μ [15]. From (1.161) it is clear that in the kaon system $|q/p|$ is close to one. In the B systems $|q/p|$ is close to one because the width difference is smaller than the mass difference. Here, however, they are comparable [15]

$$\Delta m_K = (0.5301 \pm 0.0014) \times 10^{10}\, s^{-1}, \qquad \Delta\Gamma_K = (1.1174 \pm 0.0010) \times 10^{10}\, s^{-1}\,. \tag{1.162}$$

Hence one concludes that $|q/p| - 1$ is so small, because the relative phase ϕ between M_{12} and $-\Gamma_{12}$ (cf., (1.62)) is close to zero. Expanding in ϕ one easily finds from (1.61) that

$$|M_{12}| = \frac{\Delta m_K}{2} + \mathcal{O}\left(\phi^2\right), \qquad |\Gamma_{12}| = \frac{\Delta\Gamma_K}{2} + \mathcal{O}\left(\phi^2\right), \tag{1.163a}$$

$$\frac{q}{p} = -e^{-i\phi_M}\left[1 - \phi\,\frac{\Delta\Gamma_K/2}{\Delta m_K + i\,\Delta\Gamma_K/2} + \mathcal{O}\left(\phi^2\right)\right]. \tag{1.163b}$$

Hence (1.163b) and (1.161) allow us to solve for the CP violating phase ϕ:

$$\phi = \frac{(\Delta m_K)^2 + (\Delta\Gamma_K/2)^2}{\Delta m_K \Delta\Gamma_K/2}\,\delta(\ell) \;+\; \mathcal{O}\left(\phi^2\right) = (6.6 \pm 0.2)\cdot 10^{-3}. \tag{1.164}$$

In the literature on $K \to \pi\pi$ decays the following amplitude ratios are introduced:

$$\eta_{+-} = \frac{\langle \pi^+\pi^-|K_L\rangle}{\langle \pi^+\pi^-|K_S\rangle}, \qquad \eta_{00} = \frac{\langle \pi^0\pi^0|K_L\rangle}{\langle \pi^0\pi^0|K_S\rangle}. \tag{1.165}$$

If CP were conserved, both would vanish. The moduli and phases of η_{+-} and η_{00} have been measured to be

$$\begin{aligned} |\eta_{+-}| &= (2.285 \pm 0.019)\cdot 10^{-3}, \qquad \phi_{+-} = 43.5^\circ \pm 0.6^\circ, \\ |\eta_{00}| &= (2.275 \pm 0.019)\cdot 10^{-3}, \qquad \phi_{00} = 43.4^\circ \pm 1.0^\circ, \end{aligned} \tag{1.166}$$

according to the PDG fit [15]. All three types of CP violation lead to non-zero η_{+-} and η_{00}. To separate $|\Delta S| = 2$ from $|\Delta S| = 1$ CP violation one introduces isospin states

$$\begin{aligned} |\pi^0\pi^0\rangle &= \sqrt{\frac{1}{3}}\,|\,(\pi\pi)_{I=0}\rangle - \sqrt{\frac{2}{3}}\,|\,(\pi\pi)_{I=2}\rangle, \\ |\pi^+\pi^-\rangle &= \sqrt{\frac{2}{3}}\,|\,(\pi\pi)_{I=0}\rangle + \sqrt{\frac{1}{3}}\,|\,(\pi\pi)_{I=2}\rangle, \end{aligned}$$

and isospin amplitudes

$$A_I = \langle (\pi\pi)_I\,|K^0\rangle, \qquad \overline{A}_I = \langle (\pi\pi)_I\,|\overline{K}^0\rangle, \qquad I = 0, 2. \tag{1.167}$$

The strong final state interaction of the two-pion final states is highly constrained by kinematics and conservation laws: the CP invariance of the strong interaction forbids a two-pion state to scatter into a three-pion state and the rescattering into a state with four or more pions is kinematically forbidden. Furthermore, isospin is an almost exact symmetry of QCD and forbids the rescattering between the two isospin eigenstates. Hence the final state interaction of the $I = 0$ and $I = 2$ states is only elastic and, thus, fully described by two scattering phases. This feature is known as *Watson's theorem* [87]. Hence we can write

$$\begin{aligned} A_I &= |A_I| e^{i\Phi_I} e^{i\delta_I}, \qquad \overline{A}_I = -|A_I| e^{-i\Phi_I} e^{i\delta_I}, \\ \lambda_I &= \frac{q}{p}\frac{\overline{A}_I}{A_I} = e^{-i(2\Phi_I + \phi_M)}\left[1 - \phi\frac{\Delta\Gamma_K/2}{\Delta m_K + i\,\Delta\Gamma/2}\right] + \mathcal{O}(\phi^2), \end{aligned} \tag{1.168}$$

where the two scattering phases δ_I are empirically determined to be $\delta_0 \approx 37^\circ$ and $\delta_2 \approx -7^\circ$. Several weak amplitudes (with different CP violating phases) contribute to $|A_I| e^{i\Phi_I}$, but the presence of a single strong phase allows to write A_I as in (1.168), ensuring $|\overline{A}_I/A_I| = 1$. Therefore, there is no direct CP violation in $K \to (\pi\pi)_I$. Note that our definition of A_0 and A_2 includes both the weak and strong phases, in accordance with the formalism used in B physics. In the kaon literature the A_I's are commonly defined without the factors $e^{i\delta_I}$.

A simplification arises from the experimental observation that $|A_0| \simeq 22\,|A_2|$, which is called $\Delta I = 1/2$ rule. This enhancement of $|A_0|$ allows to expand in $|A_2/A_0|$. The CP violating quantity ϵ_K reads

$$\epsilon_K = \frac{\eta_{00} + 2\,\eta_{+-}}{3} = \frac{\langle(\pi\pi)_{I=0}|K_L\rangle}{\langle(\pi\pi)_{I=0}|K_S\rangle}\left[1 + \mathcal{O}\left(\frac{A_2^2}{A_0^2}\right)\right] = \frac{1-\lambda_0}{1+\lambda_0}\,. \tag{1.169}$$

Hence ϵ_K is defined in a way that to zeroth and first order in A_2/A_0 only a single strong amplitude contributes and therefore CP violation in decay is absent. The $I = 0$ two-pion state dominates the K_S width Γ_S. Thus $\langle K^0|(\pi\pi)_{I=0}\rangle\langle(\pi\pi)_{I=0}|\overline{K}^0\rangle$ almost saturates Γ_{12}, so that the phase $\phi_M - \phi$ of $-\Gamma_{12}$ equals $-2\Phi_0$ up to tiny corrections of order A_2^2/A_0^2 and Γ_L/Γ_S. This implies that ϵ_K does not provide any additional information compared to the semileptonic asymmetry in (1.161). We find from (1.168)

$$\lambda_0 = 1 - i\,\phi\frac{\Delta m_K}{\Delta m_K + i\,\Delta\Gamma_K} + \mathcal{O}\left(\phi^2, \frac{A_2^2}{A_0^2}, \frac{\Gamma_L}{\Gamma_S}\right), \tag{1.170}$$

and (1.169) evaluates to

$$\epsilon_K = \frac{\phi}{2}\frac{\Delta m_K}{\sqrt{(\Delta m_K)^2 + (\Delta\Gamma_K/2)^2}}\,e^{i\phi_\epsilon} + \mathcal{O}\left(\phi^2, \frac{A_2^2}{A_0^2}, \frac{\Gamma_L}{\Gamma_S}\right) \quad \text{with} \quad \phi_\epsilon = \arctan\frac{\Delta m_K}{\Delta\Gamma_K/2}\,. \tag{1.171}$$

From (1.166) one finds the experimental value:

$$\epsilon_K = e^{i\,(0.97\pm0.02)\,\pi/4}\,(2.28 \pm 0.02) \times 10^{-3}\,. \tag{1.172}$$

Therefore (1.171) yields

$$\phi = (6.63 \pm 0.06) \times 10^{-3}\,, \tag{1.173}$$

in perfect agreement with (1.164). A numerical accident leads to $\Delta m_K \approx \Delta\Gamma_K/2$, which explains why the phase ϕ_ϵ in (1.171) is so close to $\pi/4$.

To first order in ϕ one finds from (1.169)

$$\epsilon_K \simeq \frac{1}{2}\,[1 - \lambda_0] \;\simeq\; \frac{1}{2}\left(1 - \left|\frac{q}{p}\right| - i\,\mathrm{Im}\,\lambda_0\right). \tag{1.174}$$

Therefore $\mathrm{Re}\,\epsilon_K$ measures CP violation in mixing and $\mathrm{Im}\,\epsilon_K$ measures interference type CP violation.

CP violation in $|\Delta S| = 1$ transitions is characterized by

$$\epsilon'_K = \frac{\eta_{+-} - \eta_{00}}{3} = \frac{\epsilon_K}{\sqrt{2}} \left[\frac{\langle (\pi\pi)_{I=2} | K_L \rangle}{\langle (\pi\pi)_{I=0} | K_L \rangle} - \frac{\langle (\pi\pi)_{I=2} | K_S \rangle}{\langle (\pi\pi)_{I=0} | K_S \rangle} \right] \left[1 + \mathcal{O}\left(\frac{A_2}{A_0} \right) \right]$$
$$= \frac{A_2}{A_0} \frac{1}{\sqrt{2}} \left[\frac{1-\lambda_2}{1+\lambda_0} - \frac{(1-\lambda_0)(1+\lambda_2)}{(1+\lambda_0)^2} \right]. \tag{1.175}$$

Next we use

$$\lambda_2 = \lambda_0 \, e^{2\,i\,(\Phi_0 - \Phi_2)}\,, \tag{1.176}$$

and expand to first order in the small phases:

$$\epsilon'_K = \frac{1}{2\sqrt{2}} \frac{A_2}{A_0} (\lambda_0 - \lambda_2) + \mathcal{O}\left(\frac{A_2^2}{A_0^2}, \phi^2, (\Phi_0 - \Phi_2)^2 \right) = \frac{1}{\sqrt{2}} \frac{A_2}{A_0} \, i \, (\Phi_2 - \Phi_0)\,. \tag{1.177}$$

A non-vanishing value of ϵ'_K implies different CP violating phases in the two isospin amplitudes and therefore $|\Delta S| = 1$ CP violation. Since experimentally $\mathrm{Re}\,\epsilon'_K > 0$, one finds $\Phi_2 > \Phi_0$. The phase of ϵ'_K is $90^\circ + \delta_2 - \delta_0 \simeq 46^\circ$ and ϵ'_K/ϵ_K is almost real and positive.

Since (1.177) does not depend on q/p, there is no contribution from CP violation in mixing to ϵ'_K. The strong phases drop out in the combination

$$\mathrm{Im}\,\frac{A_0}{A_2}\,\epsilon'_K \simeq \frac{1}{2\sqrt{2}} \left(\mathrm{Im}\,\lambda_0 - \mathrm{Im}\,\lambda_2 \right). \tag{1.178}$$

Since we work to first order in ϕ, we can set $|\lambda_I| = 1$, and therefore (1.178) purely measures interference type CP violation. From the definition in (1.175) one further finds that

$$\mathrm{Re}\,\epsilon'_K \simeq \frac{1}{6} \left(1 - \left| \frac{A_{\pi^0\pi^0}\,\overline{A}_{\pi^+\pi^-}}{\overline{A}_{\pi^0\pi^0}\,A_{\pi^+\pi^-}} \right| \right) \simeq \frac{1}{\sqrt{2}} \frac{|A_2|}{|A_0|} \sin(\delta_0 - \delta_2)\,(\Phi_2 - \Phi_0) \tag{1.179}$$

originates solely from $|\overline{A}_f/A_f| \neq 1$. Hence $\mathrm{Re}\,\epsilon'_K$ measures CP violation in decay.

Experimentally the quantity $|\eta_{00}/\eta_{+-}|^2 = 1 - 6\,\mathrm{Re}\,\epsilon'_K/\epsilon_K$ has been determined. Recent results are

$$\mathrm{Re}\,\frac{\epsilon'_K}{\epsilon_K} = (20.7 \pm 2.8) \times 10^{-4} \qquad (\mathrm{KTeV}) \quad [88]\,,$$
$$\mathrm{Re}\,\frac{\epsilon'_K}{\epsilon_K} = (15.3 \pm 2.6) \times 10^{-4} \qquad (\mathrm{NA48}) \quad [89]. \tag{1.180}$$

We therefore find from (1.177) that the difference of the CP violating phases is tiny:

$$\Phi_2 - \Phi_0 = (1.5 \pm 0.2) \cdot 10^{-4} \quad (\mathrm{KTeV})\,, \qquad \Phi_2 - \Phi_0 = (1.1 \pm 0.2) \cdot 10^{-4} \quad (\mathrm{NA48})\,. \tag{1.181}$$

1.6.2 Phenomenology of ϵ_K and ϵ'_K

In order to exploit the precise measurement of $\phi = -\arg M_{12}/\Gamma_{12}$ from ϵ_K in (1.173) one must calculate the phases of

$$M_{12} = \frac{1}{2m_K} \langle K^0 | H^{|\Delta S|=2} | \overline{K}^0 \rangle - \mathrm{Disp}\,\frac{i}{4m_K} \int \mathrm{d}^4x \, \langle K^0 | H^{|\Delta S|=1}(x)\, H^{|\Delta S|=1}(0) | \overline{K}^0 \rangle\,. \tag{1.182}$$

and

$$\Gamma_{12} = \mathrm{Abs}\,\frac{i}{2m_K}\int \mathrm{d}^4x\,\langle K^0|H^{|\Delta S|=1}(x)\,H^{|\Delta S|=1}(0)|\overline{K}^0\rangle \qquad (1.183)$$
$$= \frac{1}{2m_K}\sum_f (2\pi)^4\delta^4(p_K-p_f)\langle K^0|H^{|\Delta S|=1}|f\rangle\,\langle f|H^{|\Delta S|=1}|\overline{K}^0\rangle \simeq \frac{1}{2m_K}\,A_0^*\,\overline{A}_0\,.$$

Here Abs denotes the absorptive part of the amplitude. It is calculated by retaining only the imaginary part of the loop integration while keeping both real and imaginary parts of complex coupling constants. Analogously, the dispersive part Disp is obtained from the real part of the loop integral.

The second term in (1.182) shows that, at second order, also the $|\Delta S| = 1$ Hamiltonian contributes to M_{12}. In the B system the corresponding contribution is negligibly small. The Standard Model $|\Delta S| = 2$ Hamiltonian reads

$$H^{|\Delta S|=2} = \frac{G_F^2}{4\pi^2}\,M_W\,\Big[\lambda_c^{*2}\,\eta_1\,S(x_c)\;+\;\lambda_t^{*2}\,\eta_2\,S(x_t)$$
$$+\,2\,\lambda_c^*\,\lambda_t^*\,\eta_3\,S(x_c,x_t)\Big]\,b_K(\mu)\,Q_K(\mu) + \mathrm{h.c.} \qquad (1.184)$$

It involves the $|\Delta S| = 2$ operator

$$Q_K(\mu) = \overline{d}_L\gamma_\nu s_L\,\overline{d}_L\gamma^\nu s_L\,. \qquad (1.185)$$

In (1.184) $\lambda_q = V_{qd}V_{qs}^*$, $x_q = m_q^2/M_W^2$ and $S(x)$ is the Inami-Lim function introduced in (1.120). The third function $S(x_c, x_t)$ comes from the box diagram with one charmed and one top quark. One finds $S(x_c) \simeq x_c$, $S(x_c, x_t) \simeq x_c(0.6 - \ln x_c)$ and $S(x_t) \simeq 2.4$ for $m_t \simeq 167\,\mathrm{GeV}$ in the $\overline{\mathrm{MS}}$ scheme. Short distance QCD corrections are contained in the η_i's. In the $\overline{\mathrm{MS}}$ scheme the next-to-leading order results are $\eta_1 = 1.4 \pm 0.3$, $\eta_2 = 0.57 \pm 0.01$ and $\eta_3 = 0.47 \pm 0.04$ [90]. η_1 strongly depends on m_c and α_s, the quoted range corresponds to $m_c = 1.3\,\mathrm{GeV}$. A common factor of the QCD coefficients is $b_K(\mu)$, the kaon analogue of $b_B(\mu)$ encountered in (1.119). The matrix element of Q_K is parameterized as

$$\langle K^0|Q_K(\mu)|\overline{K}^0\rangle = \frac{2}{3}\,f_K^2\,m_K^2\,\frac{\widehat{B}_K}{b_K(\mu)}\,, \qquad (1.186)$$

where f_K is the kaon decay constant.

CP violation in the kaon system is related to the squashed unitarity triangle with sides $|\lambda_u|$, $|\lambda_c|$ and $|\lambda_t|$. In the limit $\lambda_t = 0$ all CP violation vanishes, thus CP violation is governed by the small parameter $\mathrm{Im}\,(\lambda_t/\lambda_u)$. This explains the smallness of the measured phases in (1.173) and (1.181). This pattern is a feature of the CKM mechanism of CP violation and need not hold in extensions of the Standard Model. Hence kaon physics provides a fertile testing ground for non-standard CP violation related to the first two quark generations.

The presence of the second term in (1.182) impedes the clean calculation of the mixing phase $\phi_M = \arg M_{12}$ in terms of the CKM phases. It constitutes a long distance contribution, which is not proportional to $\widehat{B}_K$. Since both terms in (1.182) have different weak

phases, ϕ_M involves the ratio of the two hadronic matrix elements. This is different from the case in $B^0-\overline{B}^0$ mixing where only one hadronic matrix element contributes in the Standard Model, which therefore cancels from ϕ_M. The long distance $|\Delta S|=1$ piece is hard to calculate and is usually eliminated with the help of the experimental value of $\Delta m_K = 2\,|M_{12}|$ in (1.162). Then, however, our expression for the mixing phase ϕ_M still depends on the hadronic parameter $\widehat{B}_K$.

The phases of both ϕ_M and $\arg\Gamma_{12}$ are close to $\arg\lambda_u$, which vanishes in the CKM phase convention. The dominant corrections to ϕ_M stems from the term proportional to λ_t^{*2} in $H^{|\Delta S|=2}$. For $\arg\Gamma_{12}$ we need the $|\Delta S|=1$ Hamiltonian, which is obtained from the $|\Delta B|=1$ Hamiltonian in (1.115) by replacing $\xi_{u,c,t}$ with $\lambda_{u,c,t}$ and replacing the b quark field in the operators by an s field. The leading contribution to $\arg(-\Gamma_{12}) \approx -2\,\Phi_0$, is proportional to $\mathrm{Im}\,\lambda_t\,\langle(\pi\pi)_{I=0}|Q_6|\overline{K}^0\rangle/|A_0|$. The $\Delta I=1/2$ enhancement of $|A_0|$ suppresses Φ_0, which is calculated to $\Phi_0 = \mathcal{O}(2\cdot 10^{-4})$ [91]. Hence in the CKM phase convention $\arg(-\Gamma_{12})$ contributes roughly 6% to the measured phase ϕ in (1.173) and one can approximate $\phi \approx \phi_M$. After expressing the CKM elements in (1.184) in terms of the improved Wolfenstein parameters the constraint from the measured value in (1.173) can be cast in the form [90,92]

$$5.3\times 10^{-4} = \widehat{B}_K A^2\,\overline{\eta}\,\left\{[1-\overline{\rho}+\Delta\,(\overline{\rho},\overline{\eta})]\,A^2\lambda^4\eta_2\,S(x_t)+\eta_3 S(x_c,x_t)-\eta_1 x_c\right\}. \qquad (1.187)$$

In the absence of the small term $\Delta\,(\overline{\rho},\overline{\eta}) = \lambda^2\,(\overline{\rho}-\overline{\rho}^2-\overline{\eta}^2)$ this equation defines a hyperbola in the $(\overline{\rho},\overline{\eta})$ plane. The largest uncertainties in (1.187) stem from $\widehat{B}_K$ and $A=|V_{cb}|/\lambda^2$, which enters the largest term in (1.187) raised to the fourth power. Hence, reducing the error of $|V_{cb}|$ improves the ϵ_K constraint.

It is more difficult to analyze ϵ'_K, because the weak phases Φ_0 and Φ_2 are much harder to compute than ϕ_M. Φ_2 is essentially proportional to $\mathrm{Im}\,\lambda_t\,\langle(\pi\pi)_{I=2}|\,Q_8\,|\overline{K}^0\rangle/|A_2|$. The two matrix elements entering $\Phi_2-\Phi_0$ are difficult to calculate and numerically tend to cancel each other. Especially there is a controversy about $\langle(\pi\pi)_{I=0}|Q_6|\overline{K}^0\rangle$ and the different theoretical estimates can accommodate for both the KTeV and the NA48 result in (1.181) [91,93]. Even after the experimental discrepancy in (1.180) is resolved, ϵ'_K will not immediately be useful to determine $\mathrm{Im}\,\lambda_t \simeq A^2\lambda^5\overline{\eta}$. Nevertheless, ϵ'_K can be useful to constrain new physics contributions [94]. For recent overviews on ϵ'_K we refer to [95].

1.6.3 $K \to \pi\nu\bar{\nu}$

Rare kaon decays triggered by loop-induced $s\to d$ transitions can provide information on λ_t and thereby on the shape of the unitarity triangle. Final states with charged leptons are poorly suited for a clean extraction of this information, because they involve diagrams with photon-meson couplings. Such diagrams are affected by long distance hadronic effects and are hard to evaluate. The decays $K^+\to\pi^+\nu\overline{\nu}$ and $K_L\to\pi^0\nu\overline{\nu}$, however, are theoretically very clean, with negligible hadronic uncertainties. The $K\to\pi$ form factors can be extracted from the well-measured $K_{\ell 3}$ decays. So far two $K^+\to\pi^+\nu\overline{\nu}$ events have been observed [96], corresponding to a branching ratio

$$\mathcal{B}(K^+\to\pi^+\nu\overline{\nu}) = \left(1.57^{+1.75}_{-0.82}\right)\times 10^{-10}\,. \qquad (1.188)$$

Experimental proposals at BNL and Fermilab aim at a measurement of $K^+ \to \pi^+\nu\overline{\nu}$ and $K_L \to \pi^0\nu\overline{\nu}$ at the 10% level. The constraint on the improved Wolfenstein parameters $(\overline{\rho},\overline{\eta})$ can be cast in the form [35]

$$\frac{\mathcal{B}(K^+ \to \pi^+\nu\overline{\nu})}{4.57\cdot 10^{-11}} = A^4 X^2(x_t)\left(1-\lambda^2\right)\left[\left(\frac{\overline{\eta}}{1-\lambda^2}\right)^2 + (\rho_0-\overline{\rho})^2\right]. \tag{1.189}$$

Here $X(x_t) \simeq 1.50$ comprises the dependence on m_t and the NLO short distance QCD corrections [97]. $\rho_0 \approx 1 + 0.27/A^2$ contains the contribution from the internal charm loop [97]. The quoted numerical value corresponds to a $\overline{\rm MS}$ mass of $m_c = 1.3\,{\rm GeV}$. The largest theoretical uncertainty in (1.189), of order 5%, stems from the charm contribution. Further the fourth power of A introduces a sizable parametric uncertainty. The equation in (1.189) describes an ellipse in the $(\overline{\rho},\overline{\eta})$ plane centered at $(\rho_0, 0)$. By inserting typical values for the Wolfenstein parameters (e.g., $\lambda = 0.22$, $A = 0.8$, $\overline{\rho} = 0.2$ and $\overline{\eta} = 0.4$) into (1.189) one finds that (1.188) is compatible with the Standard Model.

In the Standard Model the decay $K_L \to \pi^0\nu\overline{\nu}$ is CP violating. It measures interference type CP violation, the associated phase $\arg\lambda_{\pi^0\nu\overline{\nu}}$ is large, of order $\overline{\eta}/(1-\overline{\rho})$. This is in sharp contrast to the small phases we found in (1.173) and (1.181). A measurement of $\mathcal{B}(K_L \to \pi^0\nu\overline{\nu})$ establishes $\arg\lambda_{\pi^0\nu\overline{\nu}} \neq \phi$ and therefore implies CP violation in the $|\Delta S| = 1$ Hamiltonian. This is the same situation as with $\mathrm{Im}\,(\epsilon'_K\, A_0/A_2)$ in (1.178), which also proves $|\Delta S| = 1$ CP violation from the difference of two interference type CP violating phases. $K_L \to \pi^0\nu\overline{\nu}$ is even cleaner than $K^+ \to \pi^+\nu\overline{\nu}$, because the charm contribution is negligible. $\mathcal{B}(K_L \to \pi^0\nu\overline{\nu})$ is proportional to $(\mathrm{Im}\,\lambda_t)^2 \propto \overline{\eta}^2$ and therefore determines the height of the unitarity triangle

$$\frac{\mathcal{B}(K_L \to \pi^0\nu\overline{\nu})}{1.91\cdot 10^{-10}} = A^4 X^2(x_t)\,\overline{\eta}^2\left(1+\lambda^2\right). \tag{1.190}$$

Hence the two discussed branching ratios allow for a precise construction of the unitarity triangle from kaon physics alone. Moreover the ratio of the two branching ratios is almost independent of A and m_t. It allows for a determination of $\sin 2\beta$ with a similar precision as from $a_{CP}(B \to \psi K_S)$ [98]. New physics may enter $s \to d$ transitions in a different way than $b \to s$ and $b \to d$ transitions. Hence comparing of the unitarity triangles from K physics and from B physics provides an excellent test of the Standard Model.

1.7 Standard Model Expectations

This section outlines what is known about the CKM matrix at the present time, and what the pattern of expectations is for some of the most interesting processes in the Standard Model.

Since most of the existing data apart from $\sin 2\beta$ come from CP conserving measurements, it is convenient to present the constraints on the CKM matrix using the Wolfenstein parameterization. Magnitudes of CKM matrix elements are simply related to λ, A, $\bar{\rho}$, and $\bar{\eta}$. The best known of these is λ, the Cabibbo angle, which is known at the 1% level. The parameter A is determined by $|V_{cb}|$, which is known with a 5% error. The uncertainty in $\bar{\rho}$ and $\bar{\eta}$ is significantly larger. The most important constraints come from

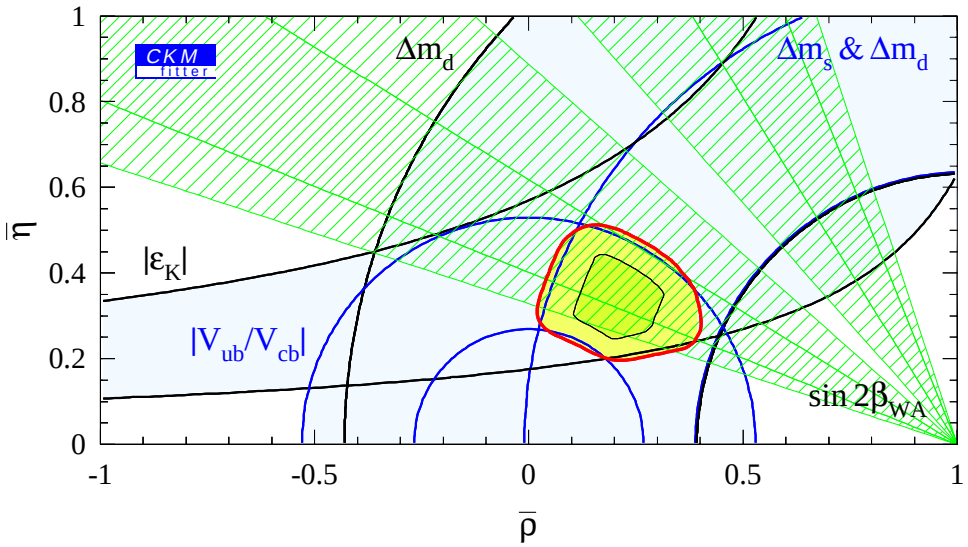

Figure 1.9: The allowed region in the $\bar{\rho} - \bar{\eta}$ plane. Also shown are the individual constraints, and the world average $\sin 2\beta$. (From Ref. [99].)

- CP violation in $K^0 - \overline{K}^0$ mixing described by the ϵ_K parameter;
- $|V_{ub}/V_{cb}|$ measured from semileptonic B decays;
- $B^0 - \overline{B}^0$ mixing;
- The lower limit on $B_s - \overline{B}_s$ mixing.

A problem in translating these to constraints on the CKM matrix is related to theoretical uncertainties. We follow the point of view adopted in the BaBar book [4] that no confidence level can be attached to model dependent theory errors. Fig. 1.9 shows the result of such an analysis from Ref. [99]. Fig. 1.10 shows the same fit on the $\sin 2\alpha - \sin 2\beta$ plane. Note that any value for $\sin 2\alpha$ would still be allowed if $|V_{ub}|$ were slightly larger, or if Δm_{B_s} were slightly smaller than their allowed ranges. Fig. 1.11 shows the allowed range in the $\sin 2\beta - \gamma$ plane, and that γ is already constrained.

Some of the uncertainties entering these constraints will be significantly reduced during Run II. The hadronic matrix elements B_K, $f_{B_d}^2 B_{B_d}$, and $f_{B_s}^2 B_{B_s}$ need to be determined by unquenched lattice QCD calculations. The theoretical uncertainties in $|V_{ub}|$ and $|V_{cb}|$ will also be reduced to the few percent level by unquenched lattice calculations of the exclusive $\overline{B}_d^0 \to \pi \ell \bar{\nu}$ and $\overline{B}_d^0 \to D^{(*)} \ell \bar{\nu}$ form factors in the region of phase space where the momentum of the final hadron is small. As discussed in Sec. 1.5.4, these lattice calculations are straightforward in principle, but a variety of uncertainties must be brought under control. The uncertainties in these two CKM matrix elements may be reduced in the next few years, even without recourse to lattice QCD, using inclusive semileptonic decays. The error in $|V_{cb}|$ may be reduced to 2–3% with precise determinations of a short distance b quark mass and by gaining more confidence about the smallness of quark-hadron duality violation. On a similar timescale the error in $|V_{ub}|$ may be reduced to the 5–10% level [100] by pursuing several model independent determinations.

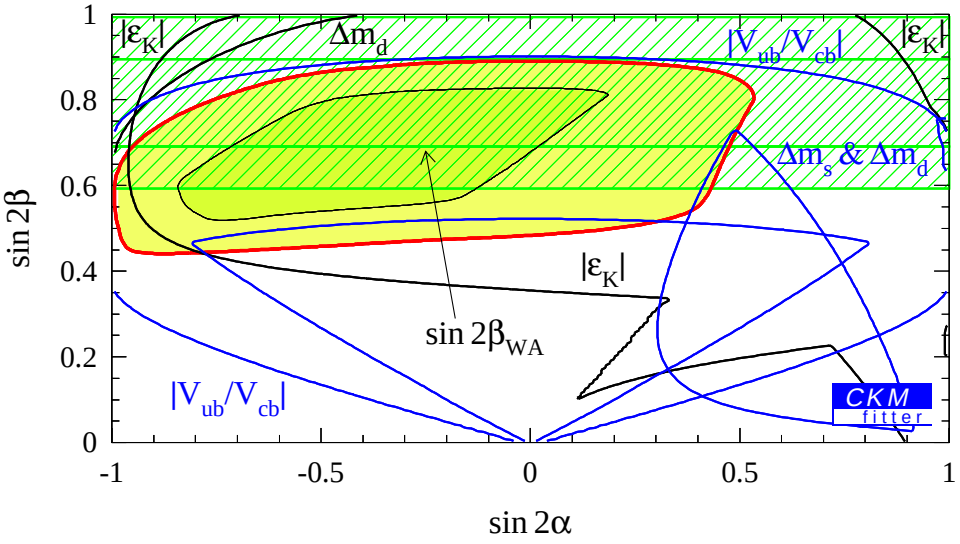

Figure 1.10: The allowed region in the $\sin 2\alpha - \sin 2\beta$ plane [99].

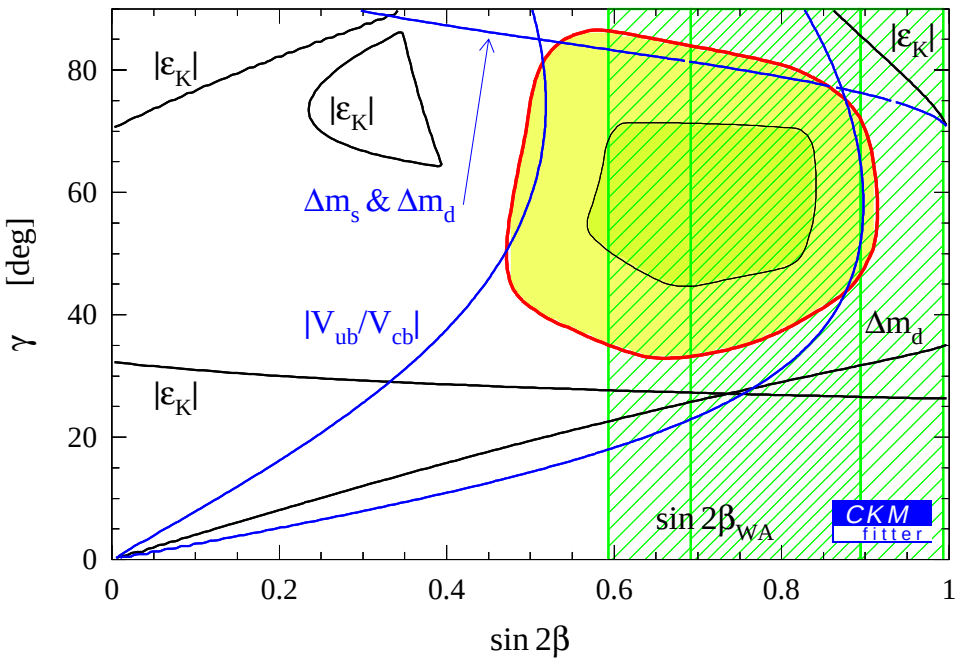

Figure 1.11: The allowed region in the $\sin 2\beta - \gamma$ plane [99].

References

[1] T. Affolder *et al.*, CDF Collaboration, Phys. Rev. D **61** (2000) 072005.

[2] B. Aubert *et al.*, BABAR Collaboration, Phys. Rev. Lett. **86** (2001) 2515.

[3] A. Abashian *et al.*, BELLE Collaboration, Phys. Rev. Lett. **86** (2001) 2509.

[4] *The BaBar Physics Book: Physics at an Asymmetric B Factory*, ed. P. F. Harrison and H. R. Quinn, SLAC-R-0504.

[5] G. C. Branco, L. Lavoura and J. P. Silva, *CP Violation* (Clarendon Press, Oxford, 1999).

[6] A. V. Manohar and M. B. Wise, *Heavy Quark Physics* (Cambridge University Press, 2000).

[7] I. I. Bigi and A. I. Sanda, *CP Violation* (Cambridge University Press, New York, 2000).

[8] *B decays at the LHC*, ed. P. Ball *et al.*, hep-ph/0003238 [CERN-TH/2000-101].

[9] See, for example, P. Langacker, in *Proceedings of the 24th International Conference on High Energy Physics*, ed. R. Kotthaus and J. H. Kühn (Springer-Verlag, Berlin, 1989).

[10] N. Cabibbo, Phys. Rev. Lett. **10** (1963) 531.

[11] M. Kobayashi and T. Maskawa, Prog. Theor. Phys. **49** (1973) 652.

[12] S. L. Glashow, J. Iliopoulos and L. Maiani, Phys. Rev. D **2** (1970) 1285.

[13] J. F. Gunion, H. E. Haber, G. L. Kane and S. Dawson, *The Higgs Hunter's Guide* (Addison-Wesley, Redwood City, Calif., 1989).

[14] C. Jarlskog, Phys. Rev. Lett. **55** (1985) 1039.

[15] D. E. Groom *et al.* [Particle Data Group], Eur. Phys. J. C **15** (2000) 1.

[16] L. Wolfenstein, preprint No. NSF-ITP-90-29 (unpublished); Phys. Rev. D **43** (1991) 151.

[17] A. J. Buras, M. E. Lautenbacher, G. Ostermaier, Phys. Rev. D **50** (1994) 3433.

[18] G. Buchalla and A. J. Buras, Phys. Rev. D **54** (1996) 6782.

[19] A. F. Falk, A. Lewandowski and A. A. Petrov, Phys. Lett. B **505** (2001) 107;
G. Buchalla and G. Isidori, Phys. Lett. B **440** (1998) 170.

[20] G. P. Lepage and S. J. Brodsky, Phys. Rev. D **22** (1980) 2157.

[21] C.-H. V. Chang and H-n. Li, Phys. Rev. D **55** (1997) 5577; T.-W. Yeh and H-n. Li, Phys. Rev. D **56** (1997) 1615; Y.-Y. Keum, H-n. Li and A. I. Sanda, Phys. Lett. B **504** (2001) 6; Phys. Rev. D **63** (2001) 054008; Y.-Y. Keum and H-n. Li, Phys. Rev. D **63** (2001) 074006.

[22] M. Beneke, G. Buchalla, M. Neubert and C. T. Sachrajda, Phys. Rev. Lett. **83** (1999) 1914; Nucl. Phys. B **591** (2000) 313; hep-ph/0007256.

[23] G. Lüders, Dan. Mat. Phys. Medd. **28** (1954) 5; W. Pauli in *Niels Bohr and the Development of Physics*, ed. W. Pauli, L. Rosenfeld and V. Weisskopf (McGraw-Hill, New York, 1955); G. Lüders, Ann. Phys. **2** (1957).

[24] V. A. Kostelecky and S. Samuel, Phys. Rev. Lett. **63** (1989) 224; **66** (1991) 1811; Phys. Rev. D **39** (1989) 683; **40** (1989) 1886. V. A. Kostelecky and R. Potting, Nucl. Phys. B **359** (1991) 545; Phys. Lett. B **381** (1996) 89; J. Ellis, J. L. Lopez, N. E. Mavromatos and D. V. Nanopoulos, Phys. Rev. D **53** (1996) 3846.

[25] V.F. Weisskopf and E.P. Wigner, Z. Phys. **63** (1930) 54; **65** (1930) 18; T. D. Lee, R. Oehme and C. N. Yang, Phys. Rev. **106** (1957) 340.

[26] L.A. Khalfin, Zh. Eksp. Teor. Fiz. **33** (1957) 1371.

[27] Y. I. Azimov, Phys. Atom. Nucl. **59** (1996) 856, and references therein.

[28] A. Angelopoulos *et al.*, CPLEAR Collaboration, Phys. Lett. B **444** (1998) 43.

[29] R. Aleksan, I. Dunietz and B. Kayser, Z. Phys. C **54** (1992) 653.

[30] L. Wolfenstein, Phys. Rev. Lett. **13** (1964) 562.

[31] J. H. Christenson, J. W. Cronin, V. L. Fitch and R. Turlay, Phys. Rev. Lett. **13** (1964) 138. Phys. Rev. **140** (1965) B74.

[32] K. G. Wilson, Phys. Rev. **179** (1969) 1499.

[33] A. J. Buras, M. Misiak and J. Urban, Nucl. Phys. B **586** (2000) 397.

[34] G. Altarelli, G. Curci, G. Martinelli and S. Petrarca, Nucl. Phys. B **187** (1981) 461; A. J. Buras and P. H. Weisz, Nucl. Phys. B **333** (1990) 66; A. J. Buras, M. Jamin, M. E. Lautenbacher and P. H. Weisz, Nucl. Phys. B **370** (1992) 69, Addendum **375** (1992) 501; Nucl. Phys. B **400** (1993) 37.

[35] G. Buchalla, A. J. Buras and M. E. Lautenbacher, Rev. Mod. Phys. **68** (1996) 1125.

[36] M. Ciuchini, E. Franco, G. Martinelli, L. Reina and L. Silvestrini, Phys. Lett. B **316** (1993) 127; M. Ciuchini, E. Franco, G. Martinelli, L. Reina and L. Silvestrini, Phys. Lett. B **334** (1994) 137; M. Ciuchini, E. Franco, L. Reina and L. Silvestrini, Nucl. Phys. B **421** (1994) 41.

[37] K. Chetyrkin, M. Misiak and M. Münz, Phys. Lett. B **400** (1997) 206.

[38] T. Inami and C. S. Lim, Progr. Theor. Phys. **65** (1981) 297, **65** (1981) 1772(E).

[39] A. J. Buras, M. Jamin and P. H. Weisz, Nucl. Phys. B **347** (1990) 491.

[40] N. Isgur and M. B. Wise, Phys. Lett. B **232**, 113 (1989); **237**, 527 (1990).

[41] E. V. Shuryak, Phys. Lett. **93B** (1980) 134; Nucl. Phys. B **198** (1982) 83.

[42] S. Nussinov and W. Wetzel, Phys. Rev. D **36** (1987) 130.

[43] M. B. Voloshin and M. A. Shifman, Sov. J. Nucl. Phys. **45** (1987) 292 [Yad. Fiz. **45** (1987) 463]; **47** (1988) 511 [**47** (1988) 801].

[44] H. D. Politzer and M. B. Wise, Phys. Lett. B **206** (1988) 681; **208** (1988) 504.

[45] E. Eichten and B. Hill, Phys. Lett. B **234** (1990) 511; **243** (1990) 427.

[46] B. Grinstein, Nucl. Phys. B **339** (1990) 253.

[47] H. Georgi, Phys. Lett. B **240** (1990) 447.

[48] A. F. Falk, B. Grinstein and M. E. Luke, Nucl. Phys. B **357** (1991) 185.

[49] A. F. Falk, H. Georgi, B. Grinstein and M. B. Wise, Nucl. Phys. B **343** (1990) 1.

[50] J.D. Bjorken, *Proceedings of the 18th SLAC Summer Institute on Particle Physics*, Stanford, California, July 1990, edited by J.F. Hawthorne (SLAC, Stanford, 1991).

[51] M. E. Luke, Phys. Lett. B **252** (1990) 447.

[52] J. Charles, A. Le Yaouanc, L. Oliver, O. Pene and J. C. Raynal, Phys. Rev. D **60** (1999) 014001.

[53] M. B. Voloshin and M. A. Shifman, Sov. J. Nucl. Phys. **41** (1985) 120; J. Chay, H. Georgi and B. Grinstein, Phys. Lett. B **247** (1990) 399.

[54] I. I. Bigi, N. G. Uraltsev and A. I. Vainshtein, Phys. Lett. B **293** (1992) 430, **297** (1993) 477(E); I. I. Bigi, M. Shifman, N. G. Uraltsev and A. Vainshtein, Phys. Rev. Lett. **71** (1993) 496.

[55] A. V. Manohar and M. B. Wise, Phys. Rev. D **49** (1994) 1310; B. Blok, L. Koyrakh, M. Shifman and A. I. Vainshtein, *ibid.* **49** (1994) 3356, **50** (1994) 3572(E); T. Mannel, Nucl. Phys. B **413** (1994) 396.

[56] E. C. Poggio, H. R. Quinn and S. Weinberg, Phys. Rev. D **13** (1976) 1958.

[57] A. F. Falk, M. B. Wise and I. Dunietz, Phys. Rev. D **51** (1995) 1183.

[58] M. Gremm, A. Kapustin, Z. Ligeti and M. B. Wise, Phys. Rev. Lett. **77** (1996) 20; A. F. Falk, M. E. Luke and M. J. Savage, Phys. Rev. D **53** (1996) 6316; Z. Ligeti, M. E. Luke, A. V. Manohar and M. B. Wise, Phys. Rev. D **60** (1999) 034019.

[59] M. Crisafulli, V. Giménez, G. Martinelli and C. T. Sachrajda, Nucl. Phys. B **457** (1995) 594; V. Giménez, G. Martinelli and C. T. Sachrajda, *ibid.* **486** (1997) 227; Phys. Lett. B **393** (1997) 124; A. S. Kronfeld and J. N. Simone, Phys. Lett. B **490** (2000) 228, **495** (2000) 441(E).

[60] K. G. Wilson, Phys. Rev. D **10** (1974) 2445.

[61] J. B. Kogut, Rev. Mod. Phys. **55** (1983) 775.

[62] M. Di Pierro, "From Monte Carlo integration to lattice quantum chromodynamics: An introduction," hep-lat/0009001 [FERMILAB-FN-699].

[63] A. X. El-Khadra, G. Hockney, A. S. Kronfeld and P. B. Mackenzie, Phys. Rev. Lett. **69** (1992) 729.

[64] P. B. Mackenzie, Nucl. Phys. B Proc. Suppl. **34** (1994) 400; C. T. H. Davies *et al.*, Phys. Rev. Lett. **73** (1994) 2654 [hep-lat/9404012]; B. J. Gough *et al.*, *ibid.* **79** (1997) 1622 [hep-ph/9610223].

[65] J. Sexton and D. Weingarten, Phys. Rev. D **55** (1997) 4025.

[66] A. Ali Khan *et al.*, CP-PACS Collaboration, Nucl. Phys. B Proc. Suppl. **83** (2000) 265, 331 [hep-lat/9911039, hep-lat/9909052]; Phys. Rev. D **64** (2001) 034505 [hep-lat/0010009].

[67] C. Bernard *et al.*, MILC Collaboration, Nucl. Phys. B Proc. Suppl. **83** (2000) 289 [hep-lat/9909121]; **94** (2001) 346 [hep-lat/0011029].

[68] M. Lüscher, Commun. Math. Phys. **104** (1986) 177; **105** (1986) 153.

[69] J. Gasser and H. Leutwyler, Ann. Phys. **158** (1984) 142.

[70] S. Sharpe and N. Shoresh, Phys. Rev. D **62** (2000) 094503 [hep-lat/0006017].

[71] K. G. Wilson, in *New Phenomena in Subnuclear Physics*, edited by A. Zichichi (Plenum, New York, 1977).

[72] K. Symanzik, in *Recent Developments in Gauge Theories*, ed. G. 't Hooft *et al.* (Plenum, New York, 1980); in *Mathematical Problems in Theoretical Physics*, edited by R. Schrader *et al.* (Springer, New York, 1982); Nucl. Phys. B **226**, 187, 205 (1983).

[73] B. Sheikholeslami and R. Wohlert, Nucl. Phys. B **259** (1985) 572.

[74] K. Jansen *et al.*, Phys. Lett. B **372** (1996) 275 [hep-lat/9512009]; M. Lüscher, S. Sint, R. Sommer, P. Weisz and U. Wolff, Nucl. Phys. B **491** (1997) 323 [hep-lat/9609035].

[75] E. Eichten, Nucl. Phys. B Proc. Suppl. **4** (1987) 170; E. Eichten and B. Hill, Phys. Lett. B **234** (1990) 511.

[76] G. P. Lepage and B. A. Thacker, Nucl. Phys. B Proc. Suppl. **4** (1987) 199; B. A. Thacker and G. P. Lepage, Phys. Rev. D **43** (1991) 196.

[77] A. X. El-Khadra, A. S. Kronfeld, and P. B. Mackenzie, Phys. Rev. D **55** (1997) 3933 [hep-lat/9604004].

[78] T. R. Klassen, Nucl. Phys. B **509** (1998) 391; Nucl. Phys. B Proc. Suppl. **73** (1999) 918.

[79] S. Collins, *et al.*, Phys. Rev. D **64** (2001) 055002 [hep-lat/0101019].

[80] A. S. Kronfeld, Phys. Rev. D **62** (2000) 014505 [hep-lat/0002008].

[81] J. Harada, A. S. Kronfeld, H. Matsufuru, N. Nakajima and T. Onogi, Phys. Rev. D **64** (2001) 074501 [hep-lat/0103026].

[82] G. Martinelli and C. T. Sachrajda, Nucl. Phys. B **559** (1999) 429 [hep-lat/9812001]; V. Giménez, L. Giusti, G. Martinelli and F. Rapuano, JHEP **0003** (2000) 018 [hep-lat/0002007].

[83] S. Hashimoto, Nucl. Phys. B Proc. Suppl. **83** (2000) 3 [hep-lat/9909136]; C. Bernard, *ibid.* **94** (2001) 159 [hep-lat/0011064].

[84] L. Maiani and M. Testa, Phys. Lett. B **245** (1990) 585.

[85] M. Lüscher, Nucl. Phys. B **354** (1991) 531.

[86] L. Lellouch and M. Lüscher, Commun. Math. Phys. **219** (2001) 31. See also Sec. 7 of L. Lellouch, Nucl. Phys. B Proc. Suppl. **94** (2001) 142 [hep-lat/0011088], for a simple summary.

[87] K. M. Watson, Phys. Rev. **88** (1952) 1163.

[88] A. Alavi-Harati *et al.*, KTeV Collaboration, Phys. Rev. Lett. 83 (1999) 22; J. Graham, KTeV Collaboration, Fermilab Seminar, `http://kpasa.fnal.gov:8080/public/epsprime/ktev2001.ps.gz`, 8 June 2001.

[89] I. Augustin *et al.*, NA48 Collaboration, Phys. Lett. B **465** (1999) 335; G. Unal, NA48 Collaboration, CERN seminar, 10 May 2001. `http://na48.web.cern.ch/NA48/Welcome/images/talks/cern_seminar01/talk.ps.gz`

[90] A. J. Buras, M. Jamin and P. H. Weisz, Nucl. Phys. B **347** (1990) 491; S. Herrlich and U. Nierste, Nucl. Phys. B **419** (1994) 292; Phys. Rev. D **52** (1995) 6505; Nucl. Phys. B **476** (1996) 27.

[91] M. Ciuchini, E. Franco, G. Martinelli and L. Reina, Phys. Lett. B **301** (1993) 263; A. Buras, M. Jamin and M. E. Lautenbacher, Nucl. Phys. B **408** (1993) 209; S. Bertolini, J. O. Eeg, M. Fabbrichesi and E. I. Lashin, Nucl. Phys. B **514** (1998) 93.

[92] U. Nierste, in *Proceedings of the Workshop on K Physics*, ed. L. Iconomidou-Fayard (Editions Frontières, Gif-Sur-Yvette, 1997), [hep-ph/9609310]; hep-ph/9510383.

[93] Y. Keum, U. Nierste and A. I. Sanda, Phys. Lett. B **457** (1999) 157; E. Pallante and A. Pich, Phys. Rev. Lett. **84** (2000) 2568; A. J. Buras, M. Ciuchini, E. Franco, G. Isidori, G. Martinelli and L. Silvestrini, Phys. Lett. B **480** (2000) 80;

[94] A. J. Buras and L. Silvestrini, Nucl. Phys. B **546** (1999) 299; A. Masiero and H. Murayama, Phys. Rev. Lett. **83** (1999) 907; A. J. Buras, G. Colangelo, G. Isidori, A. Romanino and L. Silvestrini, Nucl. Phys. B **566** (2000) 3;

[95] A. J. Buras, hep-ph/9908395; U. Nierste, Nucl. Phys. Proc. Suppl. **86** (2000) 329; M. Jamin, hep-ph/9911390; S. Bertolini, hep-ph/0002114; M. Ciuchini and G. Martinelli, hep-ph/0006056.

[96] S. Adler *et al.*, E787 Collaboration, hep-ex/0111091; Phys. Rev. Lett. **84** (2000) 3768.

[97] G. Buchalla and A. J. Buras, Nucl. Phys. B **400** (1993) 225; Nucl. Phys. B **412** (1994) 106.

[98] G. Buchalla and A. J. Buras, Phys. Lett. B **333** (1994) 221, Ref. [18]; Y. Grossman and Y. Nir, Phys. Lett. B **398** (1997) 163; Y. Nir and M. P. Worah, Phys. Lett. B **423** (1998) 319; A. J. Buras, A. Romanino and L. Silvestrini, Nucl. Phys. B **520** (1998) 3.

[99] A. Höcker, H. Lacker, S. Laplace and F. Le Diberder, Eur. Phys. J. C21 (2001) 225; and updates at `http://www.slac.stanford.edu/~laplace/ckmfitter.html`.

[100] C.W. Bauer, Z. Ligeti and M. Luke, Phys. Rev. D **64** (2001) 113004; Phys. Lett. B **479** (2000) 395. A.K. Leibovich, I. Low and I.Z. Rothstein, Phys. Lett. B **486** (2000) 86.